



**Design, synthesis and reactivity of novel  
transition metal complexes of 1,3-diketonates  
bearing perfluorinated or heterocyclic moieties**

**Jo' Del Gobbo**

Thesis to obtain the Master of Science  
Degree in

**Chemistry**

Supervisors: Prof. Luísa Margarida Martins  
Prof. Maura Pellei

**Examination Committee**

Chairperson:	Prof. Carlos Baleizão
Supervisor	Prof. Luísa Margarida Martins
Members of the committee:	Prof. Isabel Correia
	Prof. Luísa Margarida Martins

**December 2022**

## ABSTRACT

$\beta$ -Diketonate ligands hold an important place in the history of coordination chemistry and continue to be among the most ubiquitous ligands. The most unique feature is their ability to coordinate most of all known elements. The first part of the research project has been mainly focused on the syntheses of a sterically hindered  $\beta$ -diketonate, 1,3-dimesitylpropane-1,3-dione ( $\text{HL}^{\text{Mes}}$ ) and of a further sterically hindered  $\beta$ -diketonate ligand, bearing fluorinated moieties, the 1,3-bis(3,5-bis(trifluoromethyl)phenyl)-3-hydroxyprop-2-en-1-one ( $\text{HL}^{\text{CF}_3}$ ). Their reactivity has been investigated through the synthesis of the related Zn(II), Cu(II), Cu(I) and Ag(I) complexes. The second part has concerned the development of a platform for the synthesis of new N,O,O-donor chelating species as a new class of "scorpionate" ligands, based on the 3-benzylidene-2,4-pentanedione skeletal functionalized with heterocyclic rings. In particular, the 3-(phenyl(1H-pyrazol-1-yl)methyl)pentane-2,4-dione ( $\text{HL}^{\text{I}}$ ), a novel 1,3-diketonate bearing a pyrazole moiety (whose reactivity and structure have been fully studied also by X-ray diffraction analysis), and the 1-(3,5-dimethyl-1H-pyrazol-1-yl)-3-phenylpropane-1,3-dione ( $\text{HL}^{\text{JM}}$ ) containing a pyrazole unit functionalized in 3- and 5-position. Each ligand has been used to synthesize different types of metal complexes by using Zn(II), Cu(II), Cu(I) and Ag(I) acceptors with the aim to investigate the chemical properties (reactivity, stability, geometry) of the new ligands and related complexes. In the syntheses of Cu(I) and Ag(I) complexes, a phosphane coligand, such as triphenylphosphine was also used to stabilize silver and copper in +1 oxidation state. Biological studies to evaluate the antitumor and antiviral activity are in progress for some of the ligands and related metal complexes.

**Keywords:**  $\beta$ -diketones, sterically hindered  $\beta$ -diketonates, N,O,O-donor chelating species, transition metal-based complexes, phosphanes, X-ray analysis.

## RESUMO

$\beta$ -dionas têm um lugar importante na história da química de coordenação, continuando a estar dentro dos ligandos mais utilizados. A característica mais singular é a sua capacidade de coordenar muitos dos elementos conhecidos. A primeira parte deste projeto de investigação tem-se focado na síntese de uma  $\beta$ -diona impedida estereoquimicamente, dimesitylpropano-1,3-diona ( $HL^{Mes}$ ), e de outra ainda mais impedida, com grupos fluorinados, 1,3-bis(3,5-bis(trifluorometil)fenil)-3-hidroxiprop-2-en-1-ona ( $HL^{CF_3}$ ). A sua reatividade foi estudada através da síntese dos correspondentes complexos de Zn(II), Cu(II), Cu(I) e Ag(I). A segunda parte diz respeito ao desenvolvimento de uma plataforma para a síntese de novos compostos quelantes doadores por N,O,O como nova classe de “escorpionatos”, baseado no esqueleto de 3-benzilideno-2,4-pentanodiona funcionalizado com anéis heterocíclicos. Em particular, a 3-(fenil(1H-pirazol-1-il)metil)pentano-2,4-diona ( $HL^L$ ), uma nova 1,3-diona com um grupo pirazol (cuja reatividade e estrutura foram estudados por análise de difração raio-X), e a 1-(3,5-dimetil-1H-pirazol-1-il)-3-fenilpropano-1,3-diona ( $HL^M$ ) contendo um pirazol funcionalizado nas posições 3 e 5. Cada ligando foi utilizado para sintetizar diferentes complexos usando Zn(II), Cu(II), Cu(I) e Ag(I) como aceitadores, com o âmbito de investigar as propriedades químicas (reatividade, estabilidade, geometria) dos novos ligandos e respetivos complexos. Nas sínteses de complexos de Cu(I) e Ag(I), um co-ligando de fósforo, como a trifenilfosfina foi também utilizado para estabilizar cobre e prata no estado de oxidação +1. Estudos biológicos para avaliar a atividade antitumoral e antiviral estão em progresso para alguns ligandos e os seus respetivos complexos.

**Palavras-chave:**  $\beta$ -dionas;  $\beta$ -dionatos estereoquimicamente impedidos; espécies quelantes dadoras N,O,O; complexos de metais de transição; fosfina; análise de raio-X.

## Index

<b>1. INTRODUCTION</b> .....	<b>1</b>
<b>1.1. Precious metals</b> .....	<b>1</b>
<b>1.2. <math>\beta</math>-Diketones ligands and base metals</b> .....	<b>1</b>
1.2.1. Structure and tautomerism .....	2
1.2.3. Spectrochemical versus nephelauxetic series .....	4
<b>1.3. Coordination modes</b> .....	<b>4</b>
1.3.1. Neutral $\beta$ -diketones.....	4
1.3.2. Monoanionic $\beta$ -diketonates .....	5
1.3.3. Dianionic $\beta$ -diketonates.....	6
<b>1.4. Historical context</b> .....	<b>7</b>
<b>1.5. Synthesis of <math>\beta</math>-diketones</b> .....	<b>7</b>
<b>1.6. Biological and pharmacological importance of <math>\beta</math>-diketones</b> .....	<b>10</b>
1.6.1. $\beta$ -diketones as intermediates in organic synthesis.....	10
1.6.3. $\beta$ -diketones as natural products.....	11
<b>1.7. Hindered <math>\beta</math>-diketonates</b> .....	<b>13</b>
<b>1.8. Main fields of research on technological applications of metal <math>\beta</math>-diketonates</b> .....	<b>15</b>
<b>1.9 Oligo-<math>\beta</math>-diketones as versatile ligands for use in metallo-supramolecular chemistry</b> .....	<b>19</b>
<b>1.10. Diketones with substituents containing additional donor atoms</b> .....	<b>19</b>
<b>2. EXPERIMENTAL SECTION</b> .....	<b>21</b>
<b>2.1. Methods and materials</b> .....	<b>21</b>
2.1.1 Crystallographic Data Collection and Refinement.....	21
<b>2.2. Synthesis of the ligands</b> .....	<b>22</b>
<b>2.3. Synthesis of HL<sup>CF<sub>3</sub></sup> complexes</b> .....	<b>25</b>
<b>2.4. Synthesis of HL<sup>J</sup> complexes</b> .....	<b>27</b>
<b>2.5. Synthesis of HL<sup>Mes</sup> complexes</b> .....	<b>29</b>
<b>3. RESULTS AND DISCUSSION</b> .....	<b>30</b>
<b>3.1. Aim of the work</b> .....	<b>30</b>
<b>3.2. Synthesis and characterization of the ligands</b> .....	<b>31</b>
<b>3.3. Synthesis and characterization of the complexes</b> .....	<b>47</b>
<b>4. Conclusions</b> .....	<b>62</b>
<b>References</b> .....	<b>63</b>
<b>Ringraziamenti</b> .....	<b>68</b>

## Index of Figures

<b>Figure 1</b> The latest release of the IUPAC Periodic Table (dated 4 May 2022).....	1
<b>Figure 2</b> Some examples of acetylacetonates used in catalysis.....	2
<b>Figure 3</b> Structures of commonly used $\beta$ -diketones .....	3
<b>Figure 4</b> Structures of different forms of neutral $\beta$ -diketones.....	5
<b>Figure 5</b> Structures of different forms of monoanionic $\beta$ -diketones .....	6
<b>Figure 6</b> Structures of different forms of dianionic $\beta$ -diketones.....	6
<b>Figure 7</b> Structure of curcumin .....	11
<b>Figure 8</b> Biological properties of Curcumin .....	12
<b>Figure 9</b> Pharmacological properties of Curcumin.....	12
<b>Figure 10</b> Generalized structures of acac and other supporting ligands, with approximate angles between the metal-ligand axis and the sterically encumbering group .....	13
<b>Figure 11</b> The hindered $\beta$ -diketone ligand, esac (far right), next to other popular ligand frameworks, including NacNacs, NHCs, and m-terphenyls .....	14
<b>Figure 12</b> Disproportionation and trapping of copper(I) $\beta$ -diketonates .....	15
<b>Figure 13</b> Trivalent Eu(III) complexes with anionic $\beta$ -diketones showing pure red emission [64] .....	16
<b>Figure 14</b> Iron(III) $\beta$ -diketonates: CVD precursors for iron oxide film formation [66] .....	16
<b>Figure 15</b> Cyclometalated Platinum(II) metallomesogens based on half-disc-shaped $\beta$ -diketonate ligands with hexacatenar [72]. .....	17
<b>Figure 16</b> $\beta$ -diketones with different types of $R^2$ substituents .....	19
<b>Figure 17</b> Structure of ligands $HL^{Mes}$ , $HL^{CF_3}$ , $HL^J$ and $HL^{JM}$ .....	30
<b>Figure 18</b> (a) $^1H$ -, (b) $^{13}C$ - and (c) $^{19}F$ -NMR spectra of $HL^{CF_3}$ in $CDCl_3$ solution .....	33
<b>Figure 19</b> Vibrational modes of the cis enol tautomer ring .....	34
<b>Figure 20</b> IR spectra of (a) $HL^{CF_3}$ and (b) $NaL^{CF_3}$ .....	36
<b>Figure 21</b> $^1H$ -NMR spectrum of $HL^{Mes}$ in $CDCl_3$ .....	38
<b>Figure 22</b> FT-IR spectrum of (a) $HL^{Mes}$ and (b) $NaL^{Mes}\cdot H_2O$ . .....	39
<b>Figure 23</b> $^1H$ -NMR spectrum of $NaL^{Mes}\cdot H_2O$ ( <b>4</b> ) in $CDCl_3$ solution.....	40
<b>Figure 24</b> $^1H$ -NMR spectrum of $HL^J$ ( <b>5</b> ) in $CDCl_3$ solution .....	41
<b>Figure 25</b> $^1H$ -NMR spectrum of $HL^{JM}$ ( <b>6</b> ) in $CDCl_3$ solution .....	42
<b>Figure 26</b> ORTEP view of $HL^J$ ( <b>5</b> ) with thermal ellipsoids drawn at the 30% probability level. Hydrogen atoms have been omitted. ....	43
<b>Figure 27</b> Packing structure view of $HL^J$ .....	43
<b>Figure 28</b> Nonbonding interactions in $HL^J$ .....	44
<b>Figure 29</b> FT-IR spectrum of (a) $HL^J$ and (b) $HL^{JM}$ .....	46
<b>Figure 30</b> ORTEP view of $[Cu(L^{Mes})_2]$ complex ( <b>14</b> ) with thermal ellipsoids drawn at the 30% probability level. Hydrogen atoms have been omitted.....	51
<b>Figure 31</b> Solid-state molecular structure of $[Cu(L^{CF_3})_2]\cdot THF$ .....	53
<b>Figure 32</b> Packing structure view of $[Cu(L^{CF_3})_2]\cdot THF$ .....	54
<b>Figure 33</b> Solid-state molecular structure of $[Zn(L^{Mes})_2]$ ( <b>15</b> ) complex.....	54
<b>Figure 34</b> $^{31}P\{^1H\}$ -NMR spectrum of complex <b>8</b> in $CDCl_3$ at 223 K.....	56
<b>Figure 35</b> Solid-state molecular structure of $[Cu(PPh_3)_2(L^{CF_3})]$ ( <b>8</b> ) complex .....	56
<b>Figure 36</b> $^{31}P\{^1H\}$ -NMR spectrum of complex <b>10</b> in $CDCl_3$ at 223 K.....	58
<b>Figure 37</b> Coordination modes of $L^J$ and $L^{JM}$ ligands ( $L^J$ : R = H; $L^{JM}$ : R = Me) .....	58
<b>Figure 38</b> $^{31}P\{^1H\}$ -NMR spectrum of complex <b>12</b> in $CDCl_3$ solution .....	61

## Index of Schemes

<b>Scheme 1</b> Tautomerism in $\beta$ -diketones .....	3
<b>Scheme 2</b> Synthesis of the three original $\beta$ -diketones by Fischer, Combes, and Claisen.....	7
<b>Scheme 3</b> Synthesis of $\beta$ -diketones by Claisen condensation.....	8
<b>Scheme 4</b> Synthesis of $\beta$ -diketones using 1-diazo-1-lithio-acetone as starting material.....	8
<b>Scheme 5</b> Regiospecific synthesis of unsymmetrical $\beta$ -diketones .....	8
<b>Scheme 6</b> Synthesis of $\beta$ -diketones by C-acylation .....	8
<b>Scheme 7</b> Synthesis of sterically hindered $\beta$ -diketones.....	9
<b>Scheme 8</b> Improved method for synthesis of $\beta$ -diketones with different R groups .....	9
<b>Scheme 9</b> A method to favour C-acylation instead of O-acylation in the synthesis of $\beta$ -diketones .....	10
<b>Scheme 10</b> $\beta$ -diketones as intermediates in the design of heterocyclic compounds .....	10
<b>Scheme 11</b> Reaction between $\beta$ -diketone and hydrazine .....	11
<b>Scheme 12</b> Poly- $\beta$ -diketones with or without a spacer and their keto-enol tautomerism.....	18
<b>Scheme 13</b> Synthetic procedure for the ligands $\text{HL}^{\text{CF}_3}$ ( <b>1</b> ) and $\text{NaL}^{\text{CF}_3}$ ( <b>2</b> ).....	31
<b>Scheme 14</b> Synthesis of 1,3-dimesityl-propane-1,3-dione $\text{HL}^{\text{Mes}}$ ( <b>3</b> ).....	37
<b>Scheme 15</b> Synthetic procedure for the ligands $\text{HL}^{\text{J}}$ ( <b>5</b> ) and $\text{HL}^{\text{JM}}$ ( <b>6</b> ).....	40
<b>Scheme 16</b> Synthetic procedure for the species $\text{L}^{\text{A}}$ .....	41
<b>Scheme 17</b> Synthetic procedure for the Cu(II) complexes of $\text{Cu}(\text{L}^{\text{CF}_3})_2$ ( <b>7</b> ) and $\text{Cu}(\text{L}^{\text{Mes}})_2$ ( <b>14</b> ) .....	47
<b>Scheme 18</b> Synthesis of the complex $[\text{Cu}(\text{PPh}_3)_2(\text{L}^{\text{CF}_3})]$ ( <b>8</b> ).....	55
<b>Scheme 19</b> Synthesis of the complex $[\text{Ag}(\text{PPh}_3)_2(\text{L}^{\text{CF}_3})]$ ( <b>10</b> ).....	57
<b>Scheme 20</b> Synthetic procedure for the $\text{Cu}(\text{L}^{\text{J}})_2$ complex ( <b>11</b> ) .....	59
<b>Scheme 21</b> Synthetic procedure for the $\text{Zn}(\text{HL}^{\text{J}})(\text{HPz})\text{Cl}_2$ ( <b>13</b> ) complex.....	59
<b>Scheme 22</b> Synthesis of complex $[\text{Cu}(\text{PPh}_3)_2(\text{HL}^{\text{J}})]\text{PF}_6$ ( <b>12</b> ).....	60

## Index of Tables

<b>Table 1</b> Vibrational band frequencies for selected $\beta$ -diketones ( $\text{cm}^{-1}$ ) [89].....	34
<b>Table 2</b> Bond lengths ( $\text{\AA}$ ) and angles ( $^\circ$ ) for compound $\text{HL}^{\text{J}}$ .....	44
<b>Table 3</b> Stretching absorptions of the C=O bond in Cu(II) complexes of $\beta$ -diketones $[\text{Cu}(\text{L})_2]$ .....	48
<b>Table 4</b> Selected bond lengths ( $\text{\AA}$ ) and angles ( $^\circ$ ) for compound $\text{Cu}(\text{L}^{\text{Mes}})_2$ .....	51
<b>Table 5</b> Selected bond angles and lengths as determined from X-ray crystallography for new and common complexes .....	52

## Abbreviation List

acacH	2,4-Pentanedione
bzacH	1-Phenyl-1,3-butanedione
dbzmH	1,3-Diphenyl-1,3-propanedione
tmhdH	2,2,6,6-Tetramethyl-3,5-heptanedione
tfacH	1,1,1-Trifloro-2,4-pentanedione
hfacH	1,1,1,5,5,5-Hexafluoro-2,4-pentanedione

en	Ethylenediamine
bpy	2,2'-Bipyridine
phen	1,10-Phenanthroline
NacNacs	$\beta$ -Diketiminates
NHCs	N-Heterocyclic Carbenes
DPM	Dipivaloylmethane
M.P.	Melting point
FT-IR	Fourier-transform infrared spectroscopy
ATR	Attenuated Total Reflection
m	Medium
mbr	Medium broad
s	Strong
sbr	Strong broad
sh	Shoulder
vs	Very strong
vsbr	Very strong broad
w	Weak
wbr	Weak broad
NMR	Nuclear magnetic resonance
br	Broad
d	Doublet
dbr	Doublet broad
dd	Doublet of doublet
m	Multiplet
s	Singlet
sbr	Singlet broad
t	Triplet
sept	Septet
vbr	Very broad
ESI-MS	ElectroSpray Ionization Mass Spectroscopy
HPLC	High-performance liquid chromatography
TMS	Tetramethylsilane
H <sub>2</sub> O	Water
H <sub>3</sub> PO <sub>4</sub>	Phosphoric acid
C <sub>2</sub> O <sub>4</sub> <sup>2-</sup>	Oxalate
NCS <sup>-</sup>	Thiocyanate
NO <sub>2</sub> <sup>-</sup>	Nitrite
CN <sup>-</sup>	Cyanide
F <sup>-</sup>	Fluoride anion
Cl <sup>-</sup>	Chloride anion
Br <sup>-</sup>	Bromide anion
I <sup>-</sup>	Iodide anion
N <sub>3</sub> <sup>-</sup>	Azide ion
CO	Carbon monoxide
NaH	Sodium hydride
THF	Tetrahydrofuran
Na <sub>2</sub> SO <sub>4</sub>	Sodium sulfate
HCl	Hydrochloric acid
NaOH	Sodium hydroxide
MeOH	Methanol
EtOH	Ethanol
CH <sub>3</sub> CN	Acetonitrile
NH <sub>3</sub>	Ammonia
AlCl <sub>3</sub>	Aluminium trichloride
CS <sub>2</sub>	Carbon disulfide
CHCl <sub>3</sub>	Chloroform
Et <sub>2</sub> O	Diethyl ether

Et <sub>3</sub> N	Triethylamine
pz	Pyrazole
ar	Aromatic
Cu(CO <sub>2</sub> CH <sub>3</sub> ) <sub>2</sub> ·H <sub>2</sub> O	Copper acetate monohydrate
[Cu(CH <sub>3</sub> CN) <sub>4</sub> ]PF <sub>6</sub>	Tetrakis(acetonitrile)copper(I) hexafluorophosphate
PPh <sub>3</sub>	Triphenylphosphine
Zn(CH <sub>3</sub> CO <sub>2</sub> ) <sub>2</sub>	Zinc acetate anhydrous
AgNO <sub>3</sub>	Silver nitrate
ZnCl <sub>2</sub>	Zinc chloride
CuCl <sub>2</sub> ·2H <sub>2</sub> O	Copper(II) chloride dihydrate
CVD	Chemical vapor deposition
SFT	Supercritical fluid transport
LMCT	Ligand-to-Metal Charge Transfer
MLCT	Metal-to-Ligand Charge Transfer
LEDs	Light-emitting diode
RNA	Ribonucleic acid
NSAIDs	Nonsteroidal anti-inflammatory drugs
COXs	Cyclooxygenase enzymes
NF-κB	Nuclear factor kappa
AP-1	Activator protein 1



# 1. INTRODUCTION

## 1.1. Precious metals

Nowadays one of the purposes of chemistry research is the development of base metal catalysts that can compete with precious metals (**Figure 1**) [1-3]. The precious metals are those that are relatively non-abundant in Earth's crust and/or difficult to extract, including the platinum group metals and many radioactive elements. Precious metals have various economic, scalability, sustainability and toxicity problems [4, 5], but they are indispensable in homogeneous catalysis [6-9]. Further, these metals often rely on expensive ligand classes to support their chemistry. Demand for precious metals has increased over the past few decades, increasing their prices and motivating research into base metal catalysis. The earth-abundant base metals, on the other hand, are economical and generally non-toxic [10, 11]. However, there is a critical need for ligand classes that promote the high-spin reactivity exhibited by the first transition series.

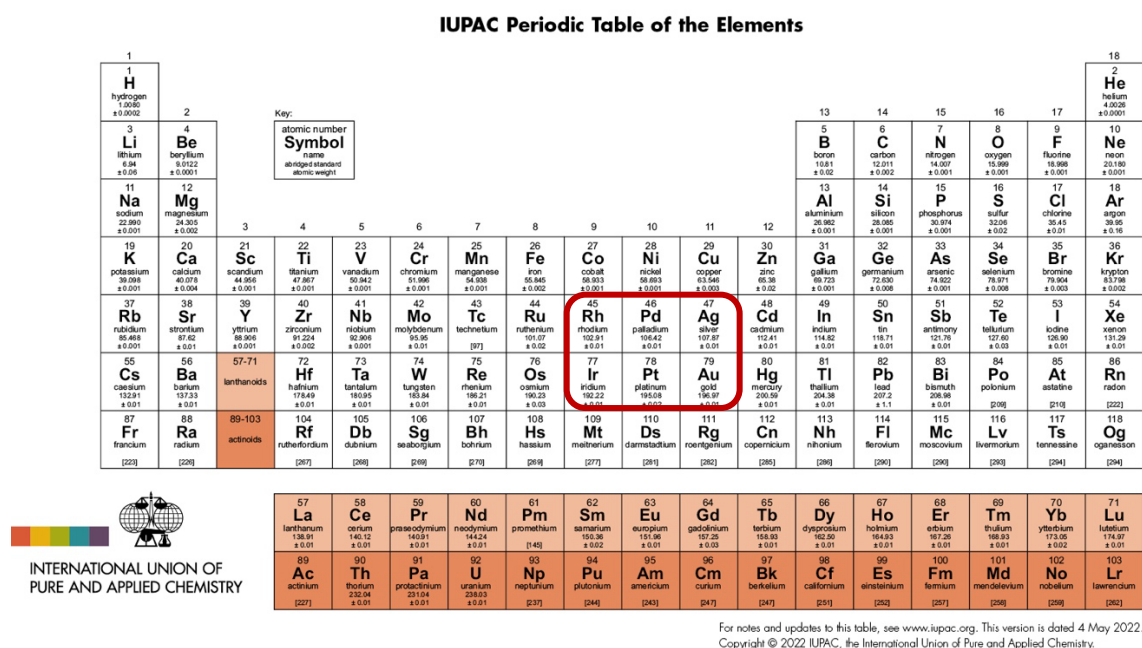
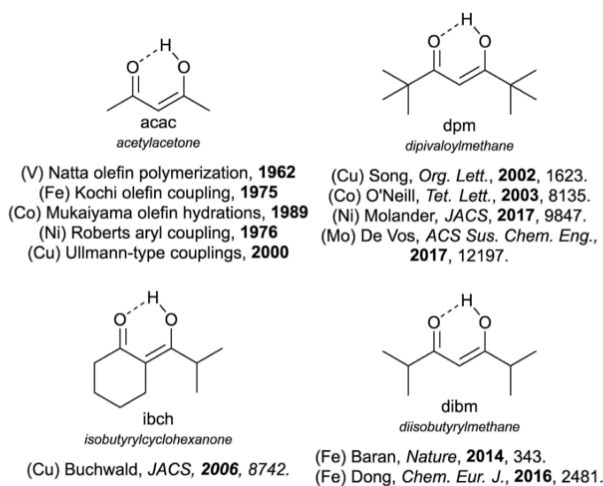


Figure 1 The latest release of the IUPAC Periodic Table (dated 4 May 2022)

## 1.2. $\beta$ -Diketones ligands and base metals

According to Goldschmidt, the base metals are distinguished by their tendency to bond with oxygen or sulfur, and so to form a slag that cooled and became the Earth's crust.  $\beta$ -Diketones, as bidentate ligands through two oxygen atoms, are well suited to coordinating these elements such as copper, lead, nickel, zinc, tin, aluminum. Metal acetylacetonates have been used in catalysis for almost a century, in a variety of important bond forming reactions (**Figure 2**) [12].



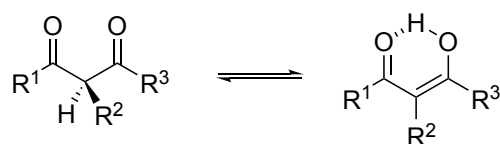
**Figure 2** Some examples of acetylacetonates used in catalysis

Classical  $\beta$ -diketones and related ligands have been studied for more than a century and their ability to give rise to a rich and interesting coordination chemistry is well documented [13]. They act under appropriate conditions as uninegative chelating  $\kappa^2$ -O,O donors, capable of stabilizing mononuclear or polynuclear complexes. Their keto-enol tautomerism was studied in solution by IR and NMR spectroscopy and in the solid state by X-ray single crystal diffraction [14-17].

Even though  $\beta$ -diketones represent one of the oldest classes of chelating ligands, their coordination chemistry continues to attract much interest, due to recent industrial applications of several of their metal derivatives. Many papers have appeared on new functionalized  $\beta$ -diketone ligands, and on the potential applications of their metal derivatives in new fields of technology. However, well-known  $\beta$ -diketones, such as acacH (acacH = 2,4-pentanedione), bzacH (bzacH = 1-phenyl-1,3-butanedione), dbzmH (dbzmH = 1,3-diphenyl-1,3-propanedione), tmhdH (tmhdH = 2,2,6,6-tetramethyl-3,5-heptanedione), tfacH (tfacH = 1,1,1-trifluoro-2,4-pentanedione) and hfacH (hfacH = 1,1,1,5,5,5-hexafluoro-2,4-pentanedione), also continue to play a key role as ligands of choice in the stabilization of otherwise unstable metallic or organometallic derivatives, or in the modulation of particular structural and/or physico-chemical properties of their metal complexes [13].

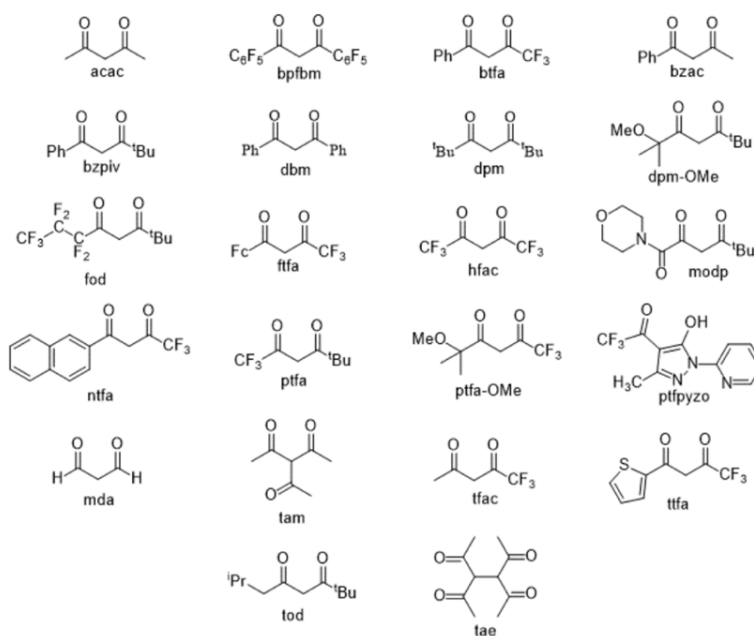
### 1.2.1. Structure and tautomerism

$\beta$ -Diketones exist as an equilibrium mixture of keto and enol tautomeric forms. Generally, the enol tautomer is more stable than the keto tautomer, due to intramolecular H-bonding and simultaneous conjugation [15] (**Scheme 1**).



*Scheme 1 Tautomerism in  $\beta$ -diketones*

Replacement of electron-withdrawing groups in  $R^1$ ,  $R^2$  and/or  $R^3$  shifts the equilibrium in favor of the enolic form. The reverse happens with electron-releasing substituents. The enolic form is favored in non-polar solvents [18]. Substitutions at the carbon atoms in the chelate ring modify the steric and electronic profile of the ligand, in turn affecting coordination properties and chemistry. Common modifications include the use of fluorinated, bulky, and/or conjugated side groups (**Figure 3**).



*Figure 3 Structures of commonly used  $\beta$ -diketones*

The enolic tautomer of  $\beta$ -diketones has served as a model for intramolecular hydrogen bonding for over a century. The oxygen-bridging proton has been described as both a “resonance assisted hydrogen bond” on the basis of crystallographic data [19, 20], and conversely as “intramolecular hydrogen bonding” on the basis of NMR data [21]. This enolic hydrogen can be replaced with a metal atom by sufficiently strong bases or Lewis acidic metals.  $\beta$ -Diketones form six-membered heterocycles with cations having at least two open coordination sites, usually metals but also some non-metals such as for example boron. The bidentate ligands exhibit the “chelate effect”, where the coordination is more effective than equivalent monodentate ligands because their dissociation is a multi-step process [22].

### 1.2.3. Spectrochemical versus nephelauxetic series

Acetylacetonate and other  $\beta$ -diketonates fall among water and hydroxide in the spectrochemical series [23], due to the electronegativity of oxygen.

#### Spectrochemical Series

Halides  $< \text{C}_2\text{O}_4^{2-} < \text{H}_2\text{O}/\text{acac} < \text{NCS}^- < \text{CH}_3\text{CN} < \text{NH}_3 < \text{en} < \text{bpy} < \text{phen} < \text{NO}_2^- < \text{PPh}_3 < \text{CN}^- < \text{CO}$

#### Nephelauxetic Series

$\text{F}^- < \text{H}_2\text{O} < \text{NH}_3 < \text{en} < \text{NCS}^- < \text{Cl}^- < \text{CN}^-/\text{acac} < \text{Br}^- < \text{N}_3^- < \text{I}^-$

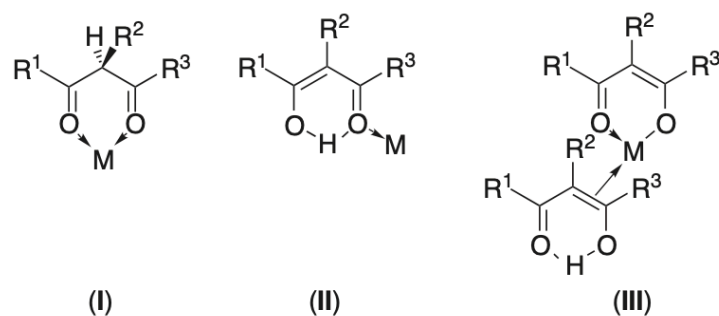
The  $\text{sp}^2$ -hybridized oxygen donor atoms occupy orbitals rather low in energy and are thus poorly de-stabilizing of the  $e_g$  orbitals on the metal. As a result of this weak splitting the  $t_{2g}$  and  $e_g$  orbitals,  $\beta$ -diketonates promote high-spin electronic configurations. On the other hand,  $\beta$ -diketonates show a “back-bonding” capability that results in an attenuation of the electrostatic repulsion, describing the inter-electron repulsion at the metal center [23]. This parameter has been used to generate the nephelauxetic series, approximating the strength of orbital overlap in the metal-chelate bonds. This effect is more pronounced for ligands with low energy  $\sigma^*$  or  $\pi^*$  orbitals which can interact with the occupied d-orbitals. This reciprocity of electrons could be construed as a covalent  $\pi$  interaction and gives rise to molecular-like solubility and volatility, intra-ligand redox communication [24], and efficient metal-ligand energy exchange [25], to name a few properties.

## 1.3. Coordination modes

A wide variety of metal  $\beta$ -diketonates have been crystallographically authenticated, and several reviews in the second half of the twentieth century have been devoted to furnishing a more comprehensive picture of the possible coordination modes of  $\beta$ -diketonates [13, 26-30]. These modes can be classified into three principal classes, including diketonates in the neutral form and diketonates in the mono- and dianionic forms.

### 1.3.1. Neutral $\beta$ -diketonates

This type includes the common examples of the O,O-bidentate ( $\kappa^2$ -O,O) keto form (**Figure 4 I**) and less common O-monodentate enol form (**Figure 4 II**) and  $\eta^2$ -C<sub>2</sub>-bonded enol form (**Figure 4 III**).



*Figure 4 Structures of different forms of neutral  $\beta$ -diketones*

### 1.3.2. Monoanionic $\beta$ -diketonates

A part from the well-known classical O,O-bidentate chelates (**Figure 5 IV**), there are examples where one (**Figure 5 V**) or both oxygen atoms (**Figure 5 VI**) coordinate to other metal centers through a second lone pair. A diketonate ligand can bridge two metal atoms in the O,O-bidentate form (**Figure 5 VII**), or coordinate in a O-monodentate cis- (**Figure 5 VIII**) or trans-mode (**Figure 5 IX**). Other known binding modes of monoanionic diketonates are those involving a carbon atom bonded to a “soft” metal, as in the C-monodentate keto form (**Figure 5 X**), in bridging C,O,O-tridentate keto form (**Figure 5 XI**), the  $\eta^3$ -C<sub>3</sub>-allylic fashion (**Figure 5 XII**), the terminal C-monodentate keto form (**Figure 5 XIII**), and the corresponding enol form (**Figure 5 XIV**). More recently, in the case of the heavier alkaline-earth metal derivatives, four additional coordination modes of monoanionic diketonates have been formally identified [28, 29]. Among them the most common is  $\eta^2$ - $\eta^2$ -O,O-bis-chelate/ $\mu^2$ - $\mu^2$ -bridging form (**Figure 5 XV**), but also the  $\eta^2$ - $\eta^2$ -O,O-bis-chelate/ $\mu^2$ - $\mu^3$ -bridging form (**Figure 5 XVI**), the  $\eta^2$ -O,O-monochelating/ $\mu^2$ - $\mu^3$ -triple-bridging form (**Figure 5 XVII**), and finally the  $\mu^2$ -O,O-monochelating/ $\mu^3$ -triple-bridging form (**Figure 5 XVIII**) have been observed.

However, these modes serve only to represent geometrical dispositions of  $\beta$ -diketonate ligands in the crystal lattice of Sr and Ba complexes, where M-O character is considered almost completely ionic. This explains the large coordination numbers of the metal, the marked deviations from planarity of the chelating ring, and the wide variation in M-O distances.

The NMR method of isotopic perturbation of equilibrium could be used in order to clarify the controversial nature of the  $\beta$ -diketonates as O,O-chelating symmetrical or not-symmetrical donor ligands in solution. A study successfully applied to the simplest dicarbonyl compounds, malonaldehyde and 2-phenylmalonaldehyde, showed the intrinsic asymmetric nature of several metal complexes containing these donor ligands even though, on the basis of NMR evidence, they appear to be symmetric chelates [31].

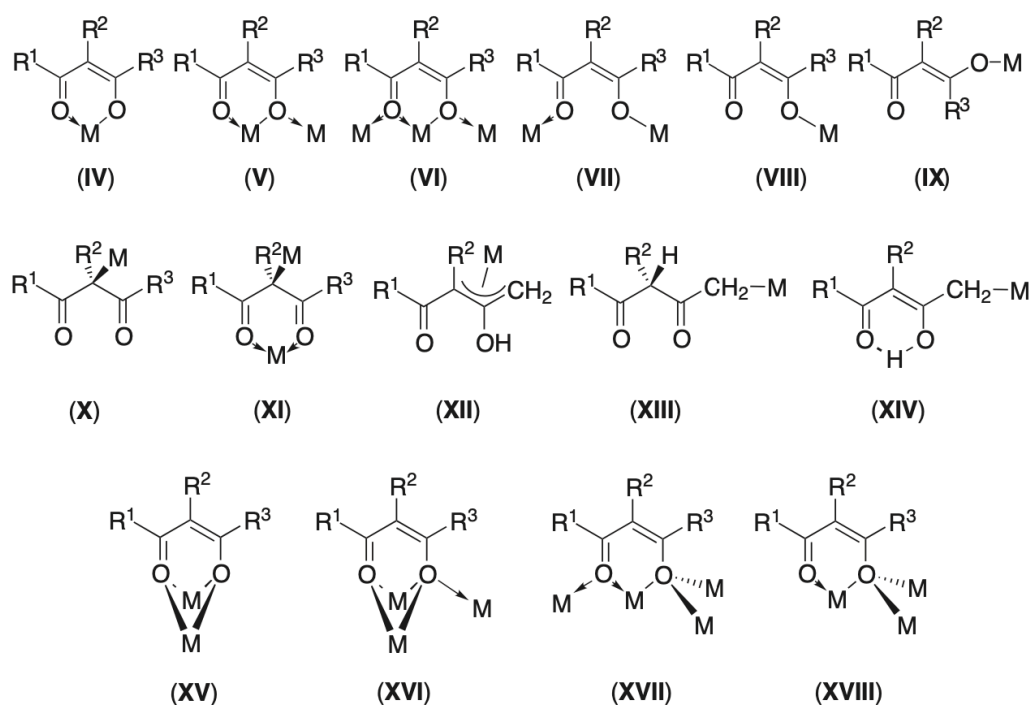


Figure 5 Structures of different forms of monoanionic  $\beta$ -diketonates

### 1.3.3. Dianionic $\beta$ -diketonates

Interesting coordination modes have been discovered in derivatives containing Pd and Pt metal ions or nonmetallic elements, where extra negative charge of the  $(\beta\text{-diketonate})^{2-}$  arises from removal of one of the methyl protons. In **Figure 6 XIX** the  $(\beta\text{-diketonate})^{2-}$  is  $\eta^3\text{-C}_3$ -tridentate to Pd through C<sub>1</sub>, C<sub>2</sub>, and C<sub>3</sub>, in an allylic fashion, whereas in **Figure 6 XX** the donor is additionally O,O-bidentate chelating toward another metal. In **Figure 6 XXI** the  $(\beta\text{-diketonate})^{2-}$  is C,O-bonded to Pt, and in **Figure 6 XXII** is O,O-bonded to a metal and C-bonded to another metal via a terminal  $-\text{CH}_2$ .

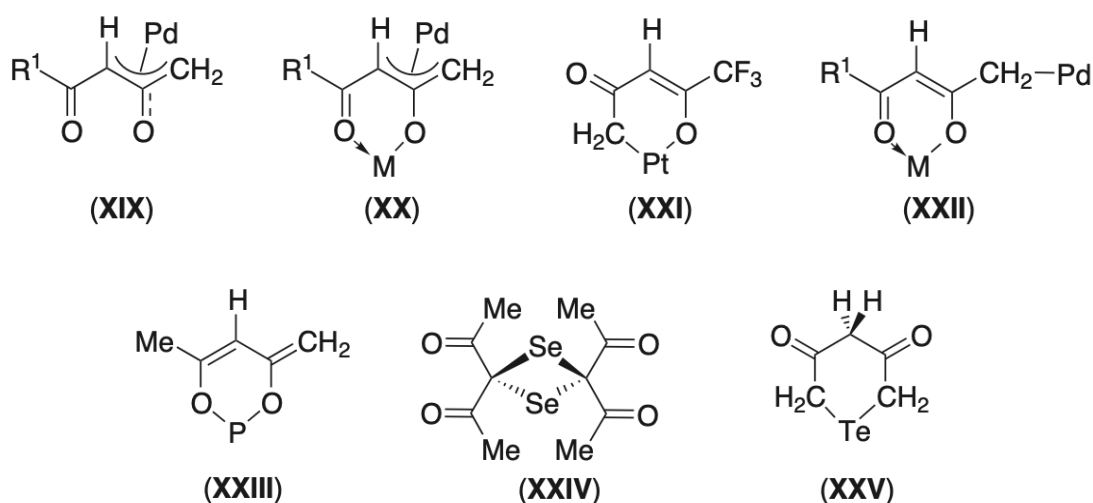
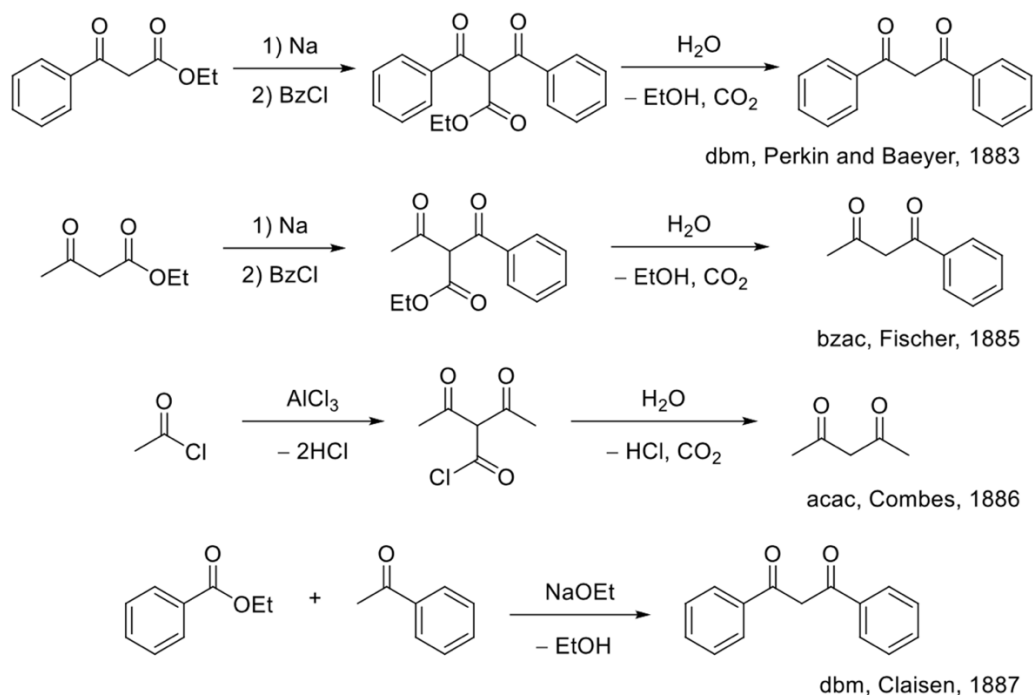


Figure 6 Structures of different forms of dianionic  $\beta$ -diketonates

## 1.4. Historical context

In 1883, Baeyer and Perkin prepared the first  $\beta$ -diketone, dibenzoylmethane (dbm), by acylation of ethyl benzoylacetate followed by decarboxylation in boiling water (**Scheme 2**).

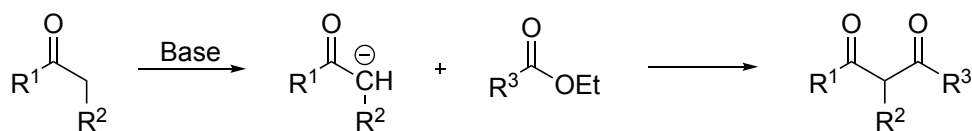


**Scheme 2** Synthesis of the three original  $\beta$ -diketones by Fischer, Combes, and Claisen

A similar synthesis of benzoylacetone was reported by Fischer in 1885, and the synthesis of acetylacetone was accomplished by Combes in 1886 by trimerization of acetyl chloride. A more direct and general procedure for the preparation of  $\beta$ -diketones was subsequently developed by Claisen in 1887. Combes described many metal acetylacetonate salts the same year, including Na, K, Mg, Al, Fe, Cu, and Pb. These preparations were contemporaneous with Werner's formulation of coordination theory for metal complexes. During the turn of the 20<sup>th</sup> century, metal diketonate salts were being used to determine and refine atomic weights. By 1914,  $\beta$ -diketonate salts were dissolved in organic solvents to give brightly colored solutions amenable to spectroscopy. In the decades that followed, their catalytic abilities slowly became realized.

## 1.5. Synthesis of $\beta$ -diketones

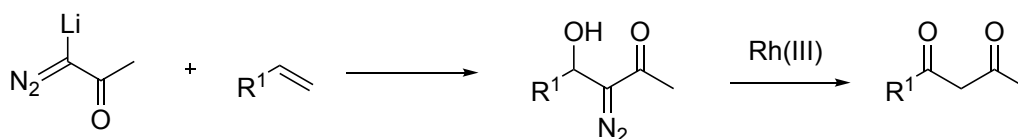
Classical  $\beta$ -diketones can be obtained from the acylation of ketones by esters (Claisen condensation), in the presence of alkali-metal hydroxides, ethoxides, hydrides, or amides as condensing agents, to enhance the relatively low reactivity of the ester carbonyl group [32, 33] (**Scheme 3**).



*Scheme 3 Synthesis of  $\beta$ -diketones by Claisen condensation*

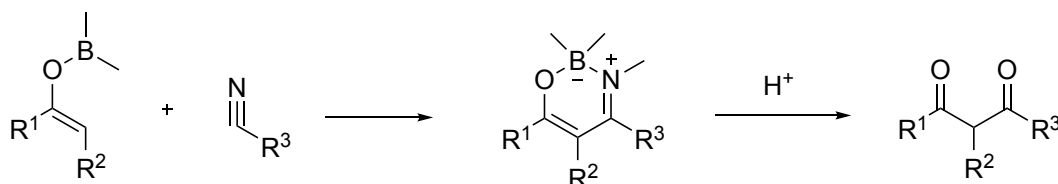
In order to avoid the difficulties which could be encountered with Claisen condensations, such as formation of regioisomers, competing O-acylation, proton exchange between the enolate and the product diketone, and generally poor yields, new synthetic approaches to modified and functionalized  $\beta$ -diketones in  $R^1$ ,  $R^2$ , and/or  $R^3$  positions have been developed.

One of the most significant enhancements has been the successful reaction of 1-diazo-1-lithio- acetone with aldehydes, followed by acid-induced transformation of the  $\alpha$ -diazo- $\beta$ -hydroxyketone thus formed into the corresponding  $\beta$ -diketone with a number of  $R^1$  groups, in the presence of  $Rh^{II}$  acetate as catalyst (**Scheme 4**).



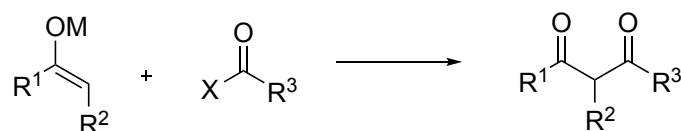
*Scheme 4 Synthesis of  $\beta$ -diketones using 1-diazo-1-lithio-acetone as starting material*

A regioselective synthesis of unsymmetrical  $\beta$ -diketones is achieved by cycloaddition of nitriles to enol boranes, giving the corresponding boroxazines that readily hydrolyze in acid conditions to  $\beta$ -diketones (**Scheme 5**).



*Scheme 5 Regioselective synthesis of unsymmetrical  $\beta$ -diketones*

Other versatile syntheses are based on C-acylation of metal (Li or Cu) enolates by acyl cyanides or chlorides (**Scheme 6**):

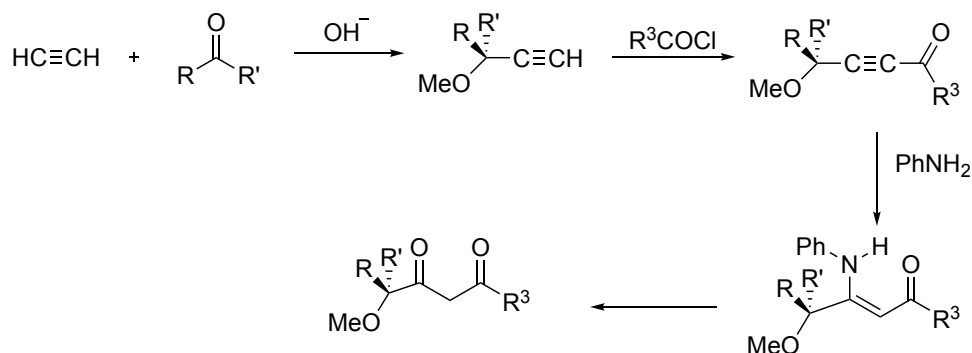


M= Li or Cu  
X= CN or Cl

*Scheme 6 Synthesis of  $\beta$ -diketones by C-acylation*

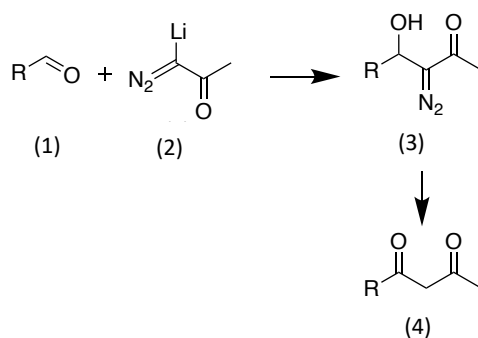


A very useful method leading to highly sterically hindered  $\beta$ -diketones with  $R^1 = \text{CRR}(\text{OMe})$ , employed for the synthesis of alkaline-earth metal-containing molecular precursors for CVD, is based on the condensation of ketones with alkynes, followed by the reaction of the product with acyl chlorides to give  $\alpha$ -acetylinic ketones. Finally, the  $\alpha$ -acetylinic ketones react with amines yielding aminovinylketones and, after hydrolysis, the resulting  $\beta$ -diketones (**Scheme 7**):



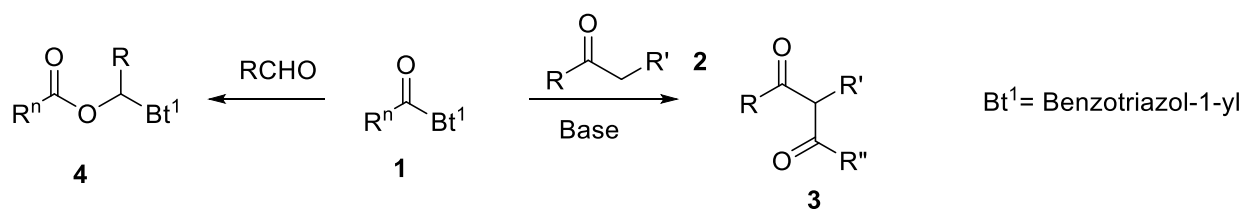
*Scheme 7 Synthesis of sterically hindered  $\beta$ -diketones*

One of the first improvement, consisted of a two steps procedure for the conversion an aldehyde (**Scheme 8 (1)**) with 1-diazo-1-lithioacetone (**Scheme 8 (2)**) followed by the acid-induced transformation of the  $\alpha$ -diazo- $\beta$ -hydroxy-keto-derivative (**Scheme 8 (3)**) into the corresponding  $\beta$ -diketone. The transformation of compound (3) in (4) occurs rapidly upon addition of a catalytic amount of rhodium(II) acetate (**Scheme 8**).



*Scheme 8 Improved method for synthesis of  $\beta$ -diketones with different R groups*

Another important process developed to favour C-acylation instead of O-acylation, consisted of the use of activated methyl ketones such as acylbenzotriazoles (**Scheme 9**). Benzotriazole is a good leaving group [34].



*Scheme 9* A method to favour C-acylation instead of O-acylation in the synthesis of  $\beta$ -diketones

## 1.6. Biological and pharmacological importance of $\beta$ -diketones

The importance of  $\beta$ -diketones in medicinal chemistry derives from the fact that they can be intermediates in the synthesis of COX-2 inhibitors, a type of nonsteroidal anti-inflammatory drugs (NSAIDs). NSAIDs relieve pain and fever and reduce inflammation. COX-2 inhibitors are approved to treat mild-to-moderate pain and inflammation caused by osteoarthritis, rheumatoid arthritis, juvenile arthritis, ankylosing spondylitis, menstrual pain (dysmenorrhea), familial adenomatous polyposis, short-term pain, such as from sports injuries.

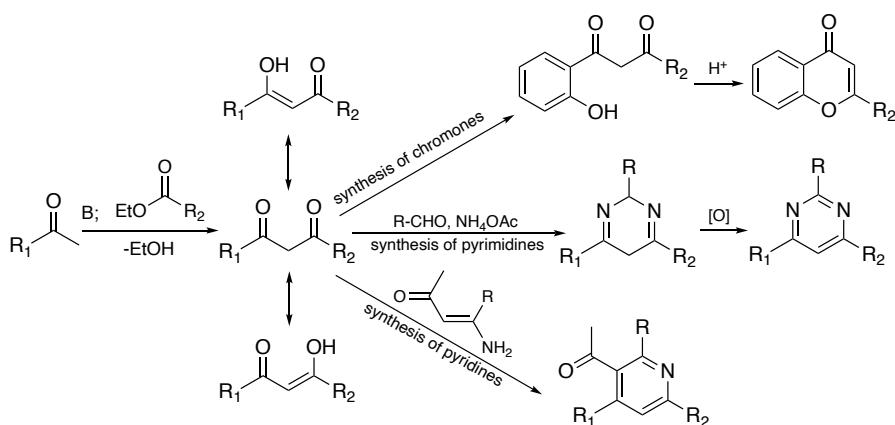
Furthermore,  $\beta$ -diketone moiety can be present in natural products such as curcuminoids, which are known for their antibacterial, neuroprotective and anticancer properties.

The third way, through which it is possible to enhance the pharmacological activity of  $\beta$ -diketones, is the design of coordination compounds (metal-based agents).

### 1.6.1. $\beta$ -diketones as intermediates in organic synthesis

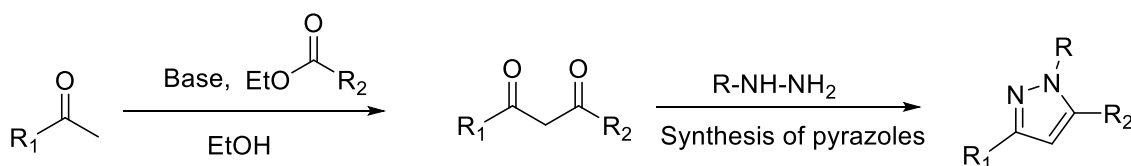
$\beta$ -Diketones represent a very important group of reagents in the synthesis of heterocyclic compounds. In particular, they are highly involved in the synthesis of 6- and 5-membered heterocyclic rings. In **Scheme 10**, some of the main processes which include the use of  $\beta$ -diketones in the design of heterocyclic compounds are reported:

Through the intramolecular cyclization reaction of 2-hydroxyaryl substituted diketones in acidic media, it is possible to obtain chromones. Moreover, pyrimidines can be synthesized by the reaction of a  $\beta$ -diketone with an aryl-aldehyde in the presence of ammonium acetate.



*Scheme 10*  $\beta$ -diketones as intermediates in the design of heterocyclic compounds

One of the most important reactions is the one which occurs between  $\beta$ -diketones and hydrazines, leading to the formation of pyrazole ring system (**Scheme 11**). The relevance of this process is imputed by the fact that it is applied as last step in the synthesis of non-steroidal anti-inflammatory drugs (NSAIDs), such as celecoxib.

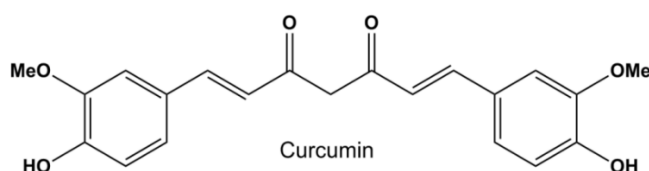


*Scheme 11* Reaction between  $\beta$ -diketone and hydrazine

The mechanism of action of NSAIDs is based on the blockage of cyclooxygenase enzymes (COXs) by sterically hindering the entrance of the physiological binder arachidonic acid. The classical NSAIDs such as aspirin, ibuprofen and flurbiprofen are non-selective and inhibit all the COXs isoforms. The peculiarity of celecoxib, is that is able to inhibit selectively COX-2 isoform.

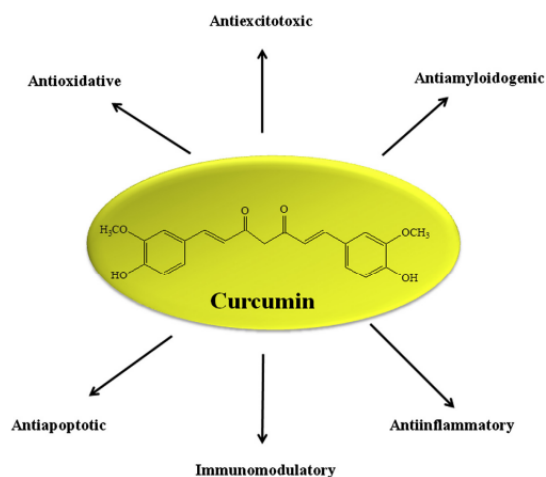
### 1.6.3. $\beta$ -diketones as natural products

The  $\beta$ -diketone moiety is not highly common in nature, but its importance derives by the fact that it is the main feature of a number of naturally occurring compounds such as the curcumins (**Figure 7**).



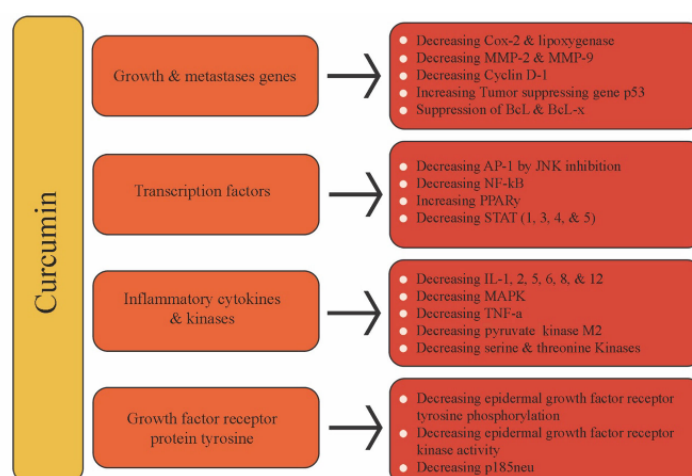
*Figure 7* Structure of curcumin

Curcumin is a low molecular weight (368.37 g/mol) polyphenolic compound with a melting temperature of approximately 183°C. Curcumin has two ferulic acid moieties bound together with an additional carbon (methane) to abridge the carboxyl groups. Curcumin has a seven carbon linker and three major functional groups including an  $\alpha,\beta$ -unsaturated  $\beta$ -diketone moiety and an aromatic O-methoxy-phenolic group. The occurrence of intramolecular hydrogen atoms transfer at the  $\beta$ -diketone chain of curcumin leads to the existence of keto and enol tautomeric conformations in equilibrium. Curcumin possesses a wide range of pharmacological properties (**Figure 8**), including anti-inflammatory, anticancer, antioxidant, wound healing, cardioprotective, antimicrobial, antihypertensive, antihyperlipidemic, antiangiogenic, antidiabetic (hypoglycemic), antipsoriasis, antithrombotic, antihepatotoxic, and analgesic uses [35].



**Figure 8** Biological properties of Curcumin

Concerning the anti-inflammatory properties of curcumin, it has been found that its natural activity is on a par with steroidal drugs and nonsteroidal drugs as indomethacin and phenylbutazone, which have dangerous side effects. Its anti-inflammatory property appears to be mediated through the inhibition of induction of cyclooxygenases, lipoxygenases, nitric oxide synthase and production of cytokines such as interferons and tumor necrosis factor, and activation of transcription factors like NF- $\kappa$ B, and AP-1 [36]. On the other hand, the antioxidant properties and the free-radical scavenging properties derive by the phenolic protons and methylene group of curcumin. Curcumin donates protons to reactive oxygen and nitrogen species and quenches them via electron transfer and H-atom abstraction. As a consequence of that, oxidative damage such as lipid peroxidation is inhibited in brain and tissues, and curcumin may be more effective than vitamin E as a free radical scavenger. Concerning the anticancer effects, curcumin has been shown to prevent carcinogenesis by affecting two processes: angiogenesis and cancer cell growth. It also suppresses cancer cell metastasis and induces cancer cell apoptosis (**Figure 9**) [37].

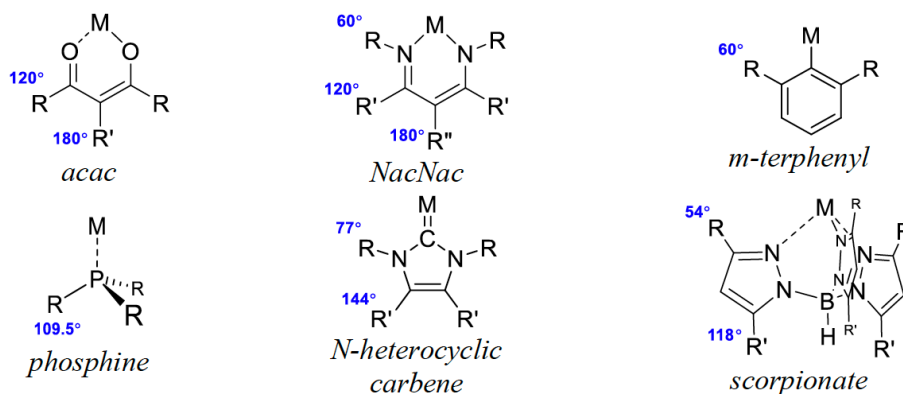


**Figure 9** Pharmacological properties of Curcumin

## 1.7. Hindered $\beta$ -diketonates

Despite being overshadowed by precious metal catalysis since the 1970s [38-40], base metal  $\beta$ -diketonates are experiencing a renaissance in this context as the desired replacement for precious metal catalysts [12, 41, 42]. However, yields of reactions catalyzed by metal acetylacetonates are erratic and vary widely with even minor structural changes to a substrate or ligand [10, 11]. Furthermore, their reaction intermediates are short-lived and non-isolable, and so their reaction mechanisms remain mysterious or contested in many cases [43]. These two problems have impeded the rational development of base metal  $\beta$ -diketonate catalysis.

One strategy that has been successfully used for several ligand classes is the application of steric hindrance to both kinetically frustrate catalytically relevant species for isolation and to better shield catalytically active species from off-cycle reactivity. This paradigm is true for phosphines [44],  $\beta$ -diketimines (NacNacs) [45], N-heterocyclic carbenes (NHCs) [46], tris(pyrazolyl)borates (scorpionates) [47, 48], and meta-terphenyls [32] and related ligands (e.g., isocyanates, carboxylates) (**Figure 10**).

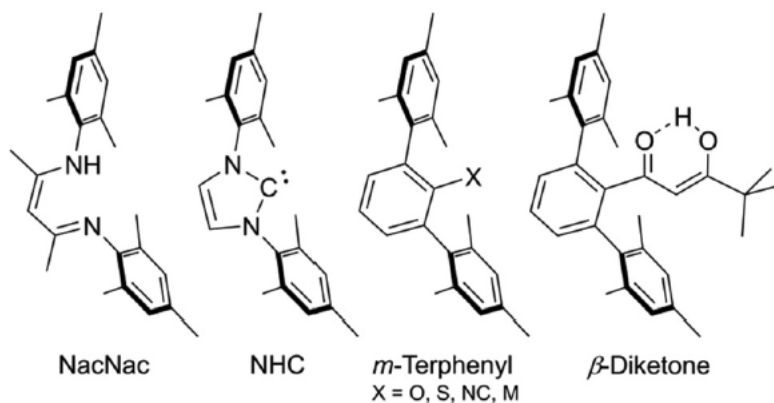


**Figure 10** Generalized structures of acac and other supporting ligands, with approximate angles between the metal-ligand axis and the sterically encumbering group

However, there has not been a study of a  $\beta$ -diketonate more sterically hindered than dipivaloylmethane (dpm) in the last half-century. One reason for this is the lack of sterically hindered  $\beta$ -diketonates, a challenge considering chelate ring substituents are directed away from the metal center. A subsequent problem is the limited steric scope of Claisen condensations, the standard reaction for preparing  $\beta$ -diketones [13]. A similar challenge among phosphines was addressed by inclusion of sterically hindering ortho-biphenyl groups, which showed a tendency for mono-chelation and dramatically improved reaction rates, yields, and substrate scopes [44].

The development of sterically hindered ligands, such as phosphanes and N-heterocyclic carbenes, was a marked improvement for the precious metal systems, imparting robust and often enantioselective reactivity to the active catalyst [8]. A common motif has become apparent for affording steric protection to reactive metal centers and isolating low-coordinate, highly-reactive species [12] (**Figure 11**).

However, the ligand frameworks which have been optimized for second- and third-row metals are often inadequate to the task of taming their first-row congeners [10]. The  $\beta$ -diketonates provide an exceptionally weak field, ionic interaction with the metal ion, offering a very different electronic environment in comparison with strong-field ligand platforms [23]. While at the same time, the ligand framework is  $\pi$ -acidic and has been described as pseudo-aromatic, speaking to the efficacy of its interaction with ligated metals [49].



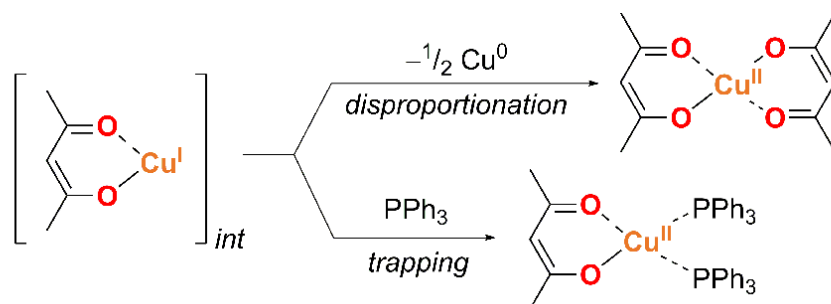
**Figure 11** The hindered  $\beta$ -diketone ligand, *esac* (far right), next to other popular ligand frameworks, including *NacNacs*, *NHCs*, and *m-terphenyls*

Reactions continue to be discovered using base metal  $\beta$ -diketonates, and it is often noted that even modestly sterically hindered ligands offer improvements over the parent acetylacetonate [50]. The hindered ligands identified often feature tert-butyl or iso-propyl substituents, which remain the most common “hindered” ligands due to synthetic limitations of the Claisen condensation [51]. Consequently, mechanisms involving base metal  $\beta$ -diketonates remain poorly understood, inhibiting further improvement (e.g., reducing the high catalyst loadings - 10 mol% vs. ppm/ppb levels for precious metals) [43, 52, 53].

The addition of steric bulk to ancillary ligands is a common approach to improving catalyst activity and selectivity, which has yet to be applied to  $\beta$ -diketonates. Previous efforts using dipivaloylmethane (DPM) and similarly sized ligands were effective in preventing the oligomerization observed in the crystal and solution phases, but left the coordination chemistry essentially unchanged. DPM obviates the first step in the pre-catalyst activation sequence and offers slightly more steric shielding of the reactive species, while leaving the manifold reactivity problem unsolved. Truly hindered  $\beta$ -diketonates have only recently been made synthetically accessible, and their coordination and catalytic support is of high interest [13].

Copper  $\beta$ -diketonates catalyze Ullmann-type coupling reactions to form C-X bonds (X = C, N, O, S, P) [42, 54]. Cu(I) is often implicated in these catalytic mechanisms, but undergoes disproportionation to Cu and Cu(II) in the absence of strong-field supporting ligands such as phosphines [55-59] (**Figure 12**). Although these represent general, base-metal-catalyzed transformations, mechanistic aspects remain poorly understood, garnering much

research effort [60]. The development of such base-metal catalysts is an important research goal for the chemical industry [10, 11].



**Figure 12** Disproportionation and trapping of copper(I)  $\beta$ -diketonates

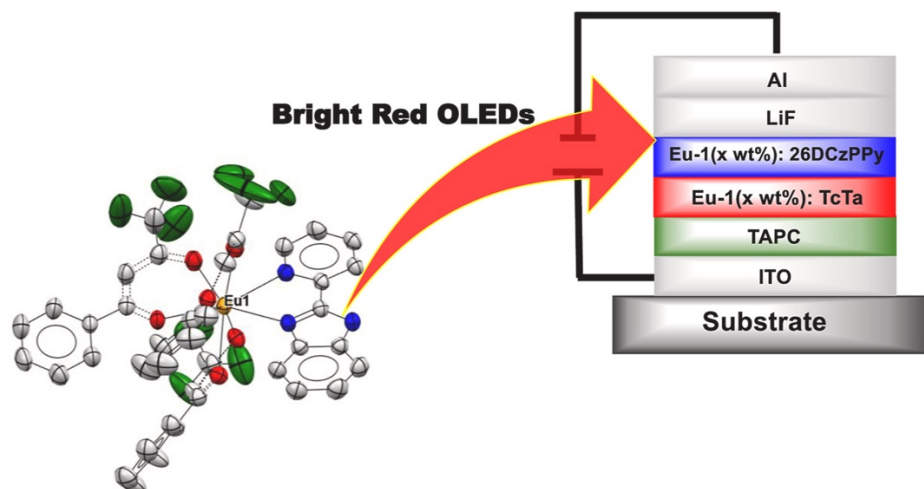
One common approach to inhibiting bimolecular reactions such as disproportionation involves the use of sterically bulky ancillary ligands to protect the reactive catalytic intermediates. For example,  $\beta$ -diketimines (i.e., NacNac ligands) have been used to stabilize Cu(I) intermediates for further reactivity studies [61]. Unfortunately, direct heteroatom substitution is infeasible with  $\beta$ -diketonates. Over the past few decades, *m*-terphenyls have emerged as popular functional groups for ancillary ligands because of their ability to direct steric bulk back toward a metal center [32].

The use of an *m*-terphenyl-functionalized  $\beta$ -diketone prevented the formation of the more stable tris( $\beta$ -diketonate) metal complexes among the early and late metals of the first transition series [12, 62].

## 1.8. Main fields of research on technological applications of metal $\beta$ -diketonates

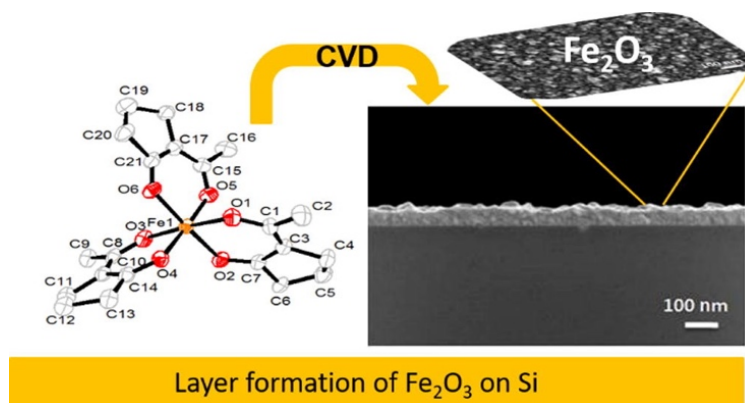
There is a growing amount of literature which especially deals with the possible applications of these complexes as components of molecular devices or as precursors in the formation of new materials. Several research groups recognized the potential of  $\beta$ -diketonates as extracting and complexing agents for the spectrophotometric determination of metal ions in dilute solutions, and for chromatographic separations. Phosphors for lighting and high efficiency electroluminescent devices for light-emitting diodes (lanthanide  $\beta$ -diketonates such as the trivalent europium(III) complexes in **Figure 13**), contrast agents for medical magnetic resonance imaging, NMR shift reagents, transport carriers of alkali metal ions across biological membranes, luminescent probes for proteins and amino acids, light-emitting sensors in fluoroimmunoassays, tags for time-resolved luminescent microscopy, magnetically addressable liquid crystals, magnetic alloys for refrigeration, superconducting materials, specific redox reagents for chemical transformation or molecular-based information, acid catalysts for sophisticated organic transformations or for the cleavage of phosphodiester bridges in RNA, fully justify the

efforts made to control the metallic sites and to selectively introduce specific metal ions into organized assemblies [63].



**Figure 13** Trivalent Eu(III) complexes with anionic  $\beta$ -diketonates showing pure red emission [64]

Cu(I) and Cu(II)  $\beta$ -diketonate adducts with ancillary Lewis bases are promising precursors for microelectronic devices and, in conjunction with alkaline-earth metal  $\beta$ -diketonates, for the generation of new, high-temperature superconducting mixed metal oxides [28, 29]. Many metal  $\beta$ -diketonates have been investigated as molecular precursors for the supercritical fluid transport (SFT) CVD technique as shown in a recent work with Fe(III)  $\beta$ -diketonates complexes (**Figure 14**) [64].

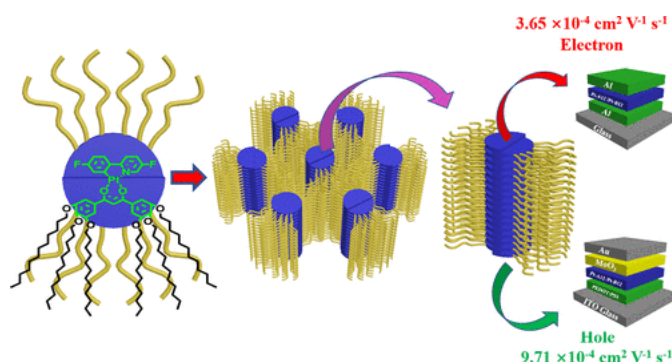


**Figure 14** Iron(III)  $\beta$ -diketonates: CVD precursors for iron oxide film formation [66]

After the serendipitous discovery of the antitumor properties of cisplatin (cis-diaminedichloro-platinum), much effort has been devoted to finding other anticancer metal agents, and several Sn, Ti, Zr, and Hf  $\beta$ -diketonates have been proven to possess interesting biological activity [65]. For example, budotitane ((EtO)<sub>2</sub>Ti(bzac)<sub>2</sub>) was the first non-Pt metal complex to reach clinical trials as a potential anticancer agent [66].



Another primary field of interest is the potential application of metal  $\beta$ -diketonates as liquid crystal phases; because of their special magnetic and electronic properties, these metal-containing materials are generally known as “metallomesogens” (**Figure 15**). Most literature in this field is devoted to the  $\beta$ -diketonates of Rh(I), Ir(I), Ni(II), Pd(I), Pt(II), and Cu(II), which have a linear or planar geometry and therefore mimic conventional organic calamitic or discotic liquid crystals [67]. Recently some lanthanide  $\beta$ -diketonate adducts, containing particular Lewis bases, were proven to exhibit interesting mesomorphic properties [68]. Transition- and lanthanide-metal derivatives also display interesting catalytic features, where the  $\beta$ -diketonates are important spectator donors for metal-intermediate species involved in several important organic reactions [69].



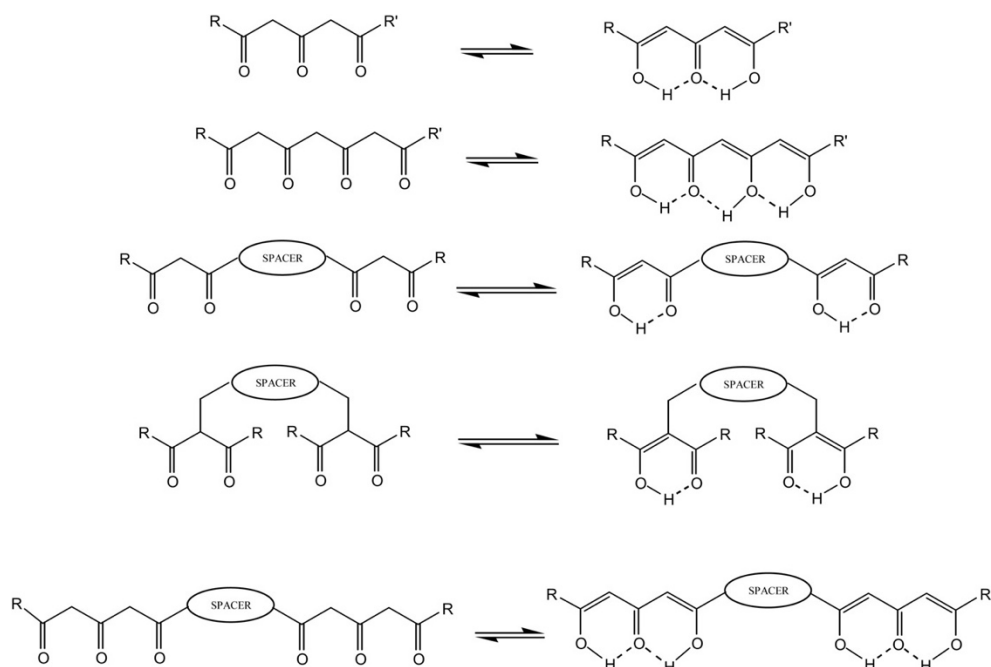
**Figure 15** Cyclometalated Platinum(II) metallomesogens based on half-disc-shaped  $\beta$ -diketonate ligands with hexacatenar [72].

The photophysical characterization both in solution and in the solid state of complexes and polymers containing d- and/or 4f- metal ions is relevant in determining the complexes with the best performance for their successful application as emitting layers in light-emitting diodes for display applications. However, the architecture of the device is also of major importance, to allow for good charge transport and recombination and thus obtain pure colours and high emission quantum efficiency. The usually broad emission from organic molecules and transition metal complexes, which occurs either from singlet or from LMCT states, requires the use of filters to obtain monochromatic colors. Further, tuning of device parameters can lead to changes in colour. Organometallic iridium(III) and lanthanide(III) phosphorescent compounds have been widely studied and applied as emitters in high efficient organic light-emitting diodes [70].

Considerable interest has been recently shown in the preparation and photophysical characterisation of heterometallic d, f-complexes, in which the strong absorption of light by MLCT transitions associated with d-block fragments, typically ruthenium(II), osmium(II), rhenium (I) or platinum(II) is used to sensitise luminescence from lanthanide(III) ions with low-energy f–f excited states. This allows near-infrared emission from lanthanide(III) ions to be generated by energy-transfer from the strongly-absorbing d-block antenna group. In the lanthanide(III) ions the emission comes from f–f transitions. Due to the core nature of the 4f electrons, which are shielded from the coordination environment by the  $5s^25p^6$  electrons, little vibrational coupling with the

environment is seen, and the emission bands are narrow and ion-specific, leading to pure colours and potentially high emission efficiencies [63].

The fields of application of the emitting lanthanide(III) complexes depend on the emission wavelength. Ions with transitions in the visible range of the spectrum are utilized for television screens and LEDs, in liquid crystals, as well as in fluoroimmunoassays and in biophysical applications. The ions which emit in the near-IR have found application in lasers and could also be useful for telecommunications and optical amplifiers. Although these complexes were successfully utilized as emitting layers in LEDs, it is more efficient to incorporate the organometallic or coordination complexes into polymers, which can additionally function as charge-transport layers to facilitate the formation and confinement of excitons. More recently, efforts were started in the utilization of polymers with covalently attached emitting complexes, to avoid phase separation during operation and consequent loss of the emitting layer. In addition, polymers have the advantage of displaying higher flexibility and mechanical stability, as well as ease in processability and device integration [71, 72].



**Scheme 12** Poly- $\beta$ -diketones with or without a spacer and their keto-enol tautomerism

The functionalization of metal  $\beta$ -diketonates complexes at the periphery of the coordination moiety or their grafting on suitable platforms gives rise to supramolecular structures capable of originating organized systems with peculiar chemical and/or physical properties. Thus, the insertion of additional donor atoms at the periphery of the chelating moiety gives rise to a series of quite interesting self-organizing systems, containing similar or dissimilar metal ions, which form planar or tridimensional metal organic frameworks with defined porosity. Furthermore, the increasing of carbonyl groups with the consequent formation of tri- or tetra-ketones and bis- $\beta$ -diketones or bis- $\beta$ -triketones (**Scheme 12**) allowed for the formation of well-defined homo- and/or heteropolynuclear complexes with peculiar physico-chemical properties, arising from the coordination of equal or different metal ions, in close connection and interacting with each other through the carbonyl bridges [63].

Moreover, these ligands generally coordinate in the equatorial plane of metal ions as copper(II), nickel(II), cobalt(II), giving rise to quite flat complexes which can contain coordinating solvents or monodentate ligands in the axial positions. These axial ligands can be exchanged by stronger coordinating ligands which, when potentially bridging linkers as 4,4'-bipyridine, pyrazine, 4,4'-trans-azopyridine, 2,2'-dipyridylamine, 1,4-diazabicyclo[2,2,2]octane, 4,4'-dipyridyl sulfide, 2,2'-bipyrimidine, self-organize into oligo- or polymeric-species with quite sophisticated architectures and new functionalities and properties [63].

In the field of nanoscale materials,  $\beta$ -diketonate ligands play an important role as assembly agents in the preparation of high-spin molecules. For example, Fe(III) and Mn(III) clusters containing  $\beta$ -diketonate donors have shown interesting magnetic anisotropic behavior, also being able to entrap alkaline ions [73].

## 1.9 Oligo- $\beta$ -diketones as versatile ligands for use in metallo-supramolecular chemistry

Over more recent years, "classical"  $\beta$ -diketone motifs have been widely incorporated into larger organic entities as metal-binding domains for use in constructing a wide range of metallo-supramolecular structures [17]. The presence of such motifs in extended ligand systems offers potential advantages when used to construct metallo-supramolecular structures. First, the ability of a  $\beta$ -diketone fragment to lose a proton on metal complexation gives the possibility of forming neutral supramolecular constructs, thus avoiding additional complexity arising from the presence of a counter ion or counter ions. Secondly, the conjugation and relative rigidity of the  $\beta$ -diketone fragments reduces the degrees of freedom in an expanded ligand system and hence tends to enhance design predictability, both with respect to the mode of metal coordination as well as to the overall architecture adopted by the assembly [63].

## 1.10. Diketones with substituents containing additional donor atoms

Ligand design is a critical step in synthesizing new and extended inorganic or organometallic structures. Many efforts were made in the last decades of the twentieth century to modify the electronic and steric properties of  $\beta$ -diketones by inserting different  $R^1$ ,  $R^2$ , and  $R^3$  substituents, which can also contain additional donor atoms, in order to prepare polyfunctional coordinating ligands as "biomimetic" agents with higher complexity and functionality (Figure 16).

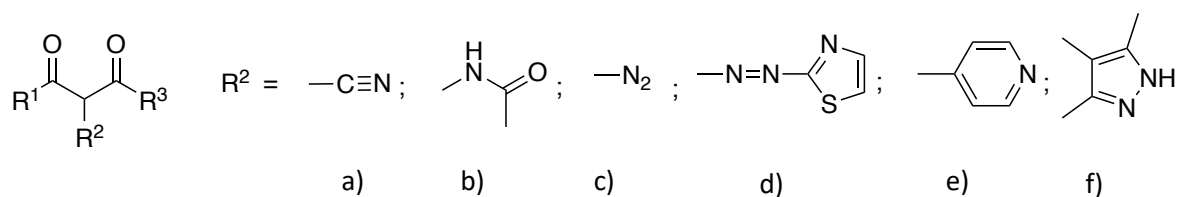


Figure 16  $\beta$ -diketones with different types of  $R^2$  substituents

The 2-cyano-1,3-diketones (**Figure 16a**) have been shown to form simple Co(II) and Cu(II) chelates stabilized by intermolecular contacts through the -CN group [74, 75] and, in the presence of dipyridylamine, a mixed-ligand binuclear Cu(II) complex with different coordination numbers and conformation in the two copper environments [76]. A new advantageous synthesis of these ligands from bis(benzotriazol-1-yl)methylimine as cyanating agent is also reported [77].

The 3-acetylamido-pentane-2,4-dione (amacH) (**Figure 16b**) is a highly enolized and acidic substance which is very soluble in water. It was first reported to form a Cu(II) complex  $[Cu(amac)_2]$  by Cotton [78], and has been used to study the kinetics of the mono complex  $M(amac)_x$  formation in aqueous solution [79]. The chemistry of the analogous 3-(hydroxyimino)-pentane-2,4-dione has also been explored [80].

The 2-diazo-1,3-diketones (**Figure 16c**) react with titanocene precursors affording 1-titana-2,n-dihetero-cyclic complexes [81]. 2-(2-thiazolylazo)-1,3-diketones (**Figure 16d**) and their corresponding metal derivatives have also been synthesized [82].

The 3-(4-pyridyl)pentane-2,4-dione(3-pyacacH) (**Figure 16e**) interacts with Cu(II) affording  $[Cu(3-pyacac)_2] \cdot 2.5H_2O \cdot 0.5thf$ , where the pyridyl fragment, aligned approximately perpendicularly to the rest of the derivative, binds a second Cu atom of another molecular unit, thus producing antiferromagnetic interactions at low temperature [83]. A donor with a pyrazolyl moiety as the R<sup>2</sup> substituent (3-pzacac) (**Figure 16f**) produced a  $[Be(3-pzacac)_2]$  complex with a supramolecular extended helical array [84].

## 2. EXPERIMENTAL SECTION

### 2.1. Methods and materials

All reagents used for the synthesis of ligands and complexes were purchased from Sigma-Aldrich and used without further purification. Elemental analyses (C, H, N, S) were performed with a Fisons Instruments EA-1108 CHNS-O Elemental Analyzer (Thermo Scientific). Melting points (M.P.) were taken on an SMP3 Stuart Scientific Instrument. FT-IR spectra were recorded from 4000 to 400  $\text{cm}^{-1}$  on a Perkin Elmer Frontier FT-IR instrument, equipped with single reflection ATR (Attenuated Total Reflection) unit (universal diamond ATR top-plate) as a sample support. IR annotations used: m = medium, mbr = medium broad, s = strong, sbr = strong broad, sh = shoulder, vs = very strong, vsbr = very strong broad, w = weak, wbr = weak broad.  $^1\text{H}$ - and  $^{31}\text{P}$ -NMR spectra were recorded with a 500 Bruker Ascend (500.1 MHz for  $^1\text{H}$  and 202,4 MHz for  $^{31}\text{P}$ ). Referencing is relative to TMS ( $^1\text{H}$ ) and 85%  $\text{H}_3\text{PO}_4$  ( $^{31}\text{P}$ ). NMR annotations used: br = broad, d = doublet, dbr = doublet broad, dd = doublet of doublet, m = multiplet, s = singlet, sbr = singlet broad, t = triplet, sept = septet, vbr = very broad. ElectroSpray Ionization Mass Spectra (ESI-MS) were obtained in positive- or negative-ion mode on a Series 1100 MSD detector HP spectrometer, using a methanol or acetonitrile mobile phases. The compounds were added to reagent grade methanol or acetonitrile to give approximately 0.1 mM solutions, injected (1  $\mu\text{L}$ ) into the spectrometer via a HPLC HP 1090 Series II fitted with an autosampler, at a flow rate of 300  $\mu\text{L}/\text{min}$ , employing nitrogen both as drying and nebulizing gas. Capillary voltages were typically 4000 V and 3500 V for the positive- and negative-ion mode, respectively. Confirmation of all major species in this ESI-MS study was aided by comparison of the observed and predicted isotope distribution patterns, the latter calculated using the IsoPro 3.1 computer program.

#### 2.1.1 Crystallographic Data Collection and Refinement

Suitable crystals of complexes **7**, **8**, **14** and **15** covered with a layer of hydrocarbon/Paratone-N oil were selected and mounted on a Cryo-loop and immediately placed in the low temperature nitrogen stream. X-ray intensity data were measured at 100 K on a Bruker SMART APEX II CCD area detector system equipped with an Oxford Cryosystems 700 series cooler, a graphite monochromator, and a Mo  $\text{K}\alpha$  fine-focus sealed tube ( $\lambda = 0.71073 \text{ \AA}$ ). Intensity data were processed using the Bruker ApexII program suite. Absorption corrections were applied by using SADABS. Initial atomic positions were located by direct methods using XS, and the structures of the compounds were refined by the least-squares method using SHELXL [85]. All the non-hydrogen atoms were refined anisotropically. X-ray structural figures were generated using Olex2 [86]. Crystals suitable for the X-ray diffraction experiment of the ligand **5** was gently picked up with a microloop wetted with paratone oil and placed on the top of the goniometer head of a kappa-geometry Oxford Diffraction Gemini EOS diffractometer, equipped with a 2 K  $\times$  2 K CCD area detector and sealed-tube Enhance (Mo) and (Cu) X-ray sources. The raw intensities were corrected for absorption, Lorentz, and polarization effects. With respect to absorption, an empirical multi-scan absorption correction based on equivalent reflections was applied by means of the scaling algorithm SCALE3 ABSPACK. Final unit cell parameters were determined by least-squares refinement of 21,955 reflections picked

during the whole experiment. Data collection, reduction, and finalization were performed with the CrysAlis Pro suite [87]. The structure was solved by intrinsic phasing in the  $P 2_1/c$  space group with SHELXT [88], and refined by full-matrix least-squares methods based on  $F_o^2$  with SHELXL [89] software integrated with the OLEX2 program [86]; there were no atoms sitting in special positions.

## 2.2. Synthesis of the ligands

### 2.2.1. Synthesis of $HL^{CF_3}$ (1)

NaH (60% in mineral oil, 11.720 mmol, 0.460 g) was washed with hexane (5 mL) at room temperature under nitrogen atmosphere. Successively, anhydrous THF was added. At the meantime, 3',5'-bis(trifluoromethyl)acetophenone (7.800 mmol, 2.000 g) was combined with methyl 3,5-bis(trifluoromethyl)benzoate (8.580 mmol, 2.320 g) in a separate flask. To this solution, the sodium hydride solution was added dropwise. The resultant mixture was heated at reflux for 36 h. Afterwards, the mixture was cooled at room temperature and a precipitate was formed adding dropwise ice-cold 10% hydrochloric acid (40 mL). The precipitate was dissolved adding diethyl ether (25 mL). The organic layer was then isolated by extraction, dried over anhydrous  $Na_2SO_4$ , filtered and concentrated under vacuum to afford an off-white solid. The solid was recrystallized in acetone to afford the whitish complex in 87% yield.

**Molar mass:** 496.033 g/mol. **M.P.:** 173 °C. **Solubility:**  $Et_2O$ , THF,  $CHCl_3$ , EtOAc, MeCN, Acetone. **FT-IR ( $cm^{-1}$ ):** 3099wbr (C-H); 1623m, 1576wbr (C=O); 1453w, 1364m, 1327w, 1276s, 1216s, 1167s, 1136vs, 1121vs, 1111vs, 939w, 959m, 939m, 924w, 907s, 894s, 844s, 793s, 731m, 694s, 681vs.  **$^1H$ -NMR** ( $CDCl_3$ , 293 K):  $\delta$  6.91 (s, 1H,  $\alpha$ -CH), 8.13 (s, 2H,  $CH_{ar}$ ), 8.46 (s, 4H,  $CH_{ar}$ ), 16.59 (s, 1H, OH).  **$^{13}C\{^1H\}$ -NMR** ( $CDCl_3$ , 293 K):  $\delta$  93.83 ( $\alpha$ -CH), 119.6, 121.8, 123.9, 126.1, 126.2, 127.3, 127.4, 132.3, 132.5, 132.8, 133.1, 136.9 ( $CH_{ar}$  and  $CF_3$ ), 183.3 (C=O).  **$^{19}F\{^1H\}$ -NMR** ( $CDCl_3$ , 293K):  $\delta$  63.11. **ESI-MS** (major negative ions, MeCN),  $m/z$  (%): 495 (60) [ $L^{CF_3}$ ]<sup>-</sup>. **Elemental Analysis** (%) calculated for  $C_{19}H_8F_{12}O_2$ : C, 45.99, H, 1.62; found: C 45.98, H 1.62.

### 2.2.2. Synthesis of $NaL^{CF_3}$ (2)

Finely ground NaOH (0.130 g, 3.000 mmol) was added to the ligand  $HL^{CF_3}$  (1.500 g, 3.000 mmol). The mixture was successively dissolved in ethanol (100 mL), giving an opalescent yellow solution. The reaction was carried out under magnetic stirring at room temperature (r.t.). Through this process the solution slowly assumed a more limpid aspect. After 4 h, the reaction was stopped and the solution was dried at reduced pressure leading to the formation of an orange solid on the bottom of the flask. The solid product was kept into the drier for a night. The solid orange with pale pink reflection was recovered (yield 85%).

**Molar mass:** 518.015 g/mol. **M.P.:** 226-230 °C. **Solubility:** MeOH, EtOH, Et<sub>2</sub>O, THF, CHCl<sub>3</sub>, EtOAc, MeCN, DMSO, Acetone. **FT-IR (cm<sup>-1</sup>):** 3677w, 3383wbr, 1628m (C=O); 1592m, 1511m, 1471m, 1421m, 1360s, 1274s, 1241m, 1189m, 1165m, 1121s, 1044m, 955w, 906s, 888w, 846m, 787s, 702m, 681s, 601m, 586m. **<sup>1</sup>H NMR (DMSO, 293K):** δ 6.57 (s, 1H, α-CH), 8.08 (s, 2H, p-CH<sub>ar</sub>), 8.48 (s, 4H, o-CH<sub>ar</sub>). **ESI-MS (major positive ions, CH<sub>3</sub>CN), m/z (%):** 541 (40) [L<sup>CF3</sup> + 2Na]<sup>+</sup>. **Elemental analysis (%)** calculated for C<sub>19</sub>H<sub>7</sub>F<sub>12</sub>NaO<sub>2</sub>: C 44.04, H 1.36; found C 41.08, H 1.74.

### 2.2.3. Synthesis of HL<sup>Mes</sup> (3)

Synthesis of precursor Al(L<sup>Mes</sup>)<sub>3</sub>: malonyl chloride (13.953 mmol, 1.915 g) was added dropwise to a mixture of mesitylene (33.965 mmol, 4.72 mL) and aluminium trichloride (37.362 mmol, 4.982 g) in carbon sulphide (100 mL) cooled at 0°C. The reaction was stirred at reflux for 24 h. The mixture was then transferred in a round-bottom flask containing HCl (37%, 20 mL), cooled at 0°C. Successively, water (80 mL) was added dropwise, and the mixture was left under constant magnetic stirring for 10 minutes. The organic phase was then separated by the aqueous phase and it was evaporated at reduced pressure giving the whitish Al(L<sup>Mes</sup>)<sub>3</sub> in 53% yield.

**Molar mass:** 949.200 g/mol. **M.P.:** >300 °C. **Solubility:** THF, CH<sub>2</sub>Cl<sub>2</sub>, CHCl<sub>3</sub>. **FT-IR (cm<sup>-1</sup>):** 3000wbr, 2970w, 2949m, 2918m, 2857w (C-H); 1611m, 1575m (C=O); 1543sbr, 1511s (C=C); 1473m, 1415sbr, 1388s, 1364vs, 1314s, 1244m, 1218m, 1165m, 1110m, 1063m, 1031mbr, 961m, 933w, 848s, 819m, 806m, 786m, 776m, 755w, 727m, 705m. **<sup>1</sup>H-NMR (CDCl<sub>3</sub>, 293 K):** δ 2.25 (s, 18H, p-CCH<sub>3</sub>), 2.26 (s, 36H, o-CCH<sub>3</sub>), 5.76 (s, 3H, COCHCOH), 6.77 (s, 12H, m-CH). **<sup>13</sup>C{<sup>1</sup>H}-NMR (CDCl<sub>3</sub>, 293 K):** δ 19.8 (o-CCH<sub>3</sub>); 21.0 (p-CCH<sub>3</sub>); 106.9 (COCHCOH); 128.0 (m-CH); 134.7, 137.4, 137.5 (C<sub>ar</sub>); 191.1 (CO). **ESI-MS (major positive ions, MeCN), m/z (%):** 147 (20) [HL<sup>Mes</sup> - COMes]<sup>+</sup>, 309 (100) [HL<sup>Mes</sup> + H]<sup>+</sup>, 331 (30) [HL<sup>Mes</sup> + Na]<sup>+</sup>, 641 (60) [Al(L<sup>Mes</sup>)<sub>2</sub>]<sup>+</sup>, 971 (40) [Al(L<sup>Mes</sup>)<sub>3</sub> + Na]<sup>+</sup>. **ESI-MS (major negative ions, MeCN), m/z (%):** 307 (100) [L<sup>Mes</sup>]<sup>-</sup>. **Elemental Analysis (%)** calculated for C<sub>63</sub>H<sub>69</sub>AlO<sub>6</sub>: C 79.72, H 7.33; found: C 79.58, H 7.30.

To the complex Al(L<sup>Mes</sup>acac)<sub>3</sub> (1.348 mmol, 1.280 g), solubilized in chloroform, concentrated HCl (37%, 10 mL) was added. The reaction mixture was stirred at reflux for 24 h. The aqueous phase was removed and the organic phase was washed with water (3 x 10 mL). The organic phase was anhydried with sodium sulphate. The mixture was filtered, and the mother liquors were evaporated under reduced pressure to give the whitish brown-orange product HL<sup>Mes</sup> in 88% yield.

**Molar mass:** 308.414 g/mol. **Solubility:** Et<sub>2</sub>O, THF, n-hexane, CH<sub>2</sub>Cl<sub>2</sub>, CHCl<sub>3</sub>, EtOAc, MeCN, DMSO, acetone. **M.P.:** 90-95 °C. **FT-IR (cm<sup>-1</sup>):** 3097wbr, 2974m, 2952m, 2918m, 2859m, 2734w (C-H); 1613vs, 1575vsbr (C=O); 1435sbr (C=C), 1377s, 1270sbr, 1166s, 1158s, 1082s, 1031sbr, 950mbr, 897m, 853vs, 816s, 772s, 728s, 720s. **<sup>1</sup>H-NMR (CDCl<sub>3</sub>, 293 K):** δ 2.31 (s, 6H, CH<sub>3</sub>), 2.34 (s, 12H, CCH<sub>3</sub>), 5.77 (s, 1H, COCHCOH), 6.90 (s, 4H, CH), 16.00 (sbr, 1H, COH). **<sup>13</sup>C{<sup>1</sup>H}-NMR (CDCl<sub>3</sub>, 293 K):** δ 19.6 (o-CCH<sub>3</sub>); 21.1 (p-CCH<sub>3</sub>); 105.5 (COCHCOH); 128.5 (m-CH); 134.5, 134.8, 138.9 (ArC); 191.2 (CO). **ESI-MS (major positive ions, MeOH), m/z (%):** 309 (100) [HL<sup>Mes</sup> + H]<sup>+</sup>, 331 (70) [HL<sup>Mes</sup> + Na]<sup>+</sup>. **ESI-MS (major negative ions, MeOH), m/z (%):** 307 (100) [L<sup>Mes</sup>]<sup>-</sup>. **Elemental Analysis (%)** calculated for C<sub>21</sub>H<sub>24</sub>O<sub>2</sub>: C, 81.78, H, 7.84; found: C, 80.35; H, 7.66.

#### 2.2.4. Synthesis of $\text{NaL}^{\text{Mes}} \cdot \text{H}_2\text{O}$ (4)

To the ligand  $\text{L}^{\text{Mes}}$  (308.414 g/mol, 2.838 mmol, 0.875 g) solubilized in MeOH (15 mL), NaOH (2.838 mmol, 0.113 g) was added. The reaction mixture was stirred at reflux for 24 h. The solution was dried at reduced pressure and the residue was recrystallized by diethyl ether and filtered. From the mother liquors, dried at reduced pressure, the light orange whitish complex  $\text{NaL}^{\text{Mes}}$  has been obtained in 74% yield.

**Molar mass:** 330.396 g/mol. **Solubility:** MeOH, EtOH, Et<sub>2</sub>O, THF, CH<sub>2</sub>Cl<sub>2</sub>, CHCl<sub>3</sub>, EtOAc, DMSO, Me<sub>2</sub>CO. **M.P.:** 325-335 °C. **FT-IR** (cm<sup>-1</sup>): 3281wbr, 3147wbr, 2971wbr, 2951wbr, 2918w, 2858w, 2732vw (C-H); 1611m, 1557mbr (C=O); 1499m (v C=C); 1417sbr, 1373s, 1298w, 1271m, 1164m, 1110m, 1028mbr, 955w, 926w, 882w, 848m, 791m, 779m, 718m. **<sup>1</sup>H-NMR** (CDCl<sub>3</sub>, 293 K): δ 2.23 (s, 6H, *p*-CCH<sub>3</sub>), 2.24 (s, 12H, *o*-CCH<sub>3</sub>), 5.29 (s, 1H, COCHCO), 6.72 (s, 4H, *m*-CH). **<sup>13</sup>C{<sup>1</sup>H}-NMR** (CDCl<sub>3</sub>, 293 K): δ 19.6 (*o*-CCH<sub>3</sub>); 20.9 (*p*-CCH<sub>3</sub>); 103.8 (COCHCOH); 127.8 (*m*-CH); 133.2, 136.1, 142.1 (ArC); 191.2 (CO). **ESI-MS** (major positive ions, MeOH), *m/z* (%): 331 (100) [ $\text{L}^{\text{Mes}} + \text{Na} + \text{H}$ ]<sup>+</sup>, 353 (40) [ $\text{L}^{\text{Mes}} + 2\text{Na}$ ]<sup>+</sup>, 683 (10) [ $2\text{L}^{\text{Mes}} + 3\text{Na}$ ]<sup>+</sup>. **ESI-MS** (major negative ions, MeOH), *m/z* (%): 307 (100) [ $\text{L}^{\text{Mes}}$ ]<sup>-</sup>, 637 (10) [ $2\text{L}^{\text{Mes}} + \text{Na}$ ]<sup>-</sup>. **Elemental Analysis** (%) calculated for C<sub>21</sub>H<sub>23</sub>NaO<sub>2</sub>: C, 76.34; H, 7.02; found: C, 70.90; H, 7.09.

#### 2.2.5. Synthesis of HL<sup>I</sup> (5)

3-benzylidene-2,4-pentadienone (1.000 g, 5.310 mmol) and an excess of triethylamine (0.628 g, 5.310 mmol) were solubilized in EtOH (20 mL). Successively, pyrazole (0.362 g, 5.310 mmol) was added and a yellow clear solution was observed. The reaction was carried out overnight under magnetic stirring, at r.t. The day after, reflux was applied to the yellow solution for 6 h giving to an intensification of the mixture's colour. During this time, the reaction was monitored by Thin Layer Chromatography. Then, the reflux was removed, and the solution was left under magnetic stirring at room temperature overnight. After 36 h the reaction was controlled by ESI-MS and it was stopped. The mixture was dried at reduced pressure and an orange oil product was observed. The oil was solubilized in Et<sub>2</sub>O and precipitated with *n*-hexane until a white precipitate was formed. The white solid product was recovered by filtration (60% yield). A batch of good quality crystals of HL<sup>I</sup>, suitable for X-ray analysis, was obtained by slow evaporation of a hexane solution of 5.

**Molar mass:** 256.122 g/mol. **M.P.:** 98-100 °C. **Solubility:** CH<sub>3</sub>OH, Et<sub>2</sub>O, THF, CH<sub>2</sub>Cl<sub>2</sub>, CHCl<sub>3</sub>, EtOAc, CH<sub>3</sub>CN, DMSO, Acetone. **FT-IR** (cm<sup>-1</sup>): 3108w (C-H); 1732m, 1699m (C=O), 1497w, 1454w, 1418w, 1394m, 1356m, 1263m, 1231w, 1198m, 1168m, 1140m, 1096m, 1046w, 965w, 916w, 893w, 757s, 729s. **<sup>1</sup>H-NMR** (CDCl<sub>3</sub>, 293 K): δ 2.03 (s, 3H, CH<sub>3</sub>), 2.22 (s, 3H, CH<sub>3</sub>), 5.32 (d, 1H, α-CH), 6.01 (d, 1H, γ-CH), 6.22 (t, 1H, 4-CH<sub>pz</sub>), 7.32-7.41 (m, 6H, CH<sub>ar</sub> and 5-CH<sub>pz</sub>), 7.50 (d, 1H, 3-CH<sub>pz</sub>). **<sup>1</sup>H-NMR** (DMSO, 293 K): δ 2.07 (s, 3H, CH<sub>3</sub>), 2.15 (s, 3H, CH<sub>3</sub>), 5.58 (d, 1H, α-CH), 6.04 (d, 1H, γ-CH), 6.18 (t, 1H, 4-CH<sub>pz</sub>), 7.26-7.50 (6H, CH<sub>ar</sub> and 5-CH<sub>pz</sub>), 7.85 (d, 1H, 3-CH<sub>pz</sub>). **<sup>13</sup>C{<sup>1</sup>H}-NMR** (CDCl<sub>3</sub>, 293 K): δ 29.9 (CH<sub>3</sub>), 30.9 (CH<sub>3</sub>), 64.2 (γ-CH), 72.6 (α-CH), 106.1 (4-CH<sub>pz</sub>), 127.5, 128.7, 128.9, 129.6 137.7 139.4



(CH<sub>ar</sub>, 3- and 5-CH<sub>pz</sub>), 200.3 (C=O), 200.0 (C=O). **ESI-MS** (major positive ions, CH<sub>3</sub>CN), *m/z* (%): 157 (30) [1-benzyl-1H-pyrazole]<sup>+</sup>, 257 (97) [HL<sup>J</sup> + H]<sup>+</sup>, 279 (98) [HL<sup>J</sup> + Na]<sup>+</sup>. **ESI-MS** (major negative ions, CH<sub>3</sub>CN), *m/z* (%): 213 (22) [HL<sup>J</sup> - CH<sub>3</sub>CO]<sup>-</sup>, 189 (15) [HL<sup>J</sup> - pz]<sup>-</sup>. **Elemental Analysis** (%) calculated for C<sub>15</sub>H<sub>16</sub>N<sub>2</sub>O<sub>2</sub>: C 70.29, H 6.29, N 10.93; found C 70.65, H 6.36, N 9.79.

### 2.2.6. Synthesis of HL<sup>JM</sup> (6)

3-benzylidene-2,4-pentanedione (0.011 mol, 2.00 g) and triethylamine (0.011 mol, 1.11 g) were solubilized in EtOH. A clear yellow solution was observed. The reaction was carried out under magnetic stirring, at r.t., for 3 h. Then, 3,5-methylpyrazole (0.011 mmol, 0.96 g) was added. No colour variation was observed. After 24 h the reaction was stopped and the yellow solution was evaporated till dryness, obtaining a colourless oil with yellow reflections. The oil was solubilized with Et<sub>2</sub>O and precipitated with *n*-hexane. The white solid formed was filtered and dried (63% yield).

**Molar mass:** 284.153 g/mol. **M.P.:** 89-91 °C dec. **Solubility:** CH<sub>3</sub>OH, CH<sub>3</sub>CH<sub>2</sub>OH, CH<sub>3</sub>CN, CHCl<sub>3</sub>, Et<sub>2</sub>O, DMSO. **FT-IR** (cm<sup>-1</sup>): 2980w (C-H); 1728m, 1699m (C=O); 1552w, 1495w, 1457w, 1421w, 1381w, 1350m, 1311w, 1244m, 1192w, 1174w, 1244m, 1192w, 1174w, 1133m, 1087w, 1022w, 951w, 897w, 776w, 763m. **<sup>1</sup>H-NMR** (CDCl<sub>3</sub>, 293K): δ 2.00-2.21 (s, 12H, CH<sub>3</sub>), 5.42 (d, 1H, γ-CH), 5.75 (s, 1H, 4-CH<sub>py</sub>), 5.82 (d, 1H, α-CH), 7.28-7.38 (m, 5H, CH<sub>ar</sub>). **<sup>13</sup>C{<sup>1</sup>H}-NMR** (CDCl<sub>3</sub>, 500 MHz): δ 10.9, 13.6 (3- and 5-CH<sub>3</sub>), 30.3, 31.6 (CH<sub>3</sub>), 60.6 (γ-CH), 72.4 (α-CH), 105.6 (4-CH<sub>py</sub>), 127.5, 128.2, 128.8, 129.0, 129.7, 138.0, 139.3, 147.3 (CH<sub>ar</sub>, 3- and 4-C<sub>py</sub>), 199.9, 200.9 (C=O). **ESI-MS** (major positive ions, CH<sub>3</sub>CN), *m/z* (%): 185 (18) [PzCHPh]<sup>+</sup>, 285 (100) [HL<sup>JM</sup> + H]<sup>+</sup>, 307 (46) [HL<sup>JM</sup> + Na]<sup>+</sup>. **ESI-MS** (major negative ions, CH<sub>3</sub>CN), *m/z* (%): 187 (42) [3-benzylpentane-2,4-dione]<sup>-</sup>. **Elemental Analysis** (%) calculated for C<sub>17</sub>H<sub>20</sub>N<sub>2</sub>O<sub>2</sub>: C 71.81, H 7.09, N 9.85; found C 72.72, H 7.49, N 8.85.

## 2.3. Synthesis of HL<sup>CF3</sup> complexes

### 2.3.1. Synthesis of Cu(L<sup>CF3</sup>)<sub>2</sub> (7)

The ligand HL<sup>CF3</sup> (1.000 mmol, 0.498 g) and Cu(CH<sub>3</sub>CO<sub>2</sub>)<sub>2</sub>·H<sub>2</sub>O (0.500 mmol, 0.100 g) were solubilized in H<sub>2</sub>O and EtOH (1:1, 20 mL:20 mL). The solution was left under constant magnetic stirring at r.t. for 1 h and then at reflux for 4 h. The reaction was stopped, and the precipitate was filtered and dried in air. The whitish complex was obtained in 94% yield. A batch of good quality crystals of [Cu(L<sup>CF3</sup>)<sub>2</sub>]·THF, suitable for X-ray analysis, was obtained by slow evaporation of a chloroform/acetone/THF solution of 7.

**Molar mass:** 1052.980 g/mol. **Solubility:** Et<sub>2</sub>O, THF, CH<sub>2</sub>Cl<sub>2</sub>, CHCl<sub>3</sub>, EtOAc, MeCN, DMSO, Acetone. **M.P.:** 181 °C. **FT-IR** (cm<sup>-1</sup>): 3099w (C-H<sub>ar</sub>); 1627m (C=O); 1564m (C=O); 1539s, 1517s, 1463m, 1395s, 1364s, 1279vs, 1187s,

1169vsbr, 1128vs, 962m, 924m, 907s, 846m, 790s, 733w, 713m. **Elemental Analysis (%)** calculated for  $C_{38}H_{14}CuF_{24}O_4$ : C 43.30, H 1.34; found: C 44.23, H 1.30.

### 2.3.2. Synthesis of $Cu(PPh_3)_2(L^{CF_3})$ (**8**)

$Cu(CH_3CN)_4PF_6$  (0.186 g, 0.500 mmol) and  $PPh_3$  (0.262 g, 1.000 mmol) were solubilized in  $CH_3CN$  (40 mL). The reaction mixture was kept under constant magnetic stirring at r.t. overnight. The next day, the ligand  $NaL^{CF_3}$  (0.260 g, 0.500 mmol) was added to the solution. After 5 h of magnetic stirring, the mixture was evaporated and the solid formed was washed in  $Et_2O$ . From the mother liquors an orange solid was precipitated, and it was crystallized using  $Et_2O$  and *n*-hexane to give the complex  $Cu(PPh_3)_2(L^{CF_3})$  in yield 60%. A batch of good quality crystals of  $Cu(PPh_3)_2(L^{CF_3})$ , suitable for X-ray analysis, was obtained by slow evaporation of a ethanol/acetone solution of **8**.

**Molar mass:** 1577.16 g/mol. **Solubility:**  $Et_2O$ , THF, *n*-hexane,  $CH_2Cl_2$ ,  $CHCl_3$ , EtOAc, MeCN, Acetone. **FT-IR ( $cm^{-1}$ ):** 3055wbr (C-H<sub>ar</sub>); 2300wbr, 1823wbr, 1625w (C=O); 1581m (C=O); 1539w, 1519w, 1500w, 1479s, 1463m, 1434m, 1416m, 1360s, 1275vs, 1247m, 1170s, 1124vs, 1096s, 1026m, 997w, 952m, 902m, 843m, 790w, 777m, 743s, 693s, 680s, 663m.  **$^1H$ -NMR** ( $CDCl_3$ , 293 K):  $\delta$  6.18 (s, 1H,  $\alpha$ -CH), 7.22-7.42 (m, 30H,  $CH_{PPh_3}$ ), 7.90 (s, 2H, *p*-CH<sub>ar</sub>), 8.11 (s, 4H, *o*-CH<sub>ar</sub>).  **$^{13}C\{^1H\}$ -NMR** ( $CDCl_3$ , 293 K):  $\delta$  92.0 ( $\alpha$ -CH), 120.2, 122.3, 123.1, 124.5, 126.7, 126.9, 128.4, 129.6, 130.8, 131.1, 131.4, 131.6, 133.1, 133.6, 133.8, 133.9 ( $CH_{ar}$ ), 144.4 (C=O), 181.6 (CO).  **$^{19}F\{^1H\}$ -NMR** ( $CDCl_3$ , 293K):  $\delta$  -62.68 (s).  **$^{31}P\{^1H\}$ -NMR** ( $CDCl_3$ , 223 K):  $\delta$  -3.683 (s). **ESI-MS** (major positive ions,  $CH_3CN$ ), *m/z* (%): 366 (40) [ $Cu(PPh_3) + CH_3CN$ ]<sup>+</sup>, 587 (100) [ $Cu(PPh_3)_2$ ]<sup>+</sup>. **ESI-MS** (major negative ions,  $CH_3CN$ ), *m/z* (%): 495 (100) [ $L^{CF_3}$ ]. **Elemental Analysis (%)** calculated for  $C_{55}H_{37}CuF_{12}O_2P_2$ : C 60.98, H 3.44; found: C 59.13, H 3.35.

### 2.3.3. Synthesis of $Zn(L^{CF_3})_2$ (**9**)

$Zn(CH_3CO_2)_2$  (0.097 g, 0.500 mmol) and  $HL^{CF_3}$  (0.524 g, 1.000 mmol) were solubilized in EtOH (15 mL) under magnetic stirring at r.t. Subsequently,  $H_2O$  was added to the flask (in a 1 to 1 ratio with EtOH). The mixture was stirred at r.t. overnight. The precipitate formed was washed with  $CHCl_3$  and kept for 2 h under magnetic stirring. It was filtered and dried under vacuum to give the  $Zn(L^{CF_3})_2$  complex in 45% yield.

**Molar mass:** 1055.87 g/mol. **Solubility:** EtOH,  $Et_2O$ , THF, *n*-hexane,  $CH_2Cl_2$ ,  $CHCl_3$ , EtOAc, MeCN, DMSO, Acetone. **M.P.:** 185 °C-188 °C. **FT-IR ( $cm^{-1}$ ):** 3356wbr (C-H<sub>ar</sub>); 1629m (C=O); 1572m (C=O); 1538m, 1516s, 1464m, 1408m, 1385m, 1361vs, 1291s, 1274vs, 1251s, 1220s, 1198s, 1170s, 1125vs, 954m, 906s, 893m, 847m, 787s, 740w, 730w, 709m.  **$^1H$ -NMR** (Acetone, 293 K):  $\delta$  7.44 (s, 2H,  $\alpha$ -CH), 8.23 (s, 4H, *p*-CH<sub>ar</sub>), 8.76 (s, 8H, *o*-CH<sub>ar</sub>).  **$^{19}F\{^1H\}$ -NMR** (Acetone, 293 K):  $\delta$  63.35 (s). **ESI-MS** (major positive ions,  $CH_3CN$ ), *m/z* (%): 640 (40) [ $Zn(L^{CF_3}) + 2H_2O$ ]<sup>+</sup>. **Elemental analysis (%)** calculated for  $C_{38}H_{14}F_{24}O_4Zn$ : C 43.23, H 1.34; found: C 41.23, H 1.34.

### 2.3.4. Synthesis of $\text{Ag}(\text{PPh}_3)_2(\text{L}^{\text{CF}_3})$ (10)

$\text{AgNO}_3$  (0.085 g, 0.500 mmol) and  $\text{PPh}_3$  (0.262 g, 1.000 mmol) were solubilized in MeOH (40 mL). The reaction mixture was stirred for 3 h at r.t., covering the flask with tinfoil.  $\text{NaL}^{\text{CF}_3}$  ligand (0.262 g, 0.500 mmol) was added with 10 mL of MeOH and the reaction was carried on for 3 h in the same conditions. The solution was evaporated to dryness and the yellow solid product was solubilized in  $\text{Et}_2\text{O}$  and precipitated in  $\text{CHCl}_3$ . A yellow opalescent mixture with a dark precipitate was formed. The yellow solution was evaporated forming of an orange oil which was dried under reduced pressure. Once dried, it was precipitated with  $\text{CHCl}_3$  and *n*-hexane. The precipitate was decanted, while the liquid solution was kept in freezer until yellow crystals have formed. The crystals were dried and characterized (yield 65%).

**Molar mass:** 1621.138 g/mol. **Solubility:** THF,  $\text{CH}_2\text{Cl}_2$ ,  $\text{CHCl}_3$ , MeCN. **M.P.:** 145-149 °C **FT-IR** ( $\text{cm}^{-1}$ ): 3056wbr, 3004wbr, 2956wbr, 2918wbr, 2318wbr, 1888wbr, 1814wbr, 1626w (C=O); 1579m (C=O); 1569m, 1479m, 1434s, 1404wbr, 1364w, 1336s, 1276s, 1257m, 1169s, 1158m, 1125s, 1095s, 1070m, 1027m, 997m, 933w, 901m, 843m, 788m, 759s, 741s, 692vs, 680vs, 618m.  **$^1\text{H-NMR}$**  ( $\text{CDCl}_3$ , 293K):  $\delta$  7.29-7.46 (m, 31H,  $\text{CH}_{\text{PPh}_3}$  and  $\alpha$ -CH), 7.87 (s, 2H,  $p$ - $\text{CH}_{\text{ar}}$ ), 8.48 (s, 4H,  $o$ - $\text{CH}_{\text{ar}}$ ).  **$^{13}\text{C}\{^1\text{H}\}$ -NMR** ( $\text{CDCl}_3$ , 293K):  $\delta$  128.8, 128.9, 129.7, 129.8, 130.2, 130.5, 130.8, 131.0, 131.9, 132.1, 132.2 (m,  $\text{CH}_{\text{ar}}$  and  $\text{CF}_3$ ); 139.7 (C=O), 169.9 (C=O).  **$^{31}\text{P}\{^1\text{H}\}$ -NMR** ( $\text{CDCl}_3$ , 293 K):  $\delta$  9.81 (sbr).  **$^{31}\text{P}\{^1\text{H}\}$ -NMR** ( $\text{CDCl}_3$ , 223 K):  $\delta$  9.64 (dd,  $J(^{107}\text{Ag}-^{31}\text{P}) = 432$  Hz,  $J(^{109}\text{Ag}-^{31}\text{P}) = 499$  Hz). **ESI-MS** (major positive ions,  $\text{CH}_3\text{CN}$ ),  $m/z$  (%): 412 (10) [ $\text{Ag}(\text{PPh}_3) + \text{CH}_3\text{CN}$ ] $^+$ , 633 (100) [ $\text{Ag}(\text{PPh}_3)_2$ ] $^+$ . **ESI-MS** (major negative ions,  $\text{CH}_3\text{CN}$ ),  $m/z$  (%): 495 (20) [ $\text{L}^{\text{CF}_3}$ ] $^-$ . **Elemental Analysis (%) calculated for  $\text{C}_{57}\text{H}_{37}\text{AgF}_{12}\text{O}_2$ :** C 58.58, H 3.31; found: C 59.66, H 3.59.

## 2.4. Synthesis of $\text{HL}^{\text{I}}$ complexes

### 2.4.1. Synthesis of $\text{Cu}(\text{L}^{\text{I}})_2$ (11)

The ligand  $\text{HL}^{\text{I}}$  (0.512 g, 2.000 mmol) and  $\text{Cu}(\text{CH}_3\text{CO}_2)_2 \cdot \text{H}_2\text{O}$  (0.199 g, 1.000 mmol) were dissolved in  $\text{CH}_3\text{OH}$  (40 mL), giving a dark green solution with blue reflex. The reaction proceeded for 12 h at r.t. under magnetic stirring. After this time the mixture becomes opalescent with a blue suspension. At the end the mixture was filtered and the obtained mother liquors were dried at reduced pressure obtaining a blue oil.  $\text{Et}_2\text{O}$  was added into the round bottom flask to purify the residue: a sky-blue precipitate was formed and removed by filtration. The obtained mother liquors were concentrated at reduced pressure and let it evaporate at room temperature. After 2 days at the bottom of the flask a petrol green solid was formed which is recovered. The petrol green complex  $\text{Cu}(\text{L}^{\text{I}})_2$  was obtained in 58% yield.

**Molar mass:** 573.156 g/mol. **Solubility:**  $\text{Et}_2\text{O}$ ,  $\text{CH}_2\text{Cl}_2$ ,  $\text{CHCl}_3$ , EtOAc, MeCN, DMSO, Acetone. **M.P.:** 76-82°C. **FT-IR** ( $\text{cm}^{-1}$ ): 3107w, 3056w, 3031wbr, 3004wbr, 2916wbr (C-H); 1732s, 1700s (C=O); 1657w, 1616w, 1517w, 1497w, 1453w, 1418m, 1394m, 1355s, 1322w, 1282sh, 1263s, 1230sh, 1917m, 1168s, 1140s, 1095s, 1069w, 1045m, 1038m, 1030sh, 966m, 916w, 893m, 869w, 879w, 757s, 728s, 702s. **ESI-MS** (major positive ions,  $\text{CH}_3\text{CN}$ ):  $m/z$

(%): 318 (30)  $[\text{Cu}(\text{L}^{\text{J}})]^+$ , 360 (50)  $[\text{Cu}(\text{L}^{\text{J}}) + \text{CH}_3\text{CN}]^+$ . **Elemental analysis** (%) calculated for  $\text{C}_{30}\text{H}_{30}\text{CuN}_4\text{O}_4$ : C 62.76, H 5.27, N 9.76; found: C 58.82, H 5.52, N 8.07.

#### 2.4.2. Synthesis of $[\text{Cu}(\text{HL}^{\text{J}})(\text{PPh}_3)_2]\text{PF}_6$ (12)

$\text{PPh}_3$  (0.525 g, 2 mmol) and  $\text{Cu}(\text{CH}_3\text{CN})_4\text{PF}_6$  (0.372 g, 1 mmol) were dissolved in  $\text{CH}_3\text{CN}$  (40 mL), giving a limpid colorless solution, that is put under magnetic stirring at r.t. for 2 h. After this time, ligand  $\text{HL}^{\text{J}}$  (0.256 g, 1.000 mmol) was added leaving the solution limpid and colorless. The reaction proceeded over night at room temperature under magnetic stirring. At the end, the solution was dried at reduced pressure giving a yellow oil. Then, using the high vacuum pump a light-yellow precipitate was formed. The light-yellow complex  $[\text{Cu}(\text{L}^{\text{J}})(\text{PPh}_3)_2]\text{PF}_6$  was obtained in 89% yield.

**Molar mass:** 988.197 g/mol. **Solubility:**  $\text{CHCl}_3$ ,  $\text{CH}_3\text{CN}$ , DMSO, Acetone. **M.P.:** 153-157 °C. **FT-IR** ( $\text{cm}^{-1}$ ): 3055wbr, 2268w, 1894wbr; 1731m, 1702m (C=O); 1586w, 1480m, 1455w, 1435s, 1407m, 1359m, 1310w, 1281m, 1167m, 1140m, 1094s, 1069m, 1027m, 998m, 918w, 875m, 832vs, 742vs, 692vs, 628m, 618m, 556vs, 516vs, 503vs, 489vs, 443s.  **$^1\text{H-NMR}$**  ( $\text{CDCl}_3$ , 293 K):  $\delta$  2.063 (s, 3H,  $\text{CH}_3$ ), 2.14 (s, 3H,  $\text{CH}_3$ ), 5.58 (d, 1H,  $\alpha\text{-CH}$ ), 6.17 (d, 1H,  $\gamma\text{-CH}$ ), 6.27 (dd, 1H, 4- $\text{CH}_{\text{pz}}$ ), 7.13-7.43 (m, 36H,  $\text{CH}_{\text{ar}}$  and 5- $\text{CH}_{\text{pz}}$ ), 7.68 (1H, 3- $\text{CH}_{\text{pz}}$ ).  **$^{31}\text{P}\{^1\text{H}\}\text{-NMR}$**  ( $\text{CDCl}_3$ , 293 K):  $\delta$  -0.86 (s), -144.21 (sept,  $J(^{19}\text{F}\text{-}^{31}\text{P}) = 712$  Hz,  $\text{PF}_6$ ). **ESI-MS** (major positive ions,  $\text{CH}_3\text{CN}$ ),  $m/z$  (%): 366 (100)  $[\text{Cu}(\text{PPh}_3) + \text{CH}_3\text{CN}]^+$ , 581 (10)  $[\text{Cu}(\text{PPh}_3)\text{HL}^{\text{J}}]^+$ , 587 (100)  $[\text{Cu}(\text{PPh}_3)_2]^+$ , 604 (20)  $[\text{Cu}(\text{PPh}_3)(\text{HL}^{\text{J}}) + \text{Na}]^+$ , 850 (15)  $[\text{Cu}(\text{PPh}_3)_3]^+$ . **Elemental analysis** (%) calculated for  $\text{C}_{51}\text{H}_{46}\text{CuF}_6\text{N}_2\text{O}_2\text{P}_3$ : C 61.91, H 4.69, N 2.83; found: C 60.75, H 4.54, N 3.53.

#### 2.4.3. Synthesis of $\text{Zn}(\text{HL}^{\text{J}})(\text{HPz})\text{Cl}_2$ (13)

The ligand  $\text{HL}^{\text{J}}$  (0.256 g, 1.000 mmol) and  $\text{ZnCl}_2$  (0.1363 g, 1.000 mmol) were dissolved in EtOH (40 mL), giving a colorless solution. The reaction proceeded for 3 h at r.t. under magnetic stirring. After that the reaction is refluxed for 3 h and then the temperature is lowered to let it proceed at room temperature overnight. At the end, the mixture was dried at reduced pressure giving a yellow oil. The residue was solubilized with anhydrous EtOH and then  $\text{Et}_2\text{O}$  and n-hexane were added into the round-bottom flask in order to purify it: a precipitate was formed, removed by decanting and dried at reduced pressure. The white complex  $\text{Zn}(\text{HL}^{\text{J}})(\text{HPz})\text{Cl}_2$  was obtained in 43% yield.

**Molar mass:** 458.025 g/mol. **Solubility:**  $\text{CHCl}_3$ , MeCN, DMSO, Acetone. **M.P.:** 135-144 °C. **FT-IR** ( $\text{cm}^{-1}$ ): 3323m, 3139w, 3116m, 2993m, 2925w (C-H); 1728s, 1701s (C=O); 1518w, 1497w, 1473w, 1455m, 1409m, 1379s, 1360m, 1332m, 1283m, 1261m, 1231s, 1207m, 1178m, 1160m, 1143m, 1125vs, 1079m, 1068m, 1051s, 1004m, 976w, 951m, 921m, 911m, 899m, 852w, 797vs, 770vs, 730vs, 705s, 661m, 630s, 607s, 587m, 571s, 522vs, 483m.  **$^1\text{H-NMR}$**  ( $\text{CD}_3\text{CN}$ , 293 K):  $\delta$  2.06 (s, 3H,  $\text{CH}_3$ ), 2.18 (s, 3H,  $\text{CH}_3$ ), 5.47 (d, 1H,  $\alpha\text{-CH}$ ), 6.12 (d, 1H,  $\gamma\text{-CH}$ ), 6.25 (t, 1H, 4- $\text{CH}_{\text{pz}}$ ), 6.57 (t, 1H,  $\text{CH}_{\text{pz}}$ ), 7.35-7.49 (m, 6H,  $\text{CH}_{\text{ar}}$  and 5- $\text{CH}_{\text{pz}}$ ), 7.63 (s, 1H, 3- $\text{CH}_{\text{pz}}$ ), 7.86 (dbr, 2H,  $\text{CH}_{\text{pz}}$ ), 11.69 (1H,  $\text{NH}_{\text{pz}}$ ). **ESI-MS** (major positive ions,  $\text{CH}_3\text{CN}$ ),  $m/z$  (%): 257  $[\text{HL}^{\text{J}} + \text{H}]^+$ , 279  $[\text{Zn}(\text{HL}^{\text{J}} - \text{Ph}) + \text{Cl}]^+$ , 355  $[\text{Zn}(\text{HL}^{\text{J}}) + \text{Cl}]^+$ .

**ESI-MS** (major negative ions, CH<sub>3</sub>CN), *m/z* (%): 171 (100) [2HPz + Cl]<sup>-</sup>. **Elemental analysis** (%) calculated for C<sub>18</sub>H<sub>20</sub>Cl<sub>2</sub>N<sub>4</sub>O<sub>2</sub>Zn: C 47.03, H 5.17, N 12.19; found C 45.99, H 4.24, N 11.29.

## 2.5. Synthesis of HL<sup>Mes</sup> complexes

### 2.5.1. Synthesis of Cu(L<sup>Mes</sup>)<sub>2</sub> (14)

The ligand NaL<sup>Mes</sup> (1.500 mmol, 0.495 g) was solubilized in a mixture of MeOH:EtOH (50:50, 15 mL) and CuCl<sub>2</sub>·2H<sub>2</sub>O (0.750 mmol, 0.128 g) was added. The reaction was left under constant magnetic stirring at r.t. for 24 h. The formation of a precipitate was observed, it was filtered and dried under reduced pressure. The grey-green Cu(L<sup>Mes</sup>)<sub>2</sub> complex, was obtained in 68% yield. A batch of good quality crystals of Cu(L<sup>Mes</sup>)<sub>2</sub>, suitable for X-ray analysis, was obtained by slow evaporation of a chloroform/hexane solution of **14**.

**Molar mass:** 678.372 g/mol. **Solubility:** MeOH, EtOH, Et<sub>2</sub>O, THF, n-hexane, CH<sub>2</sub>Cl<sub>2</sub>, CHCl<sub>3</sub>, EtOAc, MeCN, DMSO, Me<sub>2</sub>CO. **M.P.:** 297-301 °C. **FT-IR** (cm<sup>-1</sup>): 3027sh, 3009sh, 2998sh, 2952wbr, 2916w, 2856w (C-H); 1613m, 1533s (C=O); 1513s (C=C); 1472m, 1436sh, 1387s, 1367vs, 1165m, 1110m, 1054m, 1030mbr, 958w, 931wbr, 879w, 843s, 810m, 786m, 725s. **ESI-MS** (major positive ions, MeOH), *m/z* (%): 309 (5) [L<sup>Mes</sup>]<sup>+</sup>, 678 (25) [Cu(L<sup>Mes</sup>)<sub>2</sub> + H]<sup>+</sup>, 700 (100) [Cu(L<sup>Mes</sup>)<sub>2</sub> + Na]<sup>+</sup>, 716 (10) [Cu(L<sup>Mes</sup>)<sub>2</sub> + K]<sup>+</sup>. **ESI-MS** (major negative ions, MeOH), *m/z* (%): 307 (100) [L<sup>Mes</sup>]<sup>-</sup>, 387 (40) [HL<sup>Mes</sup> + Br]<sup>-</sup>. **Elemental Analysis** (%) calculated for C<sub>42</sub>H<sub>46</sub>CuO<sub>4</sub>: C 74.36; H, 6.84; Cu, 73.87; O, 6.75.

### 2.5.3. Synthesis of Zn(L<sup>Mes</sup>)<sub>2</sub> (15)

The ligand NaL<sup>Mes</sup> (1.500 mmol, 0.495 g) was solubilized in absolute EtOH (30 mL) and ZnCl<sub>2</sub> was added (0.750 mmol, 0.102 g). The reaction was left under constant magnetic stirring at r.t. for 24 h. The mixture was filtered and the precipitate was dried under reduced pressure. The light yellow complex Zn(L<sup>Mes</sup>)<sub>2</sub> was obtained in 50% yield. A batch of good quality crystals of Zn(L<sup>Mes</sup>)<sub>2</sub>, suitable for X-ray analysis, was obtained by slow evaporation of a hexane solution of **15**.

**MM:** 680.206 g/mol. **Solubility:** MeOH, EtOH, Et<sub>2</sub>O, THF, n-hexane, CH<sub>2</sub>Cl<sub>2</sub>, CHCl<sub>3</sub>, EtOAc, MeCN, DMSO, Me<sub>2</sub>CO. **M.P.:** 218-223 °C. **FT-IR** (cm<sup>-1</sup>): 3028sh, 3002sh, 2971w, 2952wbr, 2918w, 2858w (C-H); 1612m, 1546mbr (C=O), 1505s (C=C); 1472m, 1397sh, 1360s, 1301m, 1288m, 1166m, 1111w, 1089w, 1045mbr, 1032mbr, 957w, 927w, 878w, 849m, 805m, 782m, 723m. **<sup>1</sup>H-NMR** (CDCl<sub>3</sub>, 293 K): δ 2.28 (s, 6H, *p*-CCH<sub>3</sub>), 2.34 (s, 12H, *o*-CCH<sub>3</sub>), 5.71 (s, 1H, COCHCOH), 6.84 (s, 4H, *m*-CH). **<sup>13</sup>C{<sup>1</sup>H}-NMR** (CDCl<sub>3</sub>, 293 K): δ 18.9 (*o*-CCH<sub>3</sub>); 21.1 (*p*-CCH<sub>3</sub>); 105.9 (COCHCOH); 128.3 (*m*-CH); 133.7, 138.1, 138.4 (CH<sub>ar</sub>); 195.1 (C=O). **ESI-MS** (major positive ions, MeOH), *m/z* (%): 309 (20) [HL<sup>Mes</sup> + H]<sup>+</sup>, 331 (70) [HL<sup>Mes</sup> + Na]<sup>+</sup>, 679 (100) [Zn(L<sup>Mes</sup>)<sub>2</sub> + H]<sup>+</sup>, 701 (60) [Zn(L<sup>Mes</sup>)<sub>2</sub> + Na]<sup>+</sup>. **ESI-MS** (major negative ions, MeOH), *m/z* (%): 443 (100) [(L<sup>Mes</sup>)Zn + 2Cl]<sup>-</sup>, 715 (5) [(L<sup>Mes</sup>)<sub>2</sub>Zn + Cl]<sup>-</sup>. **Elemental Analysis** (%) calculated for C<sub>42</sub>H<sub>46</sub>O<sub>4</sub>Zn: C 74.16, H 6.82; found: C 69.57, H 7.00.

### 3. RESULTS AND DISCUSSION

#### 3.1. Aim of the work

My research project is focused mainly in the synthesis of first-row metal  $\beta$ -diketonate complexes with a particular attention to the copper(II) and copper(I) species, also in view of their catalytic and biological properties. The first part of my research project has been mainly focused in the preparation of first-row metal complexes of sterically hindered  $\beta$ -diketonates also bearing fluorinated moieties, the 1,3-dimesitylpropane-1,3-dione ( $\text{HL}^{\text{Mes}}$ ) and the 1,3-bis(3,5-bis(trifluoromethyl)phenyl)propane-1,3-dione ( $\text{HL}^{\text{CF}_3}$ ) (Figure 17). Another goal of the research project has been the modification of the electronic and steric properties of acetylacetonate by insertion of different substituents in 2-position ( $\text{R}^2$ ), containing additional donor atoms, in order to prepare polyfunctional coordinating ligands with higher complexity and functionality, and related metal complexes, in view of their biological activity as potential anticancer and antiviral agents. Particular attention has been paid to the development of a platform for the synthesis of new N,O,O-donor chelating species as a new class of chelating ligands based on the 3-benzylidene-2,4-pentanedione skeletal functionalized with heterocyclic rings (Figure 29). In particular, I have synthesized the 3-(phenyl(1*H*-pyrazol-1-yl)methyl)pentane-2,4-dione ( $\text{HL}^{\text{J}}$ ) and the 3-((3,5-dimethyl-1*H*-pyrazol-1-yl)(phenyl)methyl)pentane-2,4-dione ( $\text{HL}^{\text{JM}}$ ), novel 1,3-diketones bearing a pyrazole moieties, whose reactivity and structure has been fully studied also by X-ray diffraction analysis for  $\text{HL}^{\text{J}}$ . The new ligands ( $\text{HL}^{\text{J}}$  and  $\text{HL}^{\text{JM}}$ ) are really versatile N,O,O-donors because they can provide different hapticities, depending on the type of coordination environment the metal is surrounded. Moreover, based on the scientific literature, they could have potential applications both in catalysis and in medicinal chemistry and are worthy of further and deeper investigations.

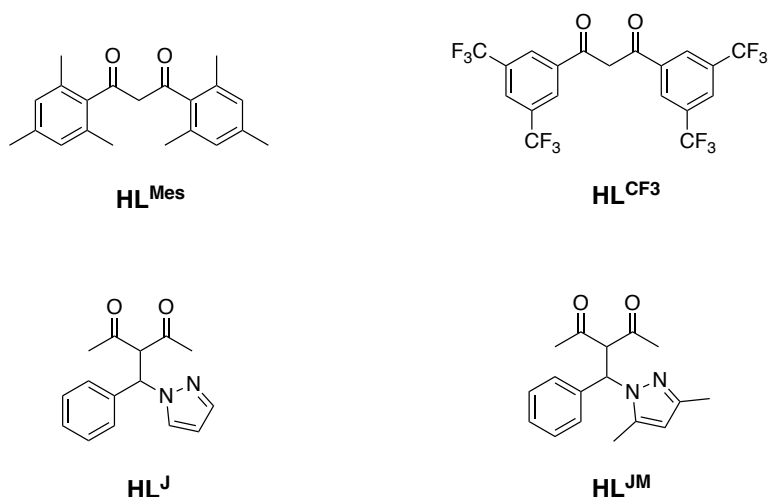


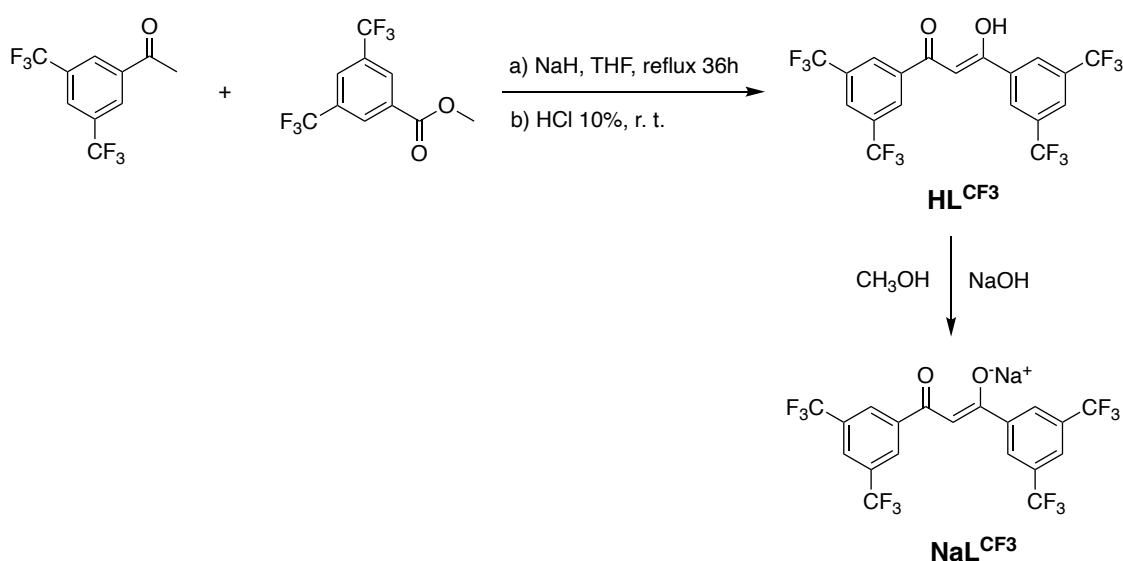
Figure 17 Structure of ligands  $\text{HL}^{\text{Mes}}$ ,  $\text{HL}^{\text{CF}_3}$ ,  $\text{HL}^{\text{J}}$  and  $\text{HL}^{\text{JM}}$

### 3.2. Synthesis and characterization of the ligands

The diketone 1,3-bis(3,5-bis(trifluoromethyl)phenyl)propane-1,3-dione (**HL<sup>CF3</sup>**) was synthesized in THF solution from a mixture of 3,5-bis(trifluoromethyl)acetophenone and 3,5-bis(trifluoromethyl)benzoate (**1**) (**Scheme 13**) by Claisen condensation, using a modified literature method utilized in the synthesis of somewhat related 1,3-bis(4-methylphenyl)propane-1,3-dione [90]. It was isolated as a white solid in 87% yield.

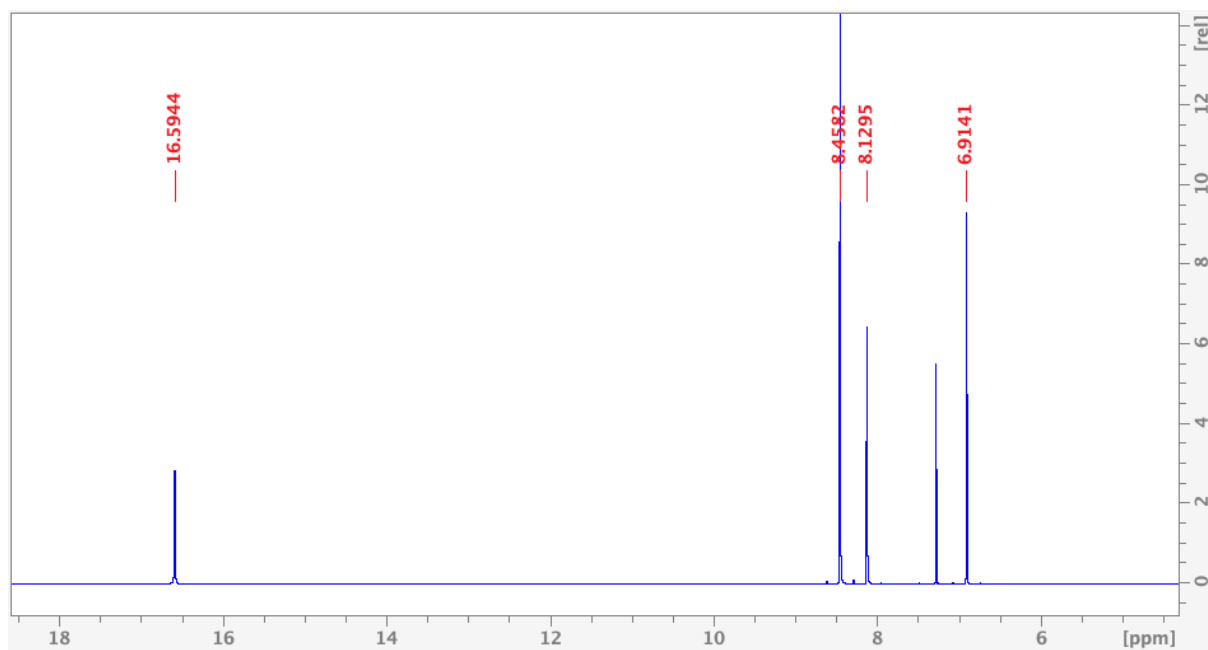
The sodium salt **NaL<sup>CF3</sup>** (**2**) was obtained by dissolving the **HL<sup>CF3</sup>** (**1**) species in an equimolar quantity of NaOH in methanol solution and it was fully characterized.

The elemental analysis has confirmed the stoichiometry of the two ligands, showing a good purity of the products, which is also confirmed by the narrow melting points.

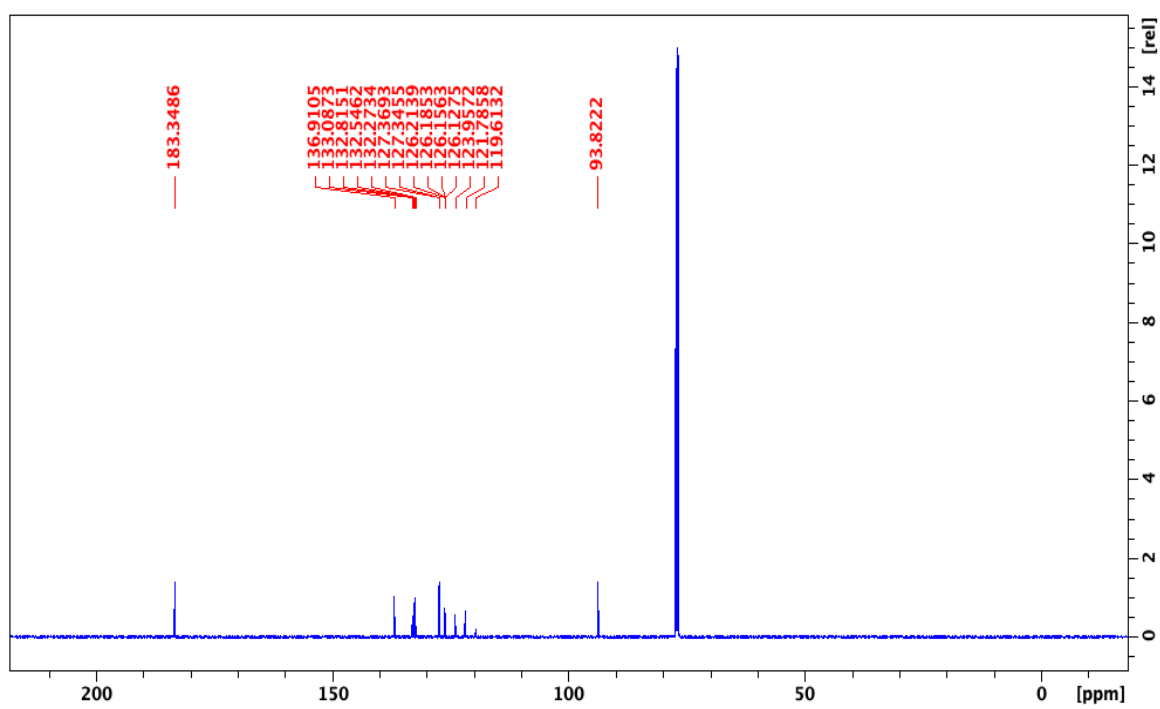


*Scheme 13* Synthetic procedure for the ligands **HL<sup>CF3</sup>** (**1**) and **NaL<sup>CF3</sup>** (**2**)

$\beta$ -Diketones are capable of keto-enol tautomerism, and the tautomers exist in equilibrium with each other in solution (Scheme 1). In most organic solvents,  $\beta$ -diketones are predominately (>90%) enolized [91]. The <sup>1</sup>H-NMR spectrum of **HL<sup>CF3</sup>** in CDCl<sub>3</sub> suggests the presence of the enol form, 1,3-bis(3,5-bis(trifluoromethyl)phenyl)-3-hydroxyprop-2-en-1-one, in solution (**Figure 18**).

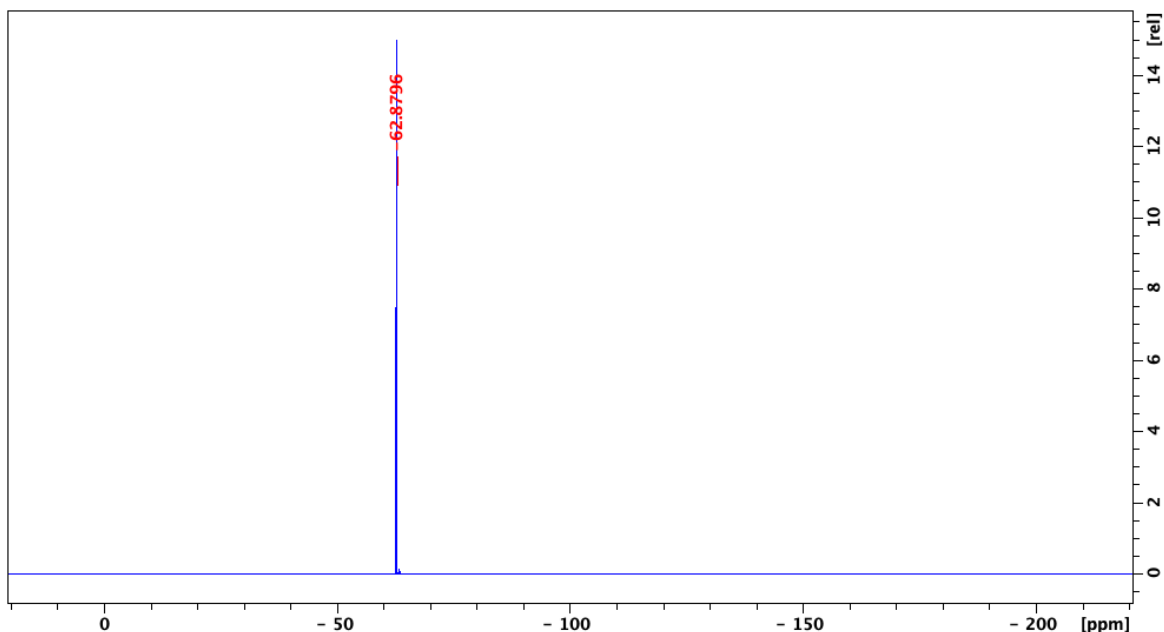


(a)



(b)





(c)

Figure 18 (a)  $^1\text{H}$ -, (b)  $^{13}\text{C}$ - and (c)  $^{19}\text{F}$ -NMR spectra of  $\text{HL}^{\text{CF}_3}$  in  $\text{CDCl}_3$  solution

In the  $^1\text{H}$ -NMR spectrum of  $\text{HL}^{\text{CF}_3}$  the 2-CH bridging and OH protons are detectable at 6.91 and 16.59 ppm, respectively. The CH protons in *ortho*- and in *para*-positions of aromatic rings are present at 8.46 and 8.13 ppm, respectively. In the  $^{13}\text{C}$ -NMR spectrum the 2-CH and C=O carbons are detectable at 93.83 and 183.5 ppm, respectively. The  $^{19}\text{F}$ -NMR shows only one signal at -63.11 ppm.

The infrared spectra of  $\beta$ -diketones show the vibrational absorptions of both the keto and enol forms if the spectra are run as neat liquids or in solvents [55, 92-94]. The enol form of  $\beta$ -diketones contains hydrogen bonds and for the study of these systems no techniques are better than those of vibrational spectroscopy. Each component of the keto-enol equilibrium should be observable, and by means of isotopic substitution it should be possible unambiguously to assign all the motions which involve the hydrogen atoms. Correlations of IR band changes,  $D_n$ , and band intensities with hydrogen bond lengths, energies and chemical shifts, enables a great deal of information to be got from the vibrational spectrum that cannot be obtained in other ways. **Figure 19** shows the most interested vibrations.

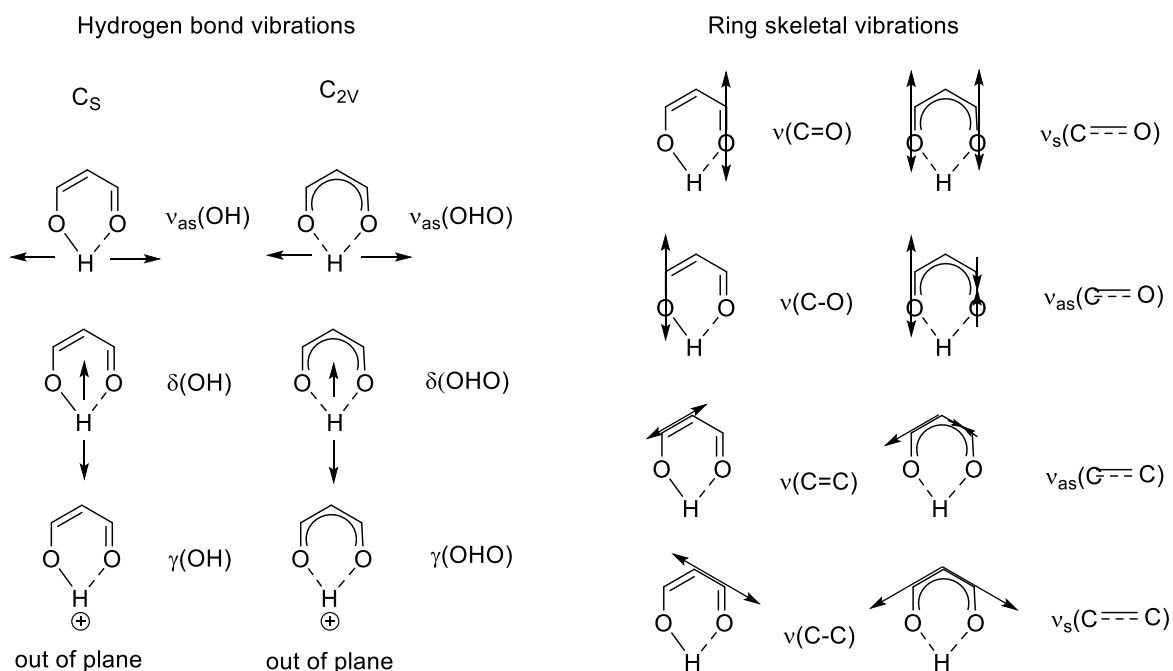


Figure 19 Vibrational modes of the cis enol tautomer ring

The most comprehensive analysis of  $\beta$ -diketones proves the  $C_s$  symmetry is the correct one for the  $\beta$ -diketones involving  $CH_3$ , Ph and  $CF_3$  groups. The band assignments are given in **Table 1**.

Table 1 Vibrational band frequencies for selected  $\beta$ -diketones ( $cm^{-1}$ ) [89].

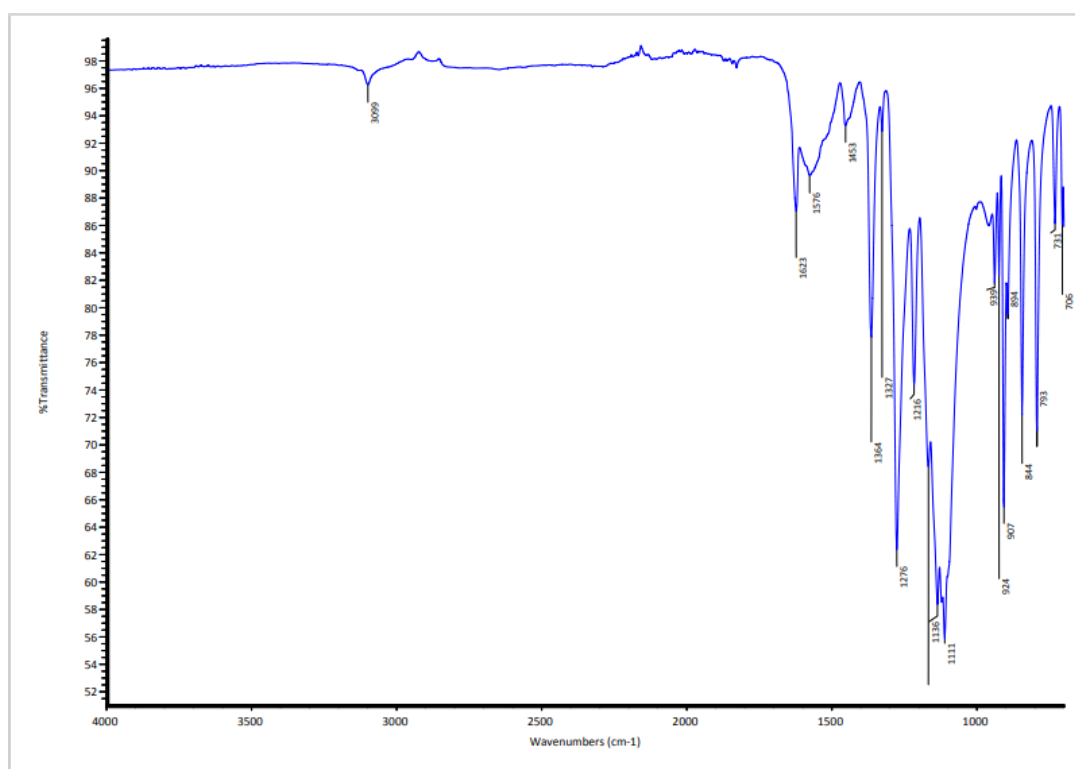
$\beta$ -diketones	$\nu_{as}(OH)$	$\gamma(OH)$	$\nu(C=O)$	$\nu(C-O)$	$\nu(C=C)$	$\nu(C-C)$
AA	2750	957	1625	1460	1600	1298
BA	2650	952	1605	1458	1580	1274
DBM	2620	975	1560	1470	1560	1282
TFAA	2900	892	1660	1427	1600	1277
HFAA	3000	856	1692	1440	1632	1289

AA = acetylacetone; BA = benzoylacetone; DBM = dibenzoylmethane; TFAA = trifluoroacetylacetone; HFAA = hexafluoroacetylacetone.

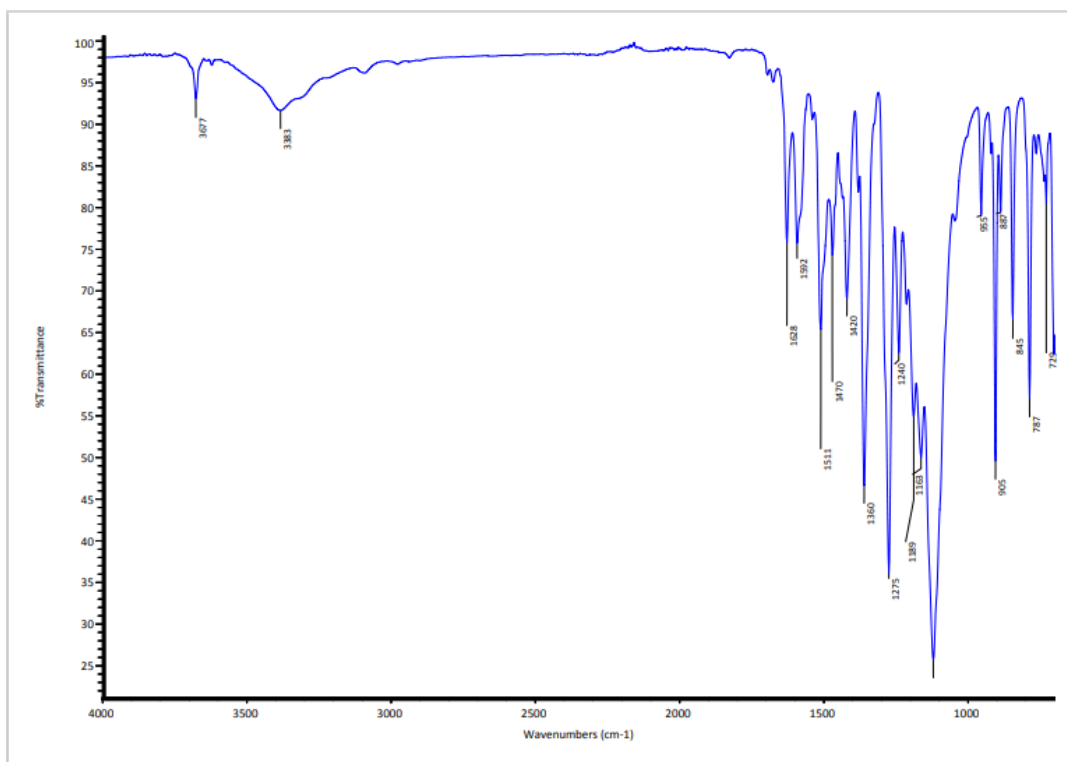
An interesting feature of the IR bands of hydrogen bonds is their broadness and intensity. For the  $\nu_{as}(OH)$  bands the intensity is not particularly strong but their broadness is, and the width at half band height of this band in acetylacetone, is nearly  $1000\text{ cm}^{-1}$ . It has, however, been noted that intensity decreases as the symmetry and strength increases, and in some cases the  $\nu_{as}(OH)$  is indistinguishable from the background noise [91, 94].

The IR spectra of  $\text{HL}^{\text{CF}_3}$  ligand was carried out on solid sample and it shows all the expected absorption band: weak absorptions in the range  $3099\text{ cm}^{-1}$  due to the C-H bonds; medium absorptions at  $1623$  and  $1576\text{ cm}^{-1}$ , due to the stretching vibrations of the C=O.

The  $^1\text{H-NMR}$  spectrum of  $\text{NaL}^{\text{CF}_3}$  was recorded in DMSO solution. It has shown a single set of resonances for the two CH protons in *ortho*- and in *para*-positions of aromatic rings at  $8.48$  and  $8.08\text{ ppm}$ , respectively. The presence of the monoanionic form was furthermore confirmed by the absence in the spectra recorded in aprotic solvents of the OH proton. In addition, in the IR spectrum the stretching vibrations of the C=O groups are shifted at  $1628\text{ cm}^{-1}$  (**Figure 20**).



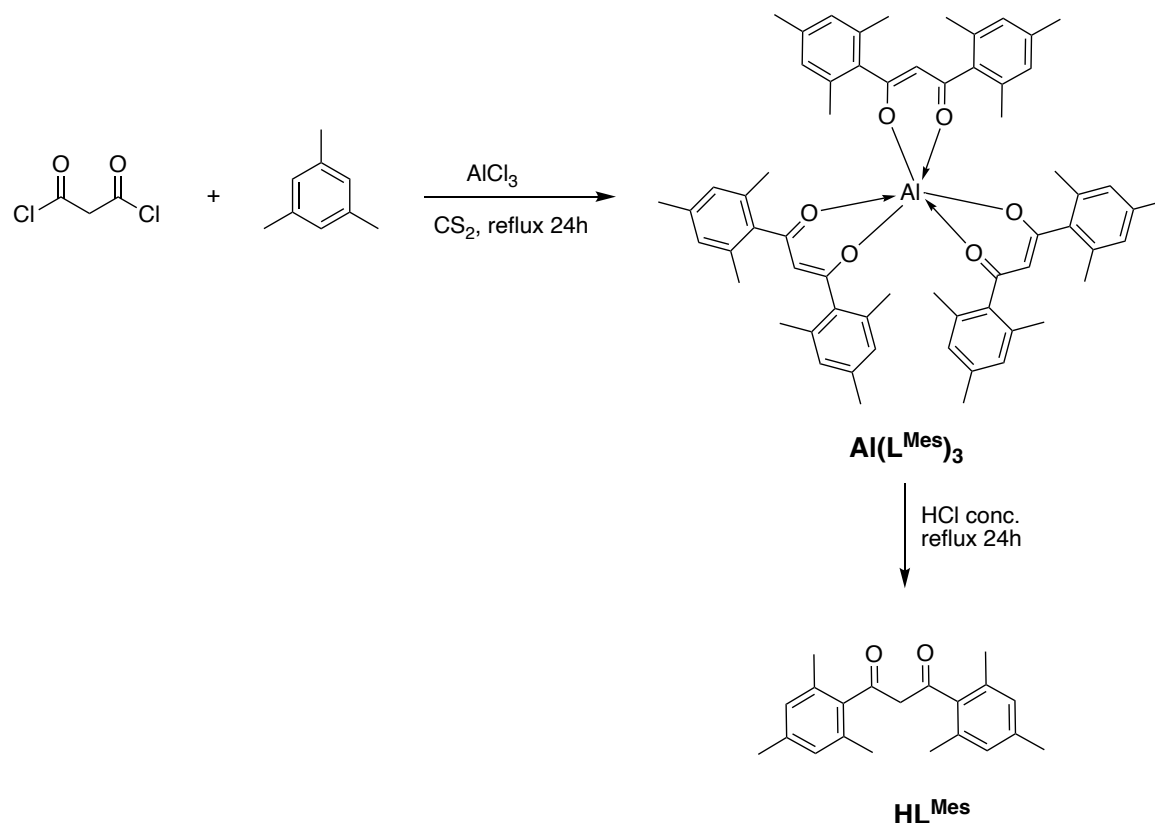
(a)



(b)

Figure 20 IR spectra of (a) HL<sup>CF3</sup> and (b) NaL<sup>CF3</sup>

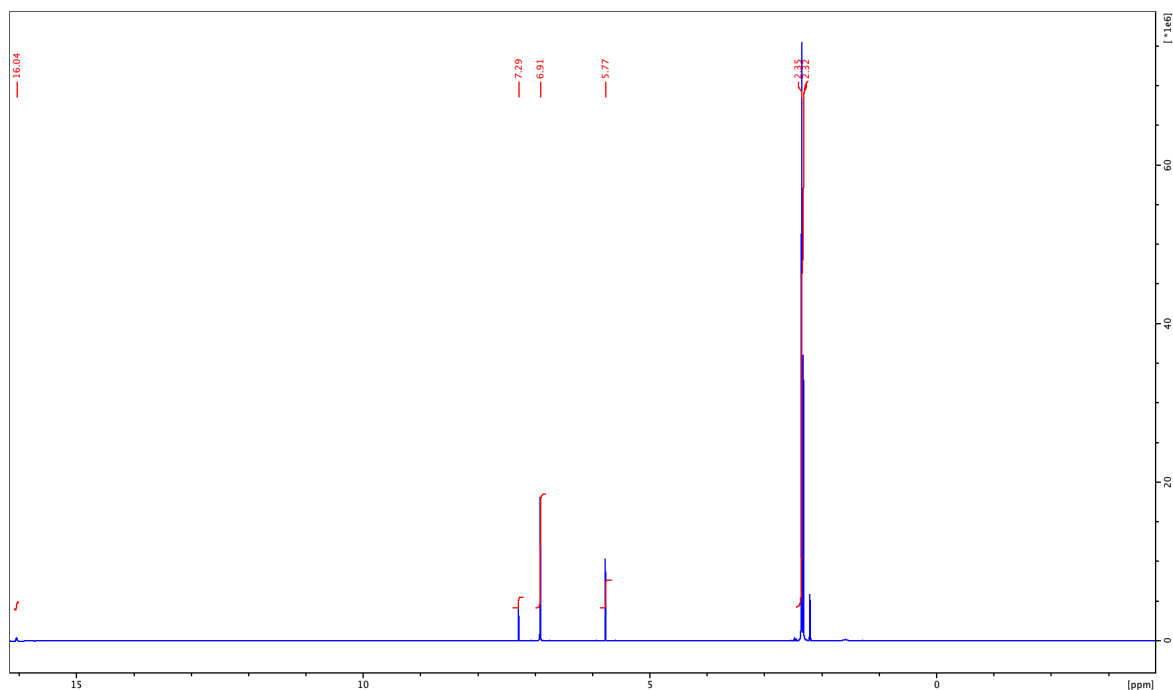
Following the method used for 1,3-bis(3,5-bis(trifluoromethyl)phenyl)propane-1,3-dione, we attempted to synthesize the 1,3-dimesityl-propane-1,3-dione compound by condensation of 2,4,6-trimethylbenzaldehyde with 2,4,6-trimethylacetophenone. However, the two reactants did not undergo condensation. We attributed the difficulty of the condensation of the two trimethyl-substituted starting materials to the high steric hindrance of the six methyl groups. As an alternative approach, we have chosen the Friedel-Crafts reaction for the synthesis of HL<sup>Mes</sup> (**3**). The synthesis began from the reaction of malonyl dichloride with mesitylene in the presence of anhydrous aluminum chloride, followed by treatment with HCl/ice (**Scheme 14**) [95].



**Scheme 14** Synthesis of 1,3-dimesityl-propane-1,3-dione  $\text{HL}^{\text{Mes}}$  (**3**)

The  $\text{Al}(\text{L}^{\text{Mes}})_3$  complex was obtained in very high yield, and it was fully characterized by FT-IR,  $^1\text{H}$ -,  $^{13}\text{C}$ -NMR and electrospray ionization mass spectrometry (ESI-MS). According to literature reports [95, 96], diketones can be obtained by acidification of the intermediate with HCl/ice. Under such mild conditions the Al(III) complex remained intact, probably due to the stability of the complex gained from the six-membered ring chelation together with the ligand steric protection. To promote the dissociation of the  $\text{Al}(\text{L}^{\text{Mes}})_3$  complex and the formation of the product, concentrated HCl was used, and the mixture was heated to reflux for 24 h under stirring. The desired 1,3-dimesityl-propane-1,3-dione ( $\text{HL}^{\text{Mes}}$ ) was then isolated in good yield and characterized by elemental analysis, FT-IR,  $^1\text{H}$ -,  $^{13}\text{C}$ -NMR and electrospray ionization mass spectrometry (ESI-MS).

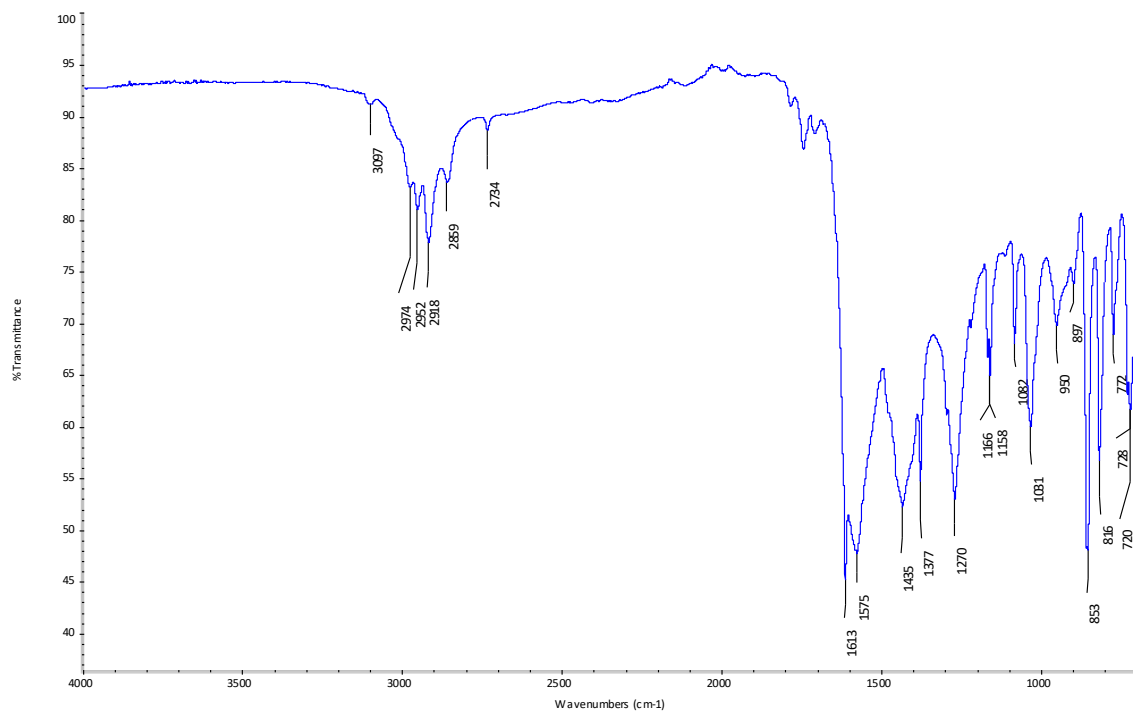
The  $^1\text{H}$ -NMR spectrum of  $\text{HL}^{\text{Mes}}$  in  $\text{CDCl}_3$  showed the characteristic enolic proton absorptions at around 16.04 ppm, the 2-CH proton at 5.77 ppm, the -CH<sub>3</sub> protons in the range 2.32-2.35 ppm and the aromatic meta-CH protons at 6.91 ppm. The 2-CH<sub>2</sub> protons of the keto form are not visible, which is an indication that the enol tautomer is the most dominant form in  $\text{CDCl}_3$  solvent (**Figure 21**).



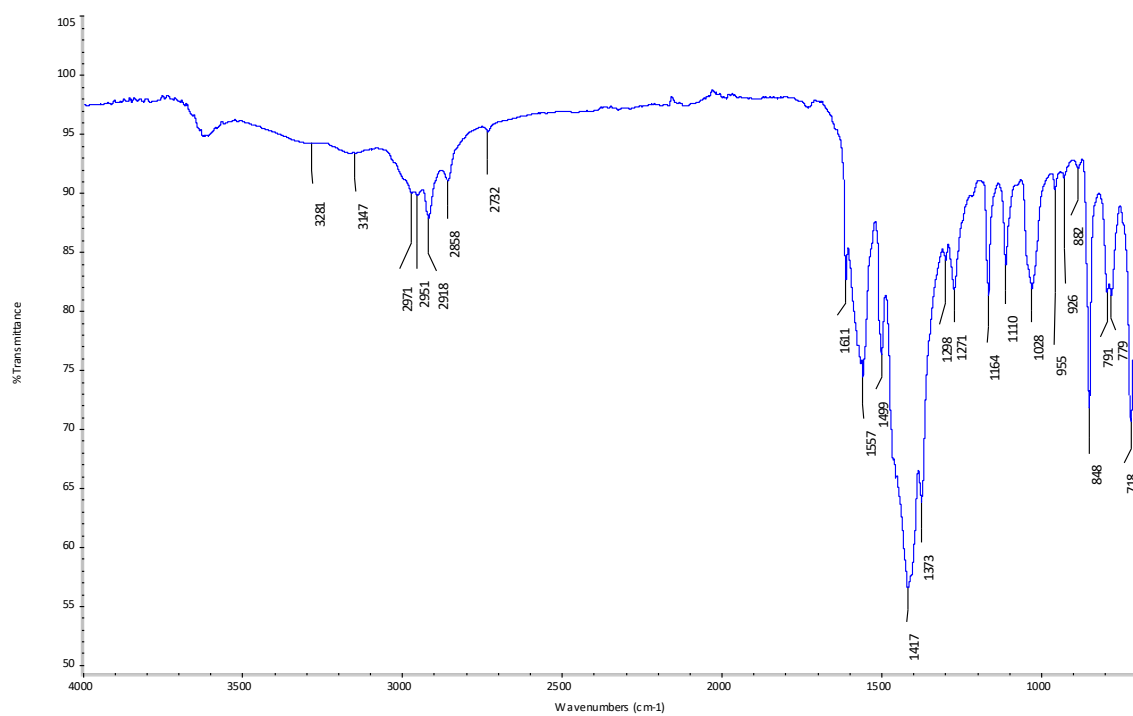
**Figure 21**  $^1\text{H-NMR}$  spectrum of  $\text{HL}^{\text{Mes}}$  in  $\text{CDCl}_3$

The IR spectrum was carried out on the solid sample of  $\text{HL}^{\text{Mes}}$  and it shows all the expected absorption bands. In particular, the band at about  $1613$  and  $1575\text{ cm}^{-1}$  are assigned to the  $\text{C=O}$  carbonyl groups, and the lower frequency band centered at  $1435\text{ cm}^{-1}$  is due to the  $\text{C=C}$  double bond. The frequency band at around  $1270\text{ cm}^{-1}$  can be assigned to the  $\text{C-O}$  vibration (**Figure 22a**).

The sodium salt  $\text{NaL}^{\text{Mes}}\cdot\text{H}_2\text{O}$  (**4**) was obtained by dissolving the  $\text{HL}^{\text{Mes}}$  species in an equimolar quantity of  $\text{NaOH}$  in methanol solution. It was then isolated in high yield and it was characterized by elemental analysis, FT-IR,  $^1\text{H}$ -,  $^{13}\text{C}$ -NMR and electrospray ionization mass spectrometry (ESI-MS). The presence of the monoanionic species was furthermore confirmed by the absence in the spectra recorded in aprotic solvents of  $\text{OH}$  proton. In addition, in the IR spectrum the stretching vibrations of the  $\text{C=O}$  groups are shifted at  $1611$  and  $1557\text{ cm}^{-1}$  (**Figure 22b**).



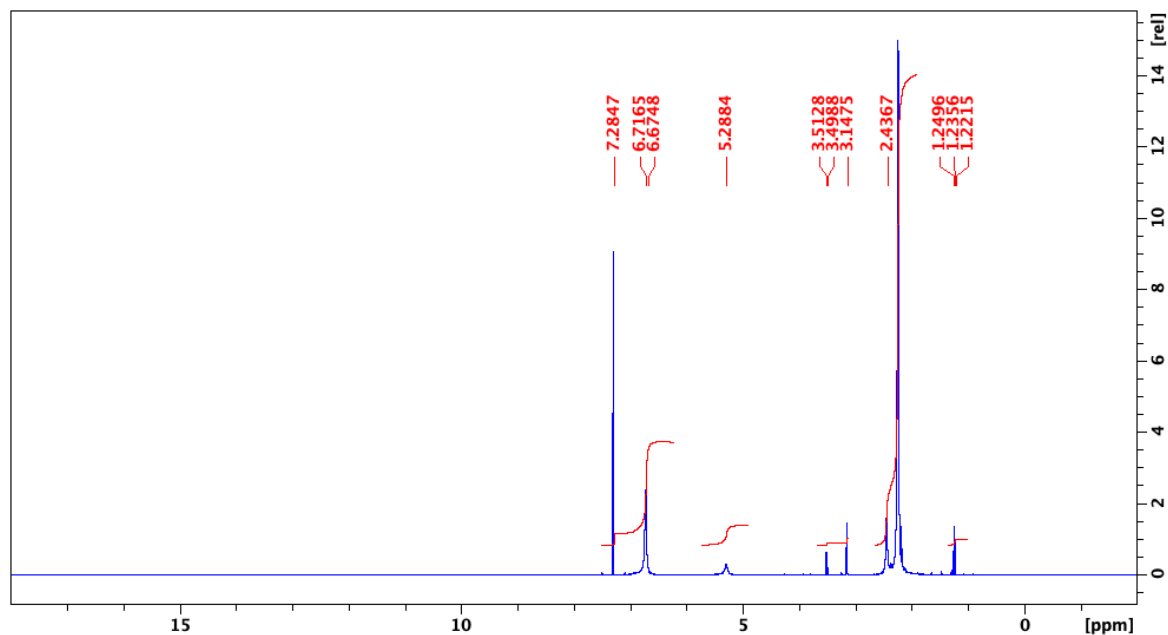
(a)



(b)

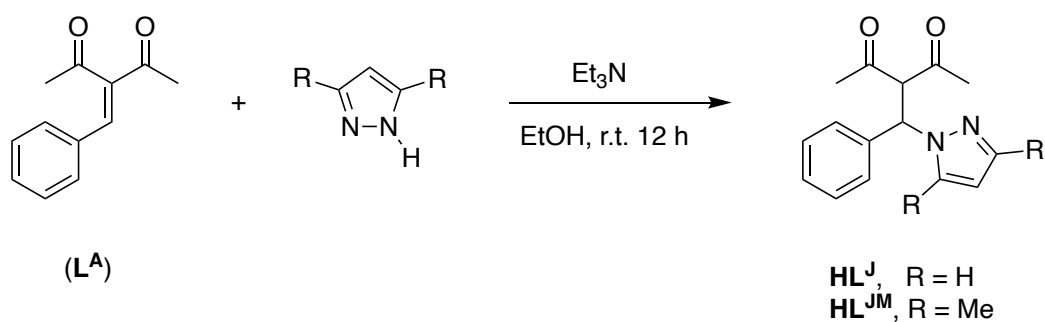
Figure 22 FT-IR spectrum of (a) HLMes and (b) NaLMes.H<sub>2</sub>O.

In **Figure 23** the  $^1\text{H-NMR}$  spectrum of  $\text{NaL}^{\text{Mes}}\cdot\text{H}_2\text{O}$  is reported.



**Figure 23**  $^1\text{H-NMR}$  spectrum of  $\text{NaL}^{\text{Mes}}\cdot\text{H}_2\text{O}$  (**4**) in  $\text{CDCl}_3$  solution

The ligands 3-(phenyl(1*H*-pyrazol-1-yl)methyl)pentane-2,4-dione,  $\text{HL}^{\text{I}}$  (**5**), and the 3-((3,5-dimethyl-1*H*-pyrazol-1-yl)(phenyl)methyl)pentane-2,4-dione,  $\text{HL}^{\text{JM}}$  (**6**), was synthesized in ethanol solution from a mixture of 3-benzylidenepentane-2,4-dione ( $\text{L}^{\text{A}}$ ) and pyrazole or 3,5-dimethyl-pyrazole under basic conditions for triethylamine ( $\text{Et}_3\text{N}$ ) (**Scheme 15**).

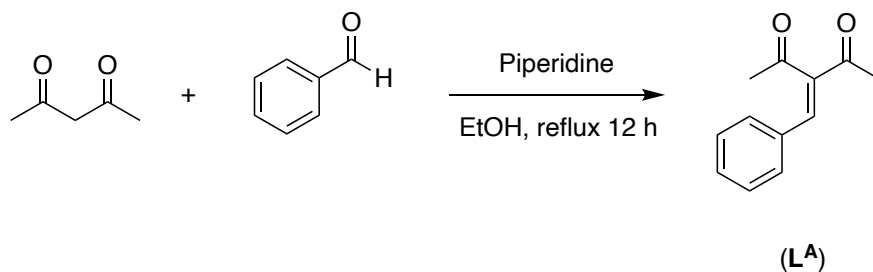


**Scheme 15** Synthetic procedure for the ligands  $\text{HL}^{\text{I}}$  (**5**) and  $\text{HL}^{\text{JM}}$  (**6**)

Pyrazoles add with surprising ease to the  $\alpha$ ,  $\beta$ -unsaturated  $\beta$ -dicarbonyl compound 3-benzylidenepentane-2,4-dione. Spontaneous, weakly exothermic reaction affords the new  $\text{HL}^{\text{I}}$  and  $\text{HL}^{\text{JM}}$  compounds which precipitate from the reaction mixture in very good yield and high purity.



The precursor 3-benzylidene-pentane-2,4-dione (**L<sup>A</sup>**) can be synthesized by Knoevenagel condensation of an equimolar amount of acetylacetone and benzaldehyde in the presence of piperidine as a catalyst (**Scheme 16**).

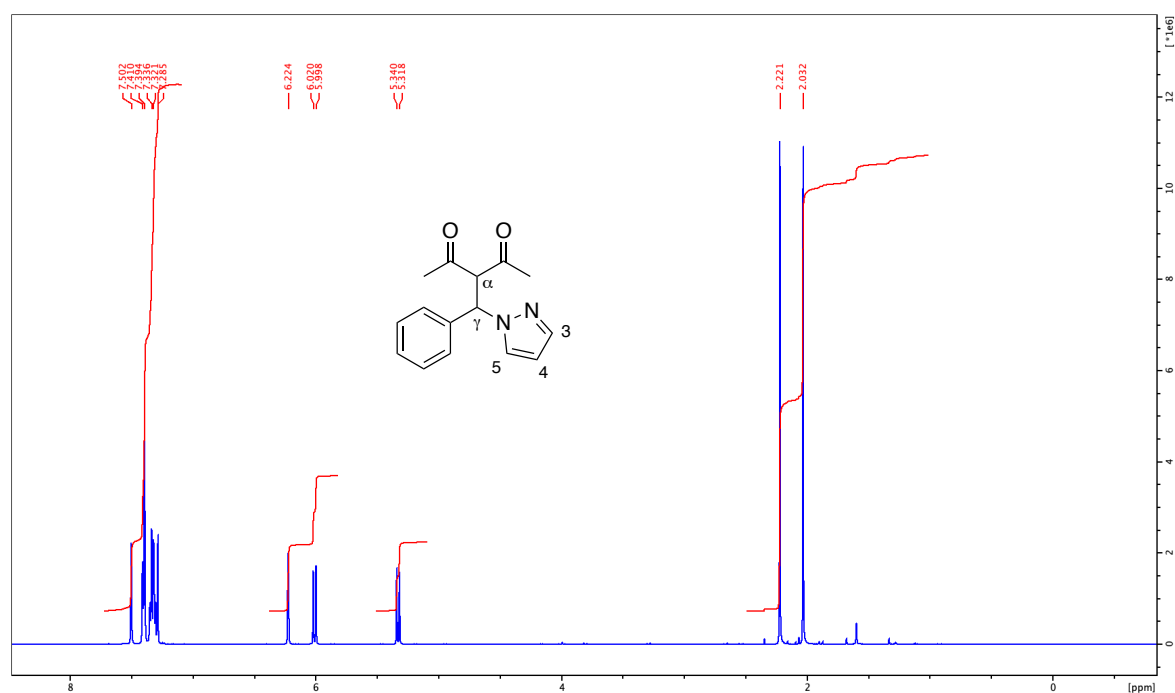


*Scheme 16 Synthetic procedure for the species L<sup>A</sup>*

The new stable species **HL<sup>I</sup>** (**5**) and **HL<sup>M</sup>** (**6**) were characterized by elemental analyses, FT-IR, <sup>1</sup>H-, <sup>13</sup>C-NMR and electrospray ionization mass spectrometry (ESI-MS).

The elemental analysis has confirmed the stoichiometry of the two ligands, showing a good purity of the products, which is also confirmed by the narrow melting points.

The <sup>1</sup>H-NMR spectra of **HL<sup>I</sup>** and **HL<sup>M</sup>** in CDCl<sub>3</sub> suggest the presence of the keto form, 3-(phenyl(1*H*-pyrazol-1-yl)methyl)pentane-2,4-dione and 3-((3,5-dimethyl-1*H*-pyrazol-1-yl)(phenyl)methyl)pentane-2,4-dione, respectively, in solution (**Figures 24** and **25**).



*Figure 24 <sup>1</sup>H-NMR spectrum of HL<sup>I</sup> (5) in CDCl<sub>3</sub> solution*

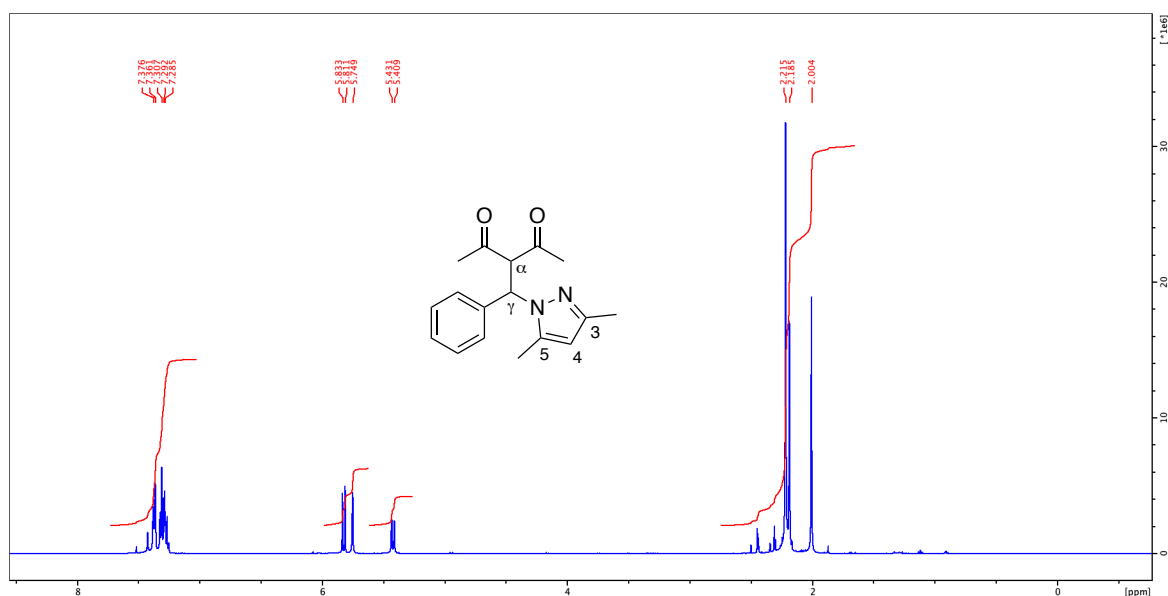


Figure 25 <sup>1</sup>H-NMR spectrum of **HL<sup>JM</sup> (6)** in CDCl<sub>3</sub> solution

In the <sup>1</sup>H-NMR spectrum of **HL<sup>J</sup>**, the 3-CH and 4-CH protons of pyrazole ring are present at 7.50 and 6.22 ppm, respectively. The 5-CH of pyrazole and the CH aromatic protons of the phenyl ring are present in the range 7.32-7.41 ppm. The α-CH and γ-CH bridging proton are present at 5.32 ppm (<sup>3</sup>J = 11.28 Hz) and 6.01 ppm (<sup>3</sup>J = 11.28 Hz). The singlets at 2.22 and 2.03 ppm are attributable to the methyl groups bonded to the β-dicarbonyl moieties.

In the <sup>13</sup>C-NMR spectrum the C=O, α-CH, γ-CH and CH<sub>3</sub> carbons are detectable at 200.3-200.0, 72.6, 64.2 and 29.9-30.9 ppm, respectively. The 4-CH carbon of the pyrazole ring is detectable at 106.10 ppm.

In the <sup>1</sup>H-NMR spectrum of **HL<sup>JM</sup>**, the CH aromatic protons are present in the range 7.28-7.38 ppm and the α-CH and γ-CH bridging proton are present at 5.82 ppm (<sup>3</sup>J = 11.11 Hz) and 5.42 ppm (<sup>3</sup>J = 11.28 Hz). The singlet at 2.21 ppm is attributable to the methyl groups bonded to the β-dicarbonyl moieties. The singlets at 2.00 and 2.18 ppm are attributable to the methyl groups of pyrazole (3-CH<sub>3</sub> and 5-CH<sub>3</sub>) and the 4-CH proton in the pyrazole ring is present as a singlet at 5.75 ppm.

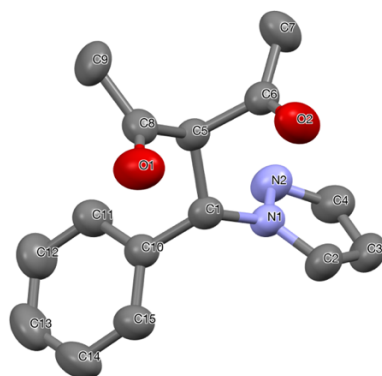
In the <sup>13</sup>C-NMR spectrum the C=O, α-CH, γ-CH and CH<sub>3</sub> carbons are detectable at 199.9-200.9, 72.4, 60.6 and 30.3-31.6 ppm, respectively. The 4-CH carbon of the pyrazole ring is detectable at 105.6 ppm.

The ESI-MS study was performed by dissolving **HL<sup>J</sup>** and **HL<sup>JM</sup>** in CH<sub>3</sub>CN and CH<sub>3</sub>CN, respectively, and recording the spectra in positive- and negative-ion mode. The molecular structure of **HL<sup>J</sup>** was confirmed by the presence of the molecular peaks at *m/z* 257 and 279 respectively, attributable to the [HL<sup>J</sup> + H]<sup>+</sup> and [HL<sup>J</sup> + Na]<sup>+</sup> species.

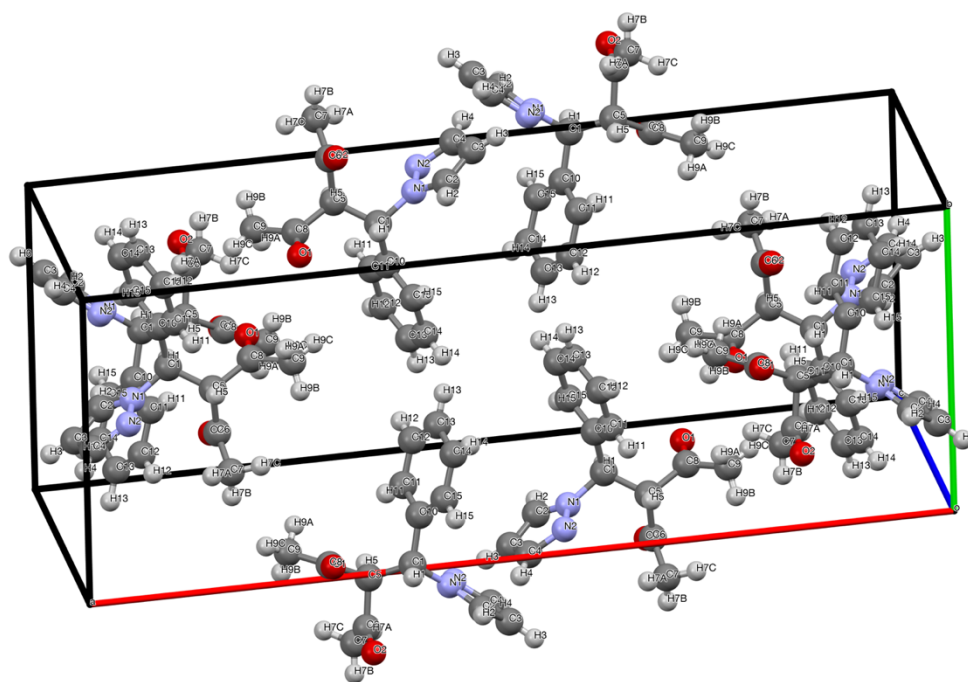
The molecular structure of **HL<sup>JM</sup>** was confirmed by the presence of the molecular peaks at *m/z* 285 and 307 respectively, attributable to the [HL<sup>JM</sup> + H]<sup>+</sup> and [HL<sup>JM</sup> + Na]<sup>+</sup> species.

Slow evaporation of a hexane solution of **HL<sup>I</sup>** afforded a batch of good quality crystals, from which a specimen of 0.60 × 0.38 × 0.22 mm was selected for the X-ray work. The X-ray crystallographic analysis of **HL<sup>I</sup>** was performed by Prof. Alessandro Dolmella of Department of Pharmaceutical and Pharmacological Sciences, University of Padova, using a kappa-geometry Oxford Diffraction Gemini EOS diffractometer, equipped with a 2K × 2K CCD area detector and sealed-tube Enhance (Mo) and (Cu) X-ray sources.

The crystallographic investigation revealed the solid-state molecular structure of the ligand **HL<sup>I</sup>** (**5**). An ORTEP [97, 98] drawing of the ligand is shown in **Figures 26** and **27**.



*Figure 26* ORTEP view of **HL<sup>I</sup>** (**5**) with thermal ellipsoids drawn at the 30% probability level. Hydrogen atoms have been omitted.



*Figure 27* Packing structure view of **HL<sup>I</sup>**.

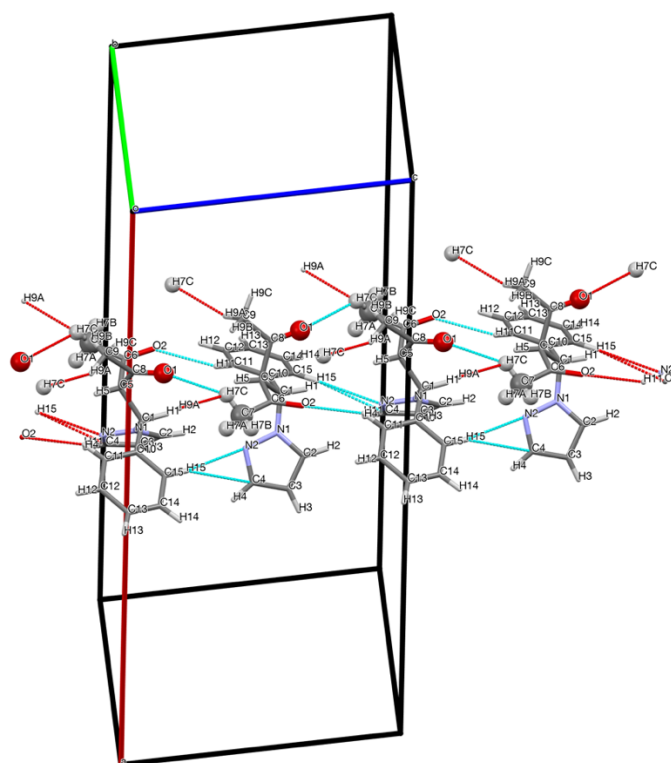


Figure 28 Nonbonding interactions in *HL'*.

The ligand shows two almost perfectly planar pyrazolyl and phenyl rings. The C(8)-O(1) and C(6)-O(2) bonds of 1.194(2) and 1.194(2) Å has instead a clear double bond character. Notably, the two carbonyl C=O moieties are in the cis conformation. Among the two methyl groups, only one has intermolecular O(1)-H(7C) interactions with the carbonyl group of a second molecule present in the same cell unit (**Figure 28**). A complete list of bond distances and angles is given in **Table 2**.

**Table 2** Bond lengths (Å) and angles (°) for compound *HL'*.

Bond lengths (Å)

O1-C8	1.194(2)	C5-C6	1.537(2)
O2-C6	1.1959(19)	C5-C8	1.532(2)
N1-N2	1.3405(18)	C6-C7	1.479(3)
N1-C1	1.4694(19)	C8-C9	1.489(3)
N1-C2	1.338(2)	C10-C11	1.379(2)
N2-C4	1.333(2)	C10-C15	1.383(2)
C1-C5	1.531(2)	C11-C12	1.385(3)
C1-C10	1.519(2)	C12-C13	1.366(3)
C2-C3	1.358(3)	C13-C14	1.364(3)
C3-C4	1.370(3)	C14-C15	1.389(3)

Angles (°)

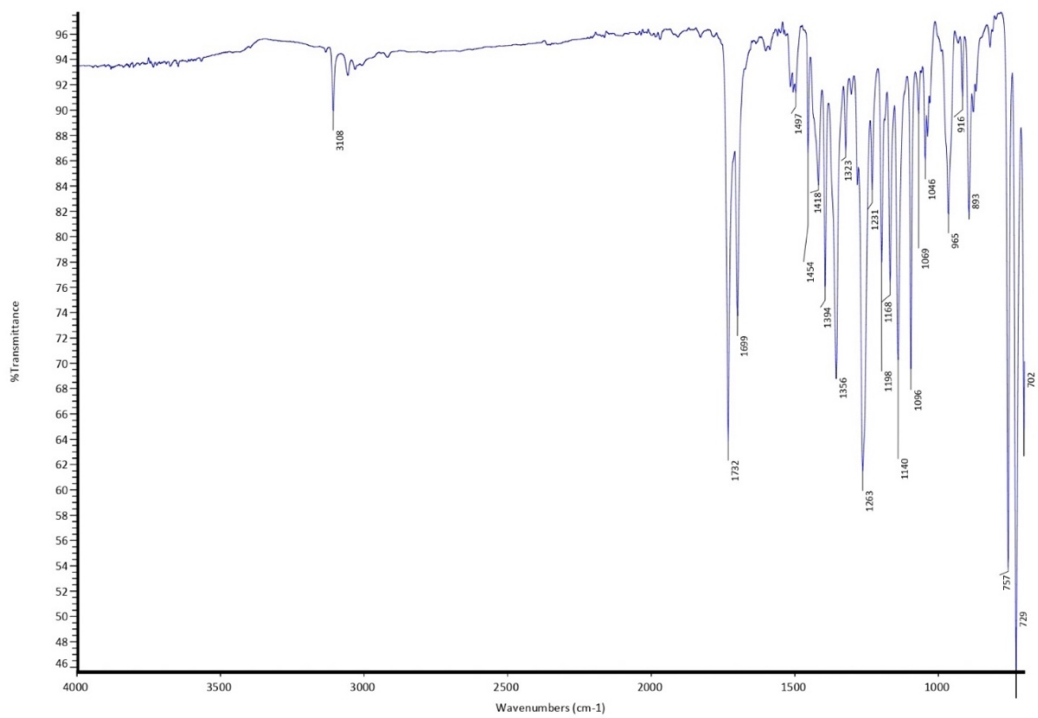
N2-N1-C1	120.54(12)	O2-C6-C7	122.94(16)
C2-N1-N2	112.19(14)	C7-C6-C5	116.90(15)

C2-N1-C1	127.27(14)	O1-C8-C5	120.37(14)
C4-N2-N1	103.66(14)	O1-C8-C9	123.12(17)
N1-C1-C5	109.98(12)	C9-C8-C5	116.46(16)
N1-C1-C10	110.71(12)	C11-C10-C1	123.05(14)
C10-C1-C5	114.08(12)	C11-C10-C15	118.44(16)
N1-C2-C3	107.09(17)	C15-C10-C1	118.48(14)
C2-C3-C4	104.79(16)	C10-C11-C12	120.59(18)
N2-C4-C3	112.27(17)	C13-C12-C11	120.5(2)
C1-C5-C6	110.76(12)	C14-C13-C12	119.7(2)
C1-C5-C8	110.34(13)	C13-C14-C15	120.4(2)
C8-C5-C6	107.38(12)	C10-C15-C14	120.42(19)
O2-C6-C5	120.14(15)		

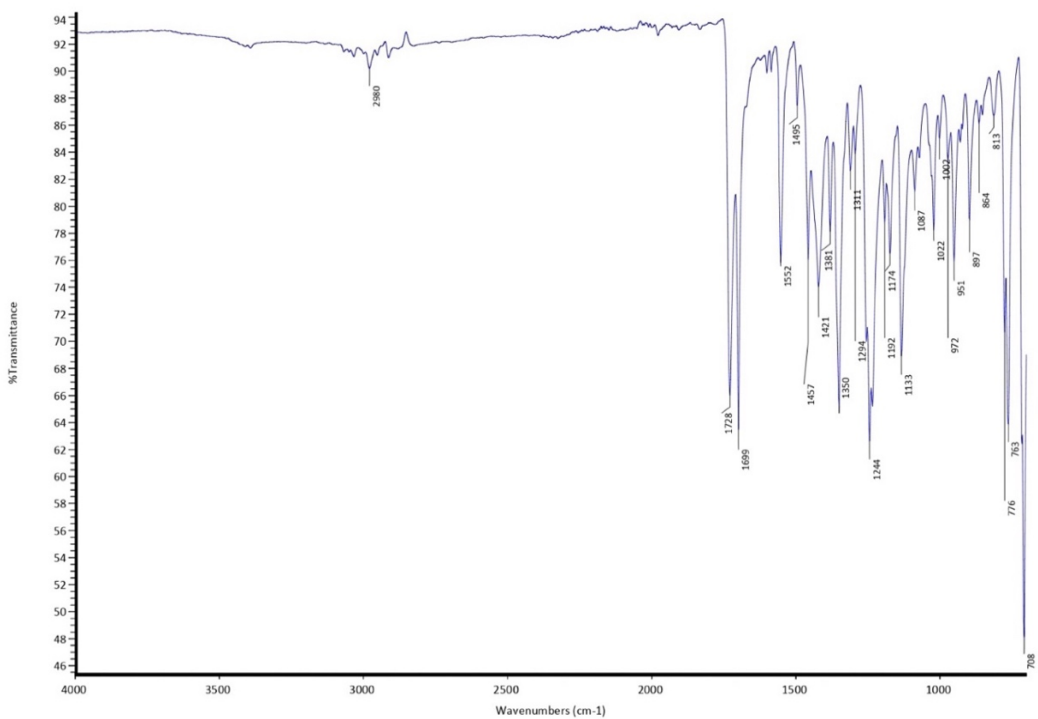
The composition of a  $\beta$ -dicarbonyl system is usually expressed as the molar percentage of the enol tautomer at equilibrium. The amount of enol is influenced by a variety of factors: solvent, temperature, the presence of other species that are capable of hydrogen bonding,  $\beta$ -substituents and  $\alpha$ -substituents. In particular, alkyl substituents on the  $\alpha$  carbon of acetylacetone lead to decreased amounts of enol. However, size alone is not the determining factor: some groups that are bulky, e.g. the chloro group, have the effect of increasing the cis enol. The bulky alkyl groups, *iso*-propyl and *sec*-butyl depressed the % enol almost to zero. A methyl group at the  $\alpha$ -position depresses the % enol not only of acetylacetone, but also of benzoylacetone from 98 to 4%, and dibenzoylmethane from 100 to 0%.

The keto form of  $\beta$ -diketones shows two carbonyl stretching frequencies,  $\nu(\text{C}=\text{O})$ , at ca. 1727 and 1707  $\text{cm}^{-1}$ . These are the in-phase and out-of-phase stretching modes of a molecule in which the dihedral angle between the two C=O groups is ca. 90° [91].

The IR spectra of **HL<sup>I</sup>** and **HL<sup>M</sup>** was carried out on solid samples and they show all the expected absorption bands (**Figure 29**).



(a)



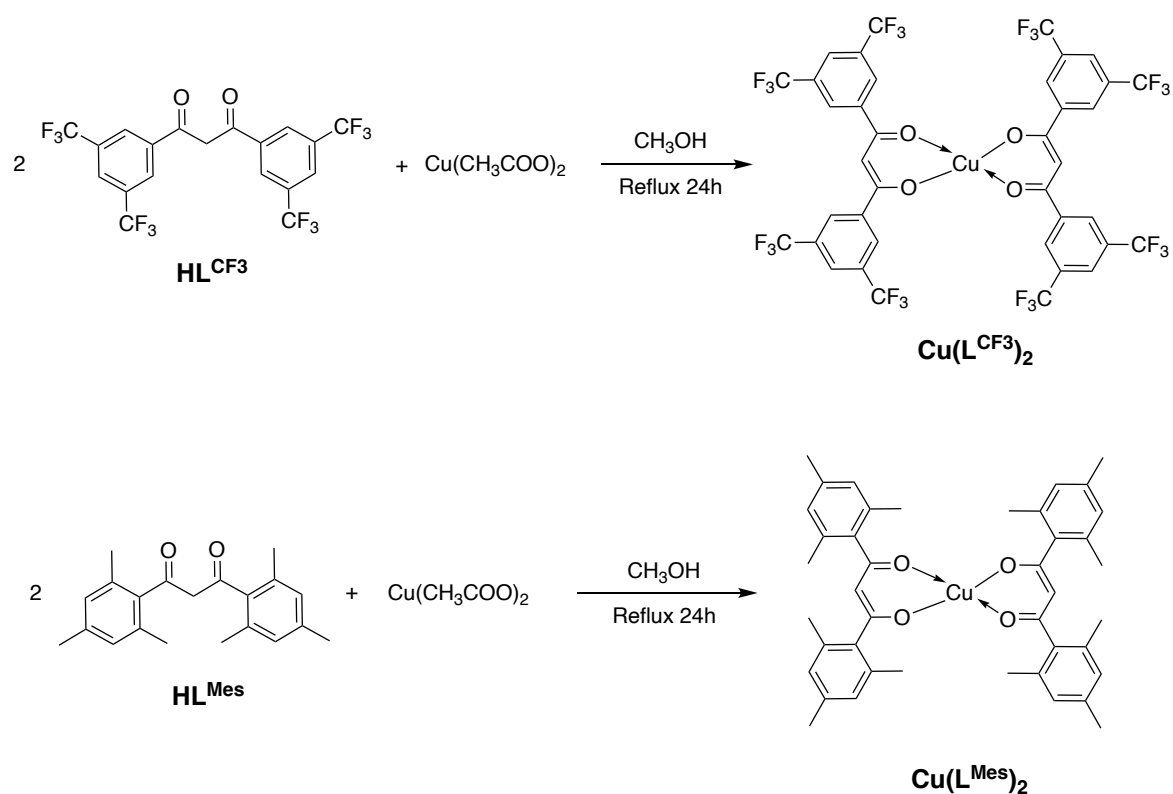
(b)

Figure 29 FT-IR spectrum of (a)  $HL^I$  and (b)  $HL^{IM}$

Weak bands in the region 2980-3108  $\text{cm}^{-1}$  are assigned to C-H stretching vibrations. The ligands also show two sharp strong bands in the regions 1732-1699  $\text{cm}^{-1}$  and 1728-1699  $\text{cm}^{-1}$  attributable to the stretching vibrations of the two carbonyl groups. The two bands at *ca.* 1500  $\text{cm}^{-1}$  correspond to C=C/C=N rings stretching. Bands in the region 1350-1394  $\text{cm}^{-1}$  are assigned to in-plane bending vibrations of the methyl groups. The out-of-plane bending vibrations of the ring C-H bonds are observed in the 776-729  $\text{cm}^{-1}$  region.

### 3.3. Synthesis and characterization of the complexes

The copper(II) complexes  $[\text{Cu}(\text{L}^{\text{CF}_3})_2]$  (**7**) and  $[\text{Cu}(\text{L}^{\text{Mes}})_2]$  (**14**) were synthesized in good yields by dissolving the corresponding ligands  $\text{HL}^{\text{CF}_3}$  (**1**) and  $\text{HL}^{\text{Mes}}$  (**3**) in a  $\text{CH}_3\text{OH}$  solution containing the acceptor  $\text{Cu}(\text{CH}_3\text{COO})_2$  (**Scheme 17**).



*Scheme 17* Synthetic procedure for the Cu(II) complexes of  $\text{Cu}(\text{L}^{\text{CF}_3})_2$  (**7**) and  $\text{Cu}(\text{L}^{\text{Mes}})_2$  (**14**)

A similar procedure was used for the synthesis of the Zn(II) complexes, containing the  $\text{HL}^{\text{CF}_3}$  (**1**) and  $\text{HL}^{\text{Mes}}$  ligands (**3**), obtaining the corresponding species  $[\text{Zn}(\text{L}^{\text{CF}_3})_2]$  (**9**) and  $[\text{Zn}(\text{L}^{\text{Mes}})_2]$  (**15**).

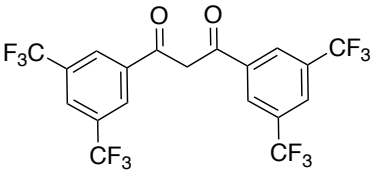
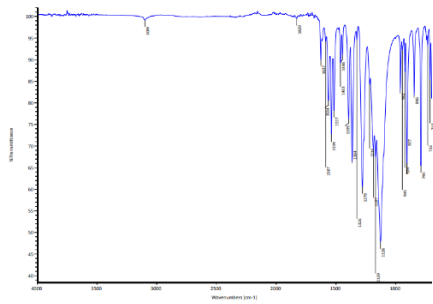
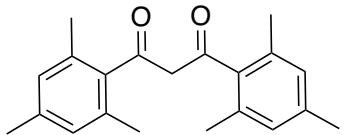
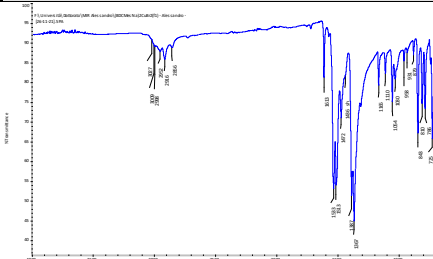
The elemental analyses have confirmed the stoichiometry of the complexes **7**, **9**, **14** and **15**, showing a good purity of the products, which is also confirmed by the narrow melting points.

The IR spectra were carried out on solid samples of **7**, **9**, **14** and **15**. They have shown all the expected absorption bands; in particular, absorptions in the range 3356-2858  $\text{cm}^{-1}$  due to the C-H bonds; medium absorptions in the range 1629-1533  $\text{cm}^{-1}$ , due to the asymmetric stretching of the C=O groups; absorptions in the range 1564-1503  $\text{cm}^{-1}$ , attributable to the C=C/C=N double bonds.

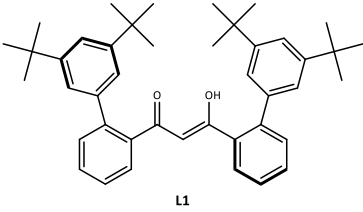
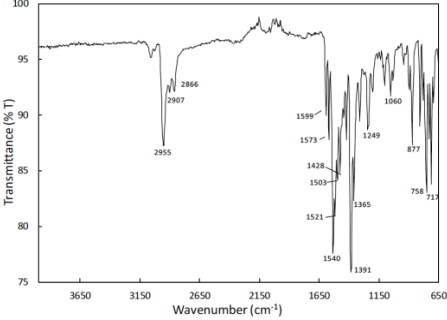
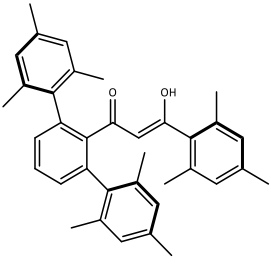
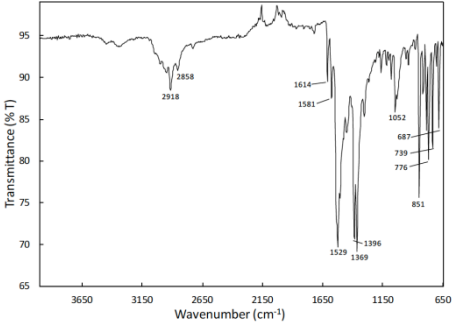
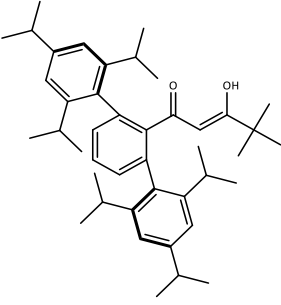
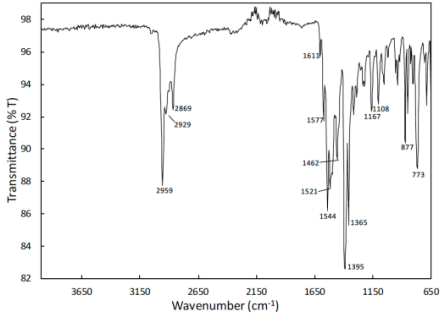
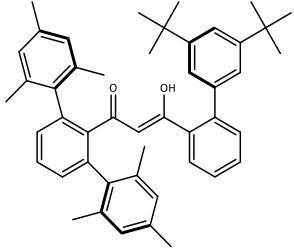
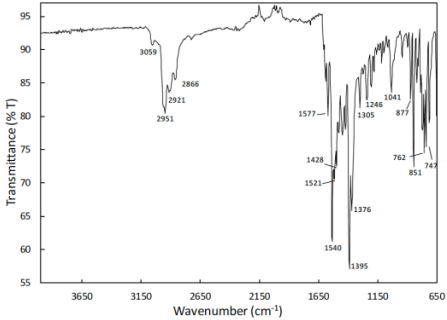
The ligand coordination sites involved in bonding with the metal ions were determined by careful comparison of the infrared absorption bands of the complexes with those of the parent ligands  $\text{HL}^{\text{CF}_3}$  and  $\text{HL}^{\text{Me}_s}$ . The relevant changes were the following: a frequency shift (4-6  $\text{cm}^{-1}$ ) in the energy carbonyl vibration; shifts to lower frequencies (3-10  $\text{cm}^{-1}$ ) in the C-C stretching of the methyl group in-plane bending vibrations. All these shifts suggest coordination of the ligand as an enolate. The 3556-2858  $\text{cm}^{-1}$  region of the spectra of all complexes shows broad bands, which may be due to lattice and/or coordinated water molecules associated with the complexes.

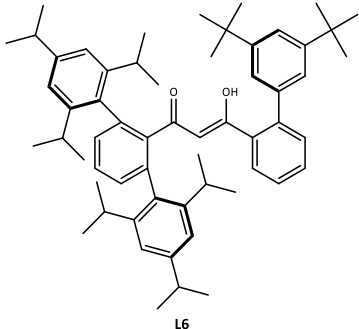
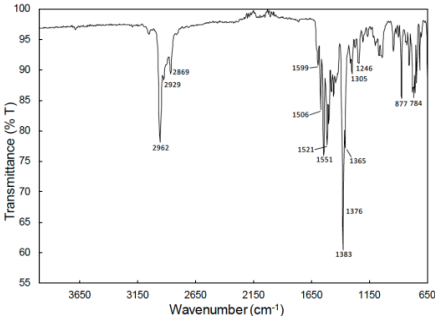
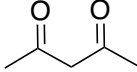
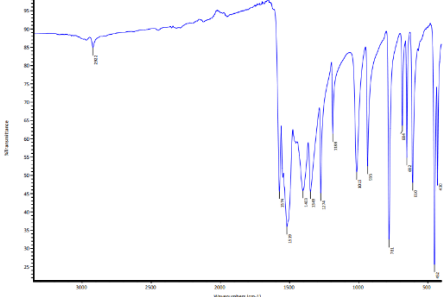
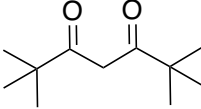
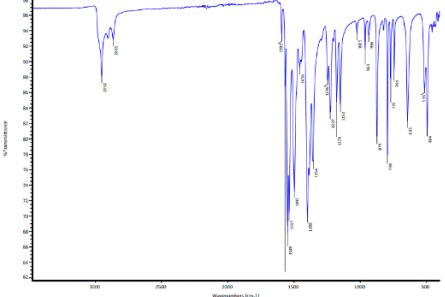
The carbonyl stretching frequencies fall in a similar range and suggest little sensitivity to steric or electronic properties. These values are comparable with those reported in the literature by various authors for analogues Cu(II) complexes supported by bulky  $\beta$ -diketones (**Table 3**).

**Table 3** Stretching absorptions of the C=O bond in Cu(II) complexes of  $\beta$ -diketones [Cu(L)<sub>2</sub>]

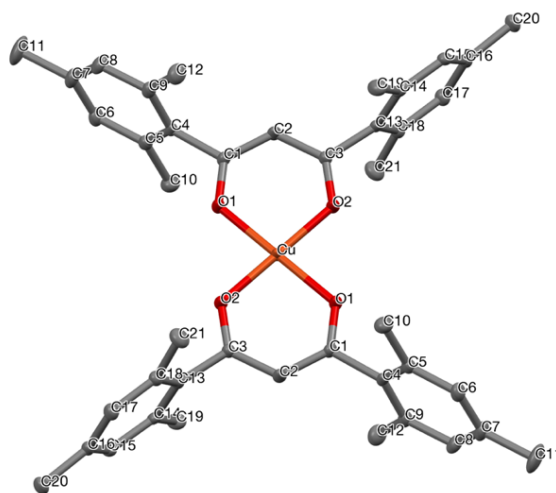
Ligand	$\nu(\text{C}=\text{O}) \text{ cm}^{-1}$	IR spectra	Ref.
	1623, 1576		
	1613, 1533		



Ligand	$\nu(\text{C}=\text{O}) \text{ cm}^{-1}$	IR spectra	Ref.
 <p style="text-align: center;"><b>L1</b></p>	1599, 1573		[59]
 <p style="text-align: center;"><b>L3</b></p>	1614, 1581		[59]
 <p style="text-align: center;"><b>L4</b></p>	1611, 1577		[59]
 <p style="text-align: center;"><b>L5</b></p>	1580, 1577		[59]

Ligand	$\nu(\text{C}=\text{O}) \text{ cm}^{-1}$	IR spectra	Ref.
 <p style="text-align: center;"><b>L6</b></p>	1599, 1572		[59]
	1574, 1519		[99]
	1549, 1537		[59]

Slow evaporation of a chloroform/hexane solution of  $[\text{Cu}(\text{L}^{\text{Mes}})_2]$  (**14**) complex afforded a batch of good quality crystals useful for the X-ray work. The X-ray crystallographic analysis was performed by Prof. Rasika Dias of Department of Chemistry and Biochemistry, The University of Texas at Arlington, USA. The crystallographic investigation revealed the solid-state molecular structure of the  $[\text{Cu}(\text{L}^{\text{Mes}})_2]$  complex. An ORTEP [97, 98] drawing of complex (**14**) is shown in **Figure 30**.



**Figure 30** ORTEP view of  $[\text{Cu}(\text{L}^{\text{Mes}})_2]$  complex (**14**) with thermal ellipsoids drawn at the 30% probability level. Hydrogen atoms have been omitted.

The neutral complex  $\text{Cu}(\text{L}^{\text{Mes}})_2$  shows a stoichiometric ratio of 1:2 between the metal and the ligand, with the Cu(II) center chelated by four oxygen atoms of two deprotonated  $\text{L}^{\text{Mes}}$  ligands in the enolic form. The two chelated rings  $\text{Cu}-\text{O}(1)-\text{C}(1)-\text{C}(2)-\text{C}(3)-\text{O}(2)$  are almost perfectly coplanar and symmetrical with respect to the metal center. A selected list of bond distances and angles is given in **Table 4**.

**Table 4** Selected bond lengths (Å) and angles (°) for compound  $\text{Cu}(\text{L}^{\text{Mes}})_2$

Bond lengths (Å)

Cu-O1	1.9166(9)
Cu-O2	1.9071(9)
O1-C1	1.2763(15)
O2-C3	1.2768(15)
C1-C2	1.3973(18)
C2-C3	1.3967(17)

Angles (°)


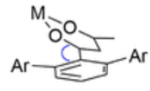
O1-Cu-O1	180.0
O2-Cu-O1	93.67(4)
O2-Cu-O1	86.33(4)
O2-Cu-O2	180.0
C1-O1-Cu	125.70(8)

C3-O2-Cu	125.98(8)
O1-C1-C2	125.33(12)
C3-C2-C1	123.88(12)
O2-C3-C2	125.28(12)

Copper(II)  $\beta$ -diketonates have a particularly regular structure across dozens of crystallographic examples [100]. Complexes exhibit nearly identical, coplanar chelate rings irrespective from steric or electronic properties of substituents.

Among the four known complexes  $\text{Cu}(\text{L}^{\text{Me}})_2$  [101],  $\text{Cu}(\text{L}^{\text{Me,Ph}})_2$  [102],  $\text{Cu}(\text{L}^{\text{Ph}})_2$  [103] e  $\text{Cu}(\text{L}^{\text{tBu}})_2$  [104], the  $\text{Cu}(\text{L}^{\text{Me}})_2$  complex has the longest Cu-O bonds, while  $\text{Cu}(\text{L}^{\text{tBu}})_2$  has the shortest, on average (**Table 5**).

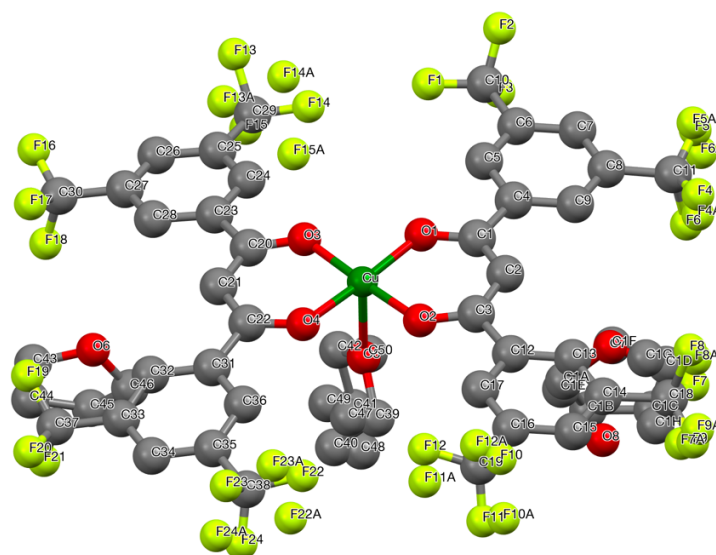
**Table 5** Selected bond angles and lengths as determined from X-ray crystallography for new and common complexes

Bond lengths (Å)				Angles (°)	
					
Complex	M–O	C–O	C–C	O–Cu–O	 Aryl-chelate dihedral
$\text{Cu}(\text{L}^{\text{Me}})_2$	1.9268(16), 1.9227(16)	1.276(3), 1.275(3)	1.403(3), 1.402(3)	93.75(7)	
$\text{Cu}(\text{L}^{\text{Me,Ph}})_2$	1.924(3), 1.918(3)	1.270(5), 1.269(5)	1.400(6), 1.405(6)	93.16(13)	14.79
$\text{Cu}(\text{L}^{\text{Ph}})_2$	1.907(4), 1.910(5)	1.285(3), 1.260(2)	1.397(3), 1.393(4)	93.30(13)	10.56
$\text{Cu}(\text{L}^{\text{tBu}})_2$	1.902(2), 1.891(2)	1.273(3), 1.276(4)	1.376(5), 1.395(5)	92.80(10)	
$\text{Cu}(\text{L}^{\text{Mes}})_2$	1.9071(9), 1.9166(9)	1.2763(15), 1.27668(15)	1.3973(18)	93.67(4), 86.33(4)	89.92

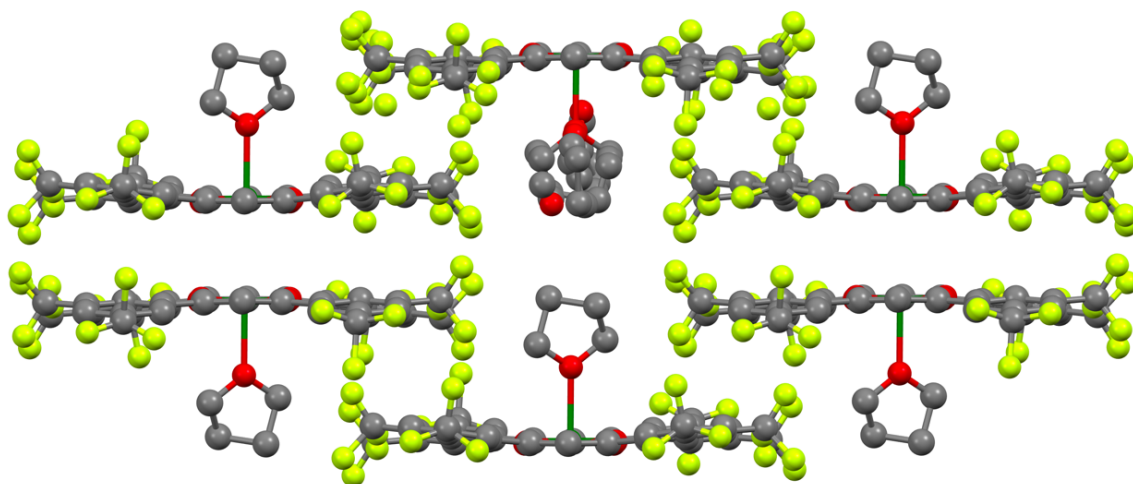
This length also decreases as the methyl groups are exchanged for phenyl, as indicated by  $\text{Cu}(\text{L}^{\text{Me,Ph}})_2$  and  $\text{Cu}(\text{L}^{\text{Ph}})_2$ . Another trend with substitution can be found in the chelate fold angles, decreasing similarly. The C–C and C–O bond lengths are indifferent to substitution, although  $\text{Cu}(\text{L}^{\text{Ph}})_2$  has a notable difference between its C–O bonds because the aryl substituents enjoy conjugation to the diketonate. In the case of  $\text{Cu}(\text{L}^{\text{Me,Ph}})_2$  and  $\text{Cu}(\text{L}^{\text{Ph}})_2$  a coplanar arrangement of the aryl and chelate rings is preferred to enjoy conjugation; however, the phenyl groups show a slight deviation from coplanarity. All four complexes are square planar. The chelate rings are highly symmetric, with many pairs of bond lengths within experimental error of each other.

Unlike the other aryl-substituted complexes, the  $\text{Cu}(\text{L}^{\text{Mes}})_2$  complex (**14**) shows a dihedral angle between the aromatic rings and the chelated ring of  $89.92^\circ$ , indicating an almost complete absence of conjugation between the aromatic and  $\beta$ -diketone rings. This rare behavior, peculiar to the mesitylene groups, can be attributed to their high steric demanding.

Slow evaporation of a chloroform/acetone/THF solution of  $[\text{Cu}(\text{L}^{\text{CF}_3})_2]$  (**7**) afforded a batch of good quality crystals useful for the X-ray investigation. The X-ray crystallographic analysis was performed by Prof. Rasika Dias of Department of Chemistry and Biochemistry, at the University of Texas at Arlington, USA. The preliminary crystallographic investigation revealed the solid-state molecular structure of  $[\text{Cu}(\text{L}^{\text{CF}_3})_2]\cdot\text{THF}$  that is reported in **Figure 31**. A packing structure view of  $[\text{Cu}(\text{L}^{\text{CF}_3})_2]\cdot\text{THF}$  is shown in **Figure 32**.

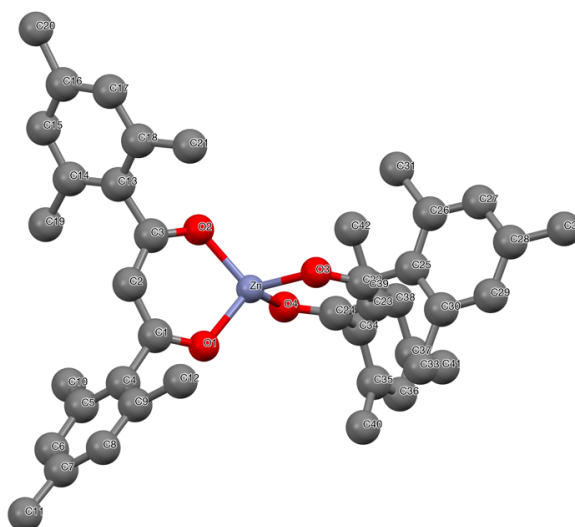


*Figure 31* Solid-state molecular structure of  $[\text{Cu}(\text{L}^{\text{CF}_3})_2]\cdot\text{THF}$



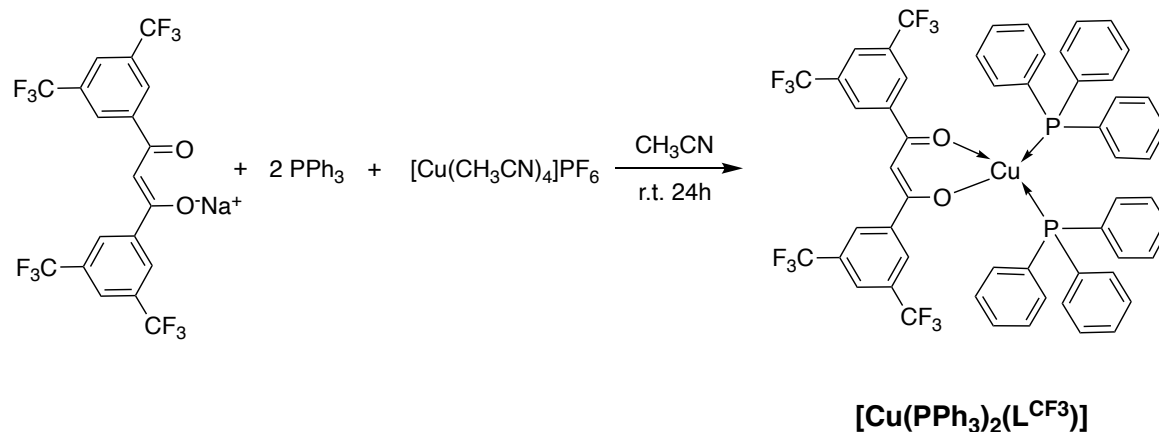
*Figure 32 Packing structure view of  $[\text{Cu}(\text{L}^{\text{CF}_3})_2]\cdot\text{THF}$*

Slow evaporation of a hexane solution of  $[\text{Zn}(\text{L}^{\text{Mes}})_2]$  (**15**) complex afforded a batch of good quality crystals useful for the X-ray investigation. The X-ray crystallographic analysis was performed by Prof. Rasika Dias of Department of Chemistry and Biochemistry, at the University of Texas at Arlington, USA. The preliminary crystallographic investigation revealed the solid-state molecular structure of  $[\text{Zn}(\text{L}^{\text{Mes}})_2]$  (**15**) that is reported in **Figure 33**.



*Figure 33 Solid-state molecular structure of  $[\text{Zn}(\text{L}^{\text{Mes}})_2]$  (**15**) complex*

The Cu(I) complex  $[\text{Cu}(\text{PPh}_3)_2(\text{L}^{\text{CF}_3})]$  (**8**) was prepared from the reaction of  $\text{PPh}_3$ ,  $\text{Cu}(\text{CH}_3\text{CN})_4\text{PF}_6$  and the sodium salt  $\text{NaL}^{\text{CF}_3}$  (Scheme 18).



*Scheme 18* Synthesis of the complex  $[\text{Cu}(\text{PPh}_3)_2(\text{L}^{\text{CF}_3})]$  (**8**)

Compound **8** is soluble in common organic solvents such as MeOH,  $\text{CHCl}_3$ ,  $\text{CH}_3\text{CN}$  and DMSO. The IR spectrum carried out on a solid sample of **8** shows all the expected bands for the  $\beta$ -diketone ligand and the triphenylphosphine co-ligand. The absorptions due to the C=O stretching are at  $1625\text{--}1581\text{ cm}^{-1}$ ; they don't significantly vary with respect to the same absorptions of the carbonyl group detectable in the spectrum of the free ligand ( $1623\text{--}1576\text{ cm}^{-1}$ ). The  $^1\text{H-NMR}$  spectrum of the Cu(I) complex, recorded in  $\text{CDCl}_3$  solution at room temperature, shows a single set of resonances for the  $\beta$ -diketone moiety, indicating that the protons of the aromatic rings are equivalents, with a slight shift due to the coordination to the metal center. The  $\text{PPh}_3$  co-ligand showed a characteristic series of peaks in the range  $7.22\text{--}7.42\text{ ppm}$ , with an integration, with respect to the ligand peaks, which confirms the 1:2 stoichiometric ratio between the  $\beta$ -diketone ligand and the phosphane co-ligand. The  $^{31}\text{P}\{\text{H}\}$ -NMR spectrum at 223 K of **8** recorded in  $\text{CDCl}_3$  solution at 223 K, gave a broad single signal at  $-3.683\text{ ppm}$  downfield shifted with respect to the value of the free phosphane ( $\delta = -5.36\text{ ppm}$ ) (Figure 34).

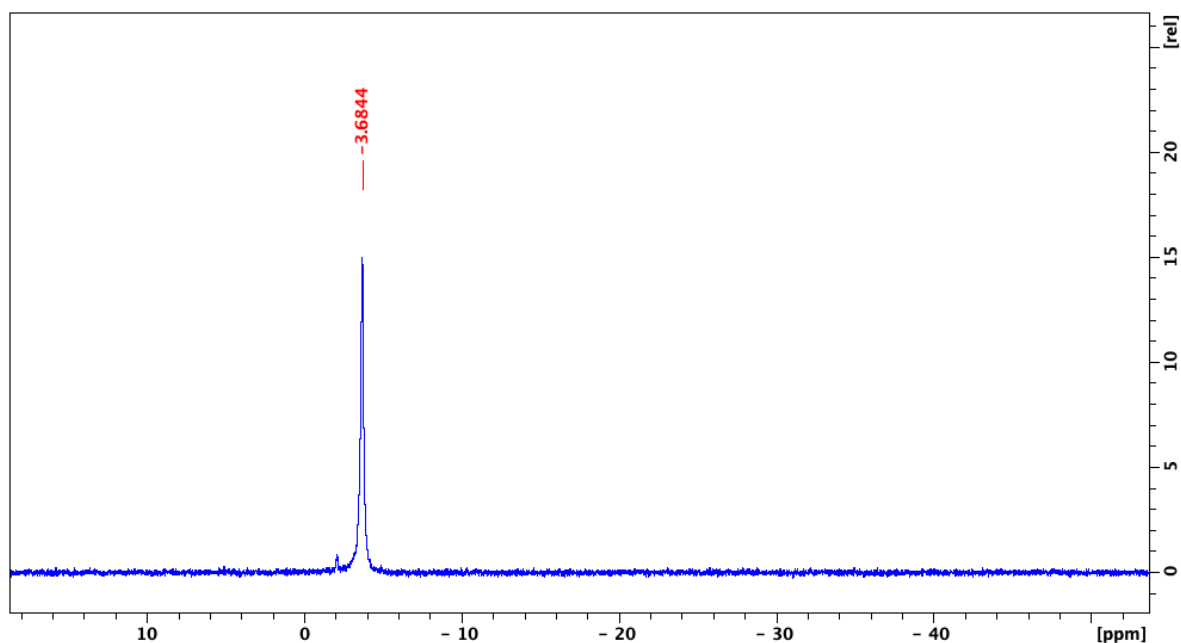


Figure 34  $^{31}\text{P}\{^1\text{H}\}$ -NMR spectrum of complex **8** in  $\text{CDCl}_3$  at 223 K

The ESI-MS study was performed by dissolving **8** in  $\text{CH}_3\text{CN}$  and recording the spectrum in positive-ion mode. The molecular structure of **8** was confirmed by the presence of the molecular peaks at  $m/z$  366 and 586, attributable to the  $[\text{Cu}(\text{PPh}_3) + \text{CH}_3\text{CN}]^+$  and  $[(\text{Cu}(\text{PPh}_3)_2)]^+$  species, being positive fragments of the dissociation of the ligand from the complex.

Slow evaporation of an ethanol/acetone solution of  $[\text{Cu}(\text{PPh}_3)_2(\text{L}^{\text{CF}_3})]$  (**8**) complex afforded a batch of good quality crystals useful for the X-ray investigation. The X-ray crystallographic analysis was performed by Prof. Rasika Dias of Department of Chemistry and Biochemistry, at the University of Texas at Arlington, USA. The preliminary crystallographic investigation revealed the solid-state molecular structure of  $[\text{Cu}(\text{PPh}_3)_2(\text{L}^{\text{CF}_3})]$  (**8**) that is shown in **Figure 35**.

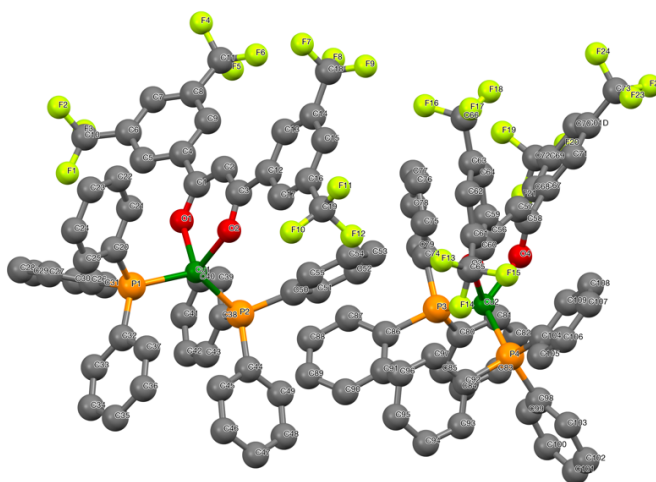
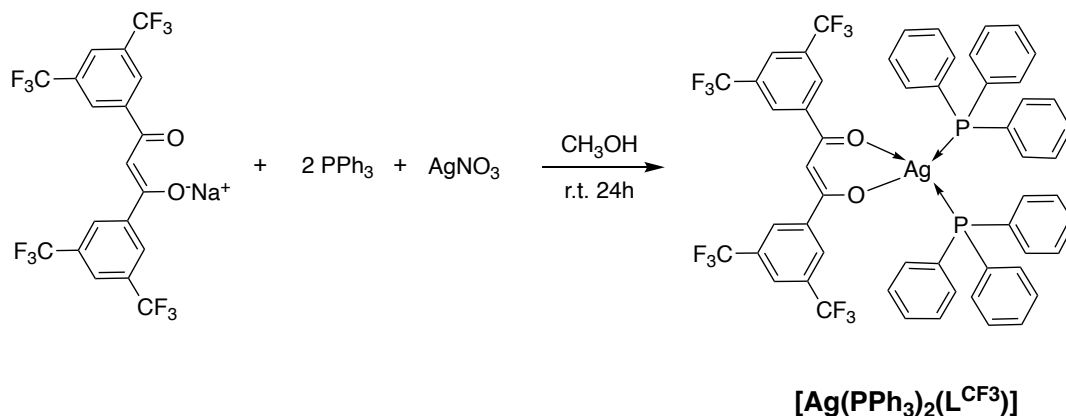


Figure 35 Solid-state molecular structure of  $[\text{Cu}(\text{PPh}_3)_2(\text{L}^{\text{CF}_3})]$  (**8**) complex



The Ag(I) complex  $[\text{Ag}(\text{PPh}_3)_2(\text{L}^{\text{CF}_3})]$  (**10**) was prepared from the reaction of  $\text{PPh}_3$ ,  $\text{AgNO}_3$  and the sodium salt  $\text{NaL}^{\text{CF}_3}$  (Scheme 19).



*Scheme 19* Synthesis of the complex  $[\text{Ag}(\text{PPh}_3)_2(\text{LCF}_3)]$  (**10**)

Compound **10** is soluble in common organic solvents such as MeOH,  $\text{CHCl}_3$ ,  $\text{CH}_3\text{CN}$  and DMSO. The IR spectrum carried out on a solid sample of **10** shows all the expected bands for the  $\beta$ -diketone ligand and the triphenylphosphine co-ligand. The absorptions due to the C=O stretching are at  $1626\text{--}1579\text{ cm}^{-1}$ ; they don't significantly vary with respect to the same absorptions of the carbonyl group detectable in the spectrum of the free ligand.

The  $^1\text{H-NMR}$  spectrum of the Ag(I) complex **10**, recorded in  $\text{CDCl}_3$  solution at room temperature, showed a single set of resonances for the  $\beta$ -diketone moiety, indicating that the protons of aromatic rings are equivalents, with a slight shift due to the coordination to the metal center. The  $\text{PPh}_3$  co-ligand showed a characteristic series of peaks at  $\delta$  7.29–7.46 ppm, with an integration, with respect to the ligand peaks, which confirms the 1:2 stoichiometric ratio between the  $\beta$ -diketone ligand and the phosphane co-ligand.

The  $^{31}\text{P}\{^1\text{H}\}$ -NMR spectrum of **10** was recorded at 223 K in  $\text{CDCl}_3$  solution. In the spectrum of **10** (Figure 36) we observed a doublet of doublet centered at 9.64 ppm with coupling constants  $J(^{107}\text{Ag}\text{--}^{31}\text{P}) = 432$  and  $J(^{109}\text{Ag}\text{--}^{31}\text{P}) = 499$  Hz. These values have confirmed the coordination of two phosphanes to the metal centre; in addition, the ratio between these two coupling constants values is in accordance with the gyromagnetic ratio of silver.

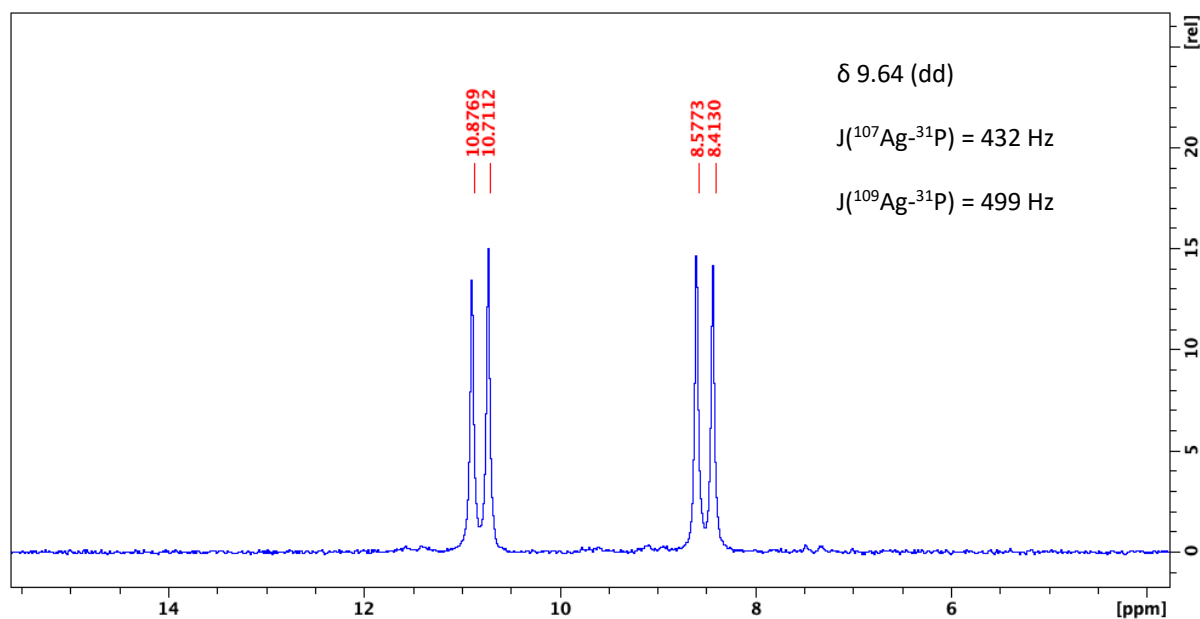


Figure 36  $^{31}\text{P}\{^1\text{H}\}$ -NMR spectrum of complex **10** in  $\text{CDCl}_3$  at 223 K

The new  $\beta$ -diketone ligands 3-(phenyl(1*H*-pyrazol-1-yl)methyl)pentane-2,4-dione (**L<sup>I</sup>**) and 3-((3,5-dimethyl-1*H*-pyrazol-1-yl)(phenyl)methyl)pentane-2,4-dione (**L<sup>IM</sup>**) having additional pyrazoles are really versatile N,O,O-donors because they can provide different hapticities, depending on the type of coordination environment of the metal (**Figure 37**).

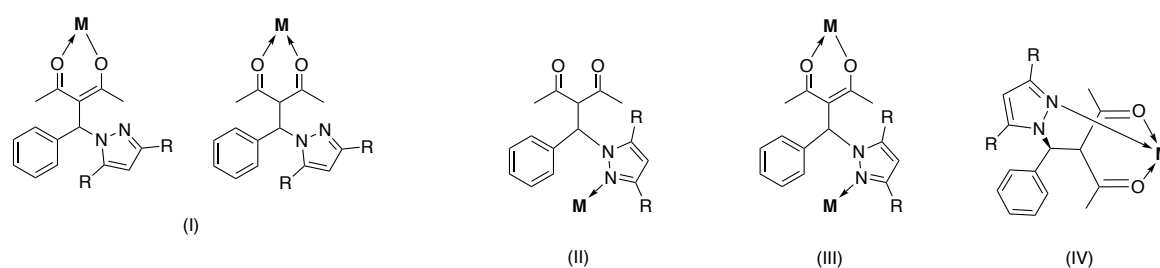
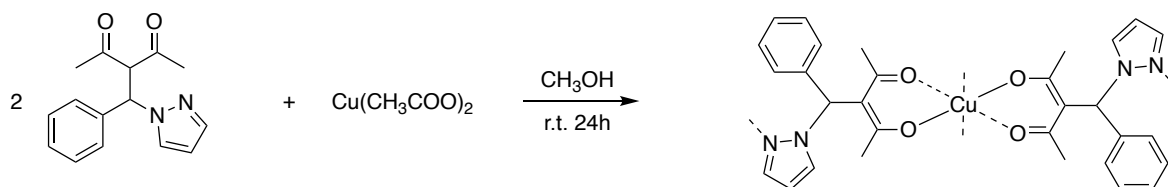


Figure 37 Coordination modes of **L<sup>I</sup>** and **L<sup>IM</sup>** ligands (**L<sup>I</sup>**: R = H; **L<sup>IM</sup>**: R = Me)

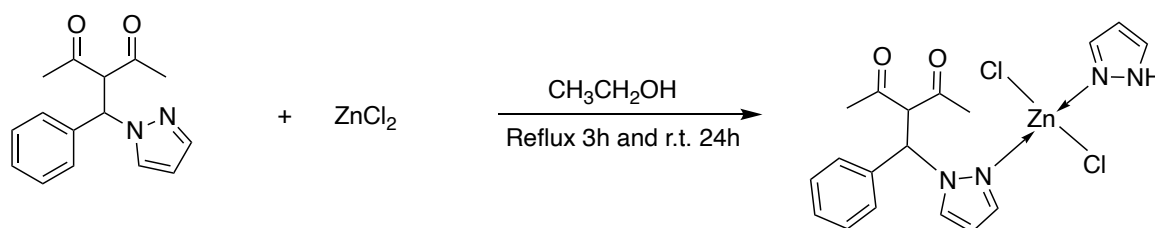
Among the classic coordination modes of  $\beta$ -diketones (Figure 4 and 5), these ligands could be coordinated to metal ions in both neutral (keto) or mono-anionic (enol) form, as  $\kappa^2$ -O,O-chelating symmetrical or not-symmetrical donors (**Figure 37 I**). In addition, they could engage the nitrogen atom of the heterocycle acting as N-monodentate ligand (**Figure 37 II**) or engaging both the two oxygen atoms of the carbonyl groups and the nitrogen atom of the pyrazole moiety acting as N,O,O-bridging ligand (**Figure 37 III**). In the neutral keto-form they could be also coordinated in the  $\kappa^3$ -N,O,O-tridentate form typical of “scorpionates” (**Figure 37 IV**).

The copper(II) complex  $[Cu(L^I)_2]$  (**11**) was synthesized in good yields by dissolving the corresponding ligand  $HL^I$  (**5**) in a  $CH_3OH$  solution containing the  $Cu(CH_3COO)_2$  acceptor (**Scheme 20**).



**Scheme 20** Synthetic procedure for the  $Cu(L^I)_2$  complex (**11**)

A different procedure was used for the synthesis of the Zn(II) complexes, containing the  $HL^I$  ligand obtaining the corresponding species  $Zn(HL^I)(HPz)Cl_2$  (**13**) (**Scheme 21**).



**Scheme 21** Synthetic procedure for the  $Zn(HL^I)(HPz)Cl_2$  (**13**) complex

The elemental analyses have confirmed the stoichiometry of the complexes **11** and **13** showing a good purity of the products, which is also confirmed by the narrow melting points.

The IR spectra was carried out on solid samples of **11** and **13**. They have shown all the expected absorption bands; in particular, absorptions in the range  $3300-2916\text{ cm}^{-1}$  due to the C-H bonds; strong absorptions in the range  $1732-1700\text{ cm}^{-1}$ , due to the asymmetric stretching of the C=O groups. The ligand coordination sites involved in bonding with the metal ions have been determined by careful comparison of the infrared absorption bands of the complexes with those of the related ligands  $HL^I$ . The relevant changes were the following: a little shift to lower frequency in the energy carbonyl vibration; shifts to lower frequencies ( $6-15\text{ cm}^{-1}$ ) in the C-C stretching of the methyl group in-plane bending vibrations. All these shifts could suggest coordination of the ligand in the keto form. The absorptions of carbonyl stretching vary little with respect to the same absorptions of the carbonyl group detectable in the spectrum of the free ligand ( $1732-1699\text{ cm}^{-1}$ ), therefore a coordination involving the nitrogen of pyrazole in the ligand moiety is also plausible.

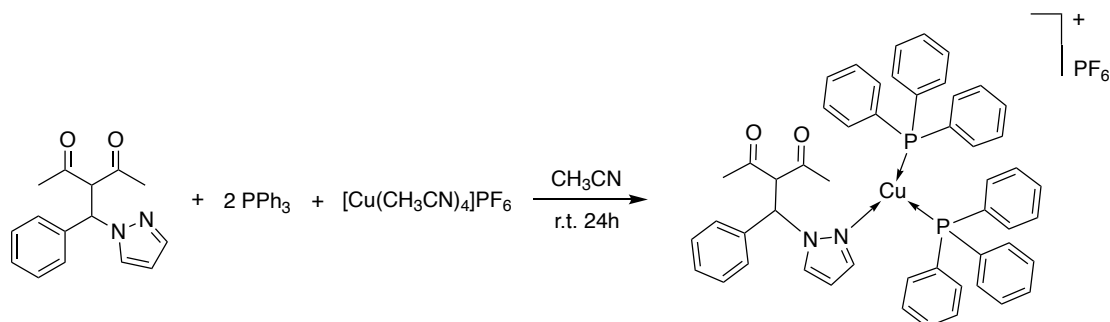
In the  $^1H$ -NMR spectrum, recorded in  $CD_3CN$  for complex **13**, the 3-CH and 4-CH protons of the pyrazole ring are present at 7.63 and 6.25 ppm, respectively. The 5-CH proton of the pyrazole and the CH aromatic protons of the

phenyl ring are present in the range 7.35-7.49 ppm. The  $\alpha$ -CH and  $\gamma$ -CH bridging protons are present at 5.47 ppm ( $^3J = 11.28$  Hz) and 6.12 ppm ( $^3J = 11.28$  Hz). The singlets at 2.18 and 2.06 ppm are attributable to the methyl groups bonded to the  $\beta$ -dicarbonyl moieties. The signal at 6.57 (4-CH), the broad doublet at 7.86 (3- and 5-CH) and the singlet at 11.69 (NH) show the presence of another pyrazole moiety in the complex. This pyrazole moiety is probably due to the decomposition of the ligand in solution in these specific reaction conditions. Therefore, the low yield for the synthesis of **13** could confirm this assumption.

The ESI-MS study was performed by dissolving complexes **11** and **13** in CH<sub>3</sub>CN, recording the spectra in positive- and negative-ion mode. The molecular structure of **11** was confirmed by the presence of the molecular peaks at  $m/z$  318 and 360 respectively, attributable to the [Cu(L<sup>I</sup>)]<sup>+</sup> and [Cu(L<sup>I</sup>) + CH<sub>3</sub>CN]<sup>+</sup> species.

The molecular structure of **13** was confirmed by the presence of the molecular peaks at  $m/z$  257, 279 and 355 respectively, attributable to the [L<sup>I</sup>H + H]<sup>+</sup>, [Zn(L<sup>I</sup> - Ph) + Cl]<sup>+</sup> and [Zn(HL<sup>I</sup>) + Cl]<sup>+</sup> species. The ESI-MS spectrum of **13** in CH<sub>3</sub>CN recorded in negative-ion mode shows peak at  $m/z$  171 attributable to the [2Pz + Cl]<sup>-</sup> aggregate.

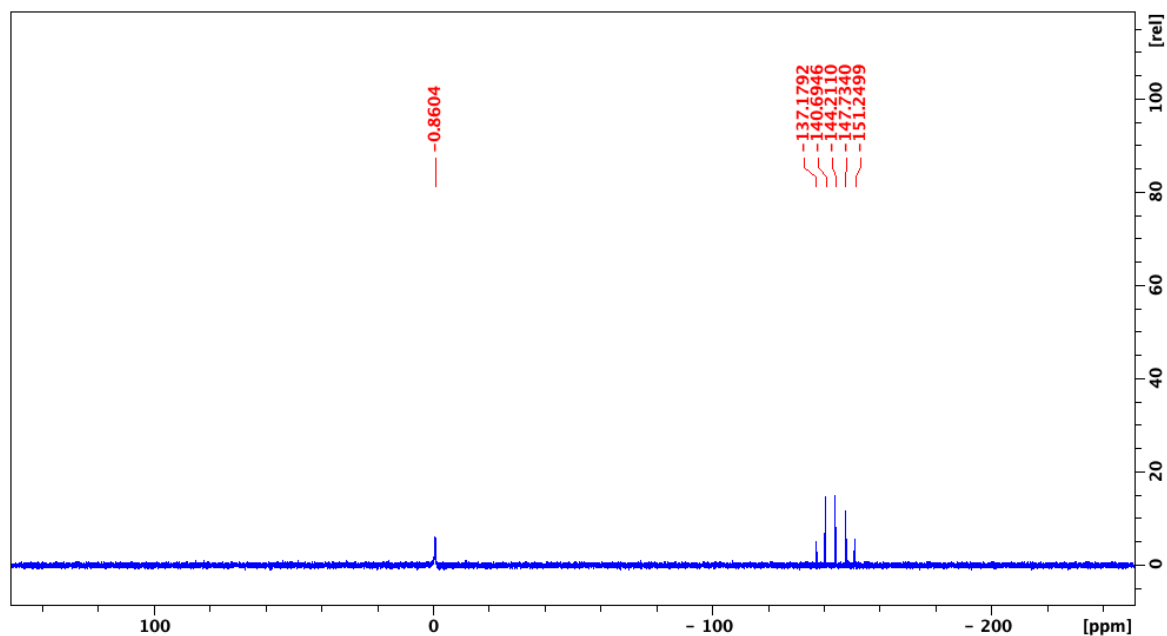
The Cu(I) complex [Cu(PPh<sub>3</sub>)<sub>2</sub>(HL<sup>I</sup>)]PF<sub>6</sub> (**12**) was prepared from the reaction of PPh<sub>3</sub>, Cu(CH<sub>3</sub>CN)<sub>4</sub>PF<sub>6</sub> and ligand HL<sup>I</sup> in CH<sub>3</sub>CN solution (Scheme 22).



Scheme 22 Synthesis of complex [Cu(PPh<sub>3</sub>)<sub>2</sub>(HL<sup>I</sup>)]PF<sub>6</sub> (**12**)

Compound **12** is soluble in common organic solvents such as CHCl<sub>3</sub>, CH<sub>3</sub>CN and DMSO. The IR spectrum carried out on a solid sample of **12** shows all the expected bands for the  $\beta$ -diketone ligand and the triphenylphosphine coligand. The absorptions due to the C=O stretching are at 1731-1702 cm<sup>-1</sup>; they don't significantly vary with respect to the same absorptions of the carbonyl group detectable in the spectrum of the free ligand (1732-1699 cm<sup>-1</sup>). In a lower frequency region, complex **12** shows a broad strong band at 832 cm<sup>-1</sup> due to the stretching vibrations of the PF<sub>6</sub><sup>-</sup> anion. The  $\delta$ (PF<sub>6</sub>) bending vibrations in the spectra of all hexafluorophosphate complexes are observed as a narrow strong band at 556 cm<sup>-1</sup>. In the <sup>1</sup>H-NMR spectra of **12**, recorded in CDCl<sub>3</sub> solution at room temperature, the 3-CH and 4-CH protons of the pyrazole ring are present at 7.68 and 6.27 ppm, respectively. The 5-CH proton of the pyrazole ring and the CH aromatic protons of the phenyl rings are present in the range 7.13-7.43 ppm. The  $\alpha$ -CH and  $\gamma$ -CH bridging protons are present at 5.58 ppm ( $^3J = 11.28$  Hz) and 6.17 ppm ( $^3J = 11.28$  Hz). The singlets at 2.14 and 2.06 ppm are attributable to the methyl groups bonded to the  $\beta$ -dicarbonyl moieties.

The  $^{31}\text{P}\{^1\text{H}\}$ -NMR spectrum of the Cu(I) complex **12**, recorded in  $\text{CDCl}_3$  solution at room temperature, gave a broad singlet at -0.86 ppm downfield shifted with respect to the value of the free phosphane ( $\delta = -5.36$  ppm)) (**Figure 38**). In the spectrum the characteristic septet centered at -144.21 ppm is due to the  $\text{PF}_6^-$  counterion.



**Figure 38**  $^{31}\text{P}\{^1\text{H}\}$ -NMR spectrum of complex **12** in  $\text{CDCl}_3$  solution

The ESI-MS study was performed by dissolving **12** in  $\text{CH}_3\text{CN}$  and recording the spectra in positive- and negative-ion mode. The molecular structure of **12** was confirmed by the presence of the peaks at  $m/z$  366 and 587, attributable to the  $[(\text{Cu}(\text{PPh}_3) + \text{CH}_3\text{CN})^+]$  and  $[(\text{Cu}(\text{PPh}_3)_2)^+]$  species, being positive fragments of the dissociation of the ligand from the complex. The ESI-MS spectrum of **12** in  $\text{CH}_3\text{CN}$  recorded in negative-ion mode shows peak at  $m/z$  145 attributable to the  $\text{PF}_6^-$  aggregate, confirming the presence of the counterion ( $\text{PF}_6^-$ ).

## 4. Conclusions

The research project was mainly focused in the synthesis of first-row metal complexes of sterically hindered  $\beta$ -diketonates also bearing fluorinated moieties. In particular, 1,3-dimesitylpropane-1,3-dione (**HL<sup>Mes</sup>**) and of a further sterically hindered  $\beta$ -diketonate ligand, bearing fluorinated moieties, the 1,3-bis(3,5-bis(trifluoromethyl)phenyl)-3-hydroxyprop-2-en-1-one (**HL<sup>CF3</sup>**) have been synthesized and fully characterized. Their reactivity has been investigated through the synthesis of the related Zn(II), Cu(II), Cu(I) and Ag(I) complexes, with a particular attention to the Cu(II) and Cu(I) species, also in view of their catalytic and biological properties. Notably, **Cu(L<sup>Mes</sup>)<sub>2</sub>** complex was fully characterized by X-ray crystallographic analysis in order to define its solid-state molecular structure. Additionally, preliminary X-ray crystallographic data of **Cu(L<sup>CF3</sup>)<sub>2</sub>**, **Cu(PPh<sub>3</sub>)<sub>2</sub>(L<sup>CF3</sup>)** and **Zn(L<sup>Mes</sup>)<sub>2</sub>** complexes were obtained.

Furthermore, the modification of the electronic and steric properties of acetylacetonate was examined by insertion of different substituents in 2-position, containing additional donor atoms, in order to prepare polyfunctional coordinating ligands with higher complexity and functionality, and related metal complexes, in view of their biological activity as potential anticancer and antiviral agents. In particular, the 3-(phenyl(1*H*-pyrazol-1-yl)methyl)pentane-2,4-dione (**HL<sup>1</sup>**) and the 3-((3,5-dimethyl-1*H*-pyrazol-1-yl)(phenyl)methyl)pentane-2,4-dione (**HL<sup>JM</sup>**) have been synthesized; they are novel 1,3-diketones bearing a pyrazole moieties, whose reactivity and structure were fully studied also by X-ray diffraction analysis for **HL<sup>1</sup>**. The new ligands (**HL<sup>1</sup>** and **HL<sup>JM</sup>**) are really versatile N,O,O-donors because they can provide different hapticities, depending on the type of coordination environment the metal is surrounded.

The free ligands and the metal complexes have been fully spectroscopically and analytically characterized by elemental analysis, FT-IR, ESI-MS(+/-), <sup>1</sup>H-, <sup>13</sup>C-, <sup>19</sup>F- and <sup>31</sup>P-NMR. Biological studies to evaluate the antitumor and antiviral activity are in progress for some of the ligands and related metal complexes. Moreover, based on the scientific literature, they could have potential applications both in catalysis and in medicinal chemistry. For these reasons, the research work is worthy of further and deeper investigations of the properties of this class of compounds, as well as of the synthesis of novel analogous ligands and related complexes.

## References

1. Ivanova, S.; Martínez, T. M. Special Issue Catalysis by Precious Metals, Past and Future. *Catalysts* **2020**, *10*, (2), 247.
2. Chirik, P.; Morris, R. Getting Down to Earth: The Renaissance of Catalysis with Abundant Metals. *Acc. Chem. Res.* **2015**, *48*, (9), 2495.
3. Ludwig, J. R.; Schindler, C. S. Catalyst: Sustainable Catalysis. *Chem* **2017**, *2*, (3), 313-316.
4. Johansson Seechurn, C. C. C.; Kitching, M. O.; Colacot, T. J.; Snieckus, V. Palladium-catalyzed cross-coupling: A historical contextual perspective to the 2010 nobel prize. *Angew. Chem., Int. Ed.* **2012**, *51*, (21), 5062-5085.
5. Izatt, R. M., *Metal Sustainability: Global Challenges, Consequences, and Prospects*. 2016; p 527.
6. Dennis, J. M.; White, N. A.; Liu, R. Y.; Buchwald, S. L. Breaking the Base Barrier: An Electron-Deficient Palladium Catalyst Enables the Use of a Common Soluble Base in C-N Coupling. *J. Am. Chem. Soc.* **2018**, *140*, (13), 4721-4725.
7. Zhang, D.; Wang, Q. Palladium catalyzed asymmetric Suzuki-Miyaura coupling reactions to axially chiral biaryl compounds: Chiral ligands and recent advances. *Coord. Chem. Rev.* **2015**, *286*, 1-16.
8. Diez-Gonzalez, S., *N-Heterocyclic Carbenes: From Laboratory Curiosities to Efficient Synthetic Tools*. 2nd ed.; The Royal Society of Chemistry: 2017.
9. Crabtree, R. H. NHC ligands versus cyclopentadienyls and phosphines as spectator ligands in organometallic catalysis. *J. Organomet. Chem.* **2005**, *690*, (24-25), 5451-5457.
10. Hayler, J. D.; Leahy, D. K.; Simmons, E. M. A Pharmaceutical Industry Perspective on Sustainable Metal Catalysis. *Organometallics* **2019**, *38*, (1), 36-46.
11. Blakemore, D. C.; Castro, L.; Churcher, I.; Rees, D. C.; Thomas, A. W.; Wilson, D. M.; Wood, A. Organic synthesis provides opportunities to transform drug discovery. *Nat. Chem.* **2018**, *10*, (4), 383-394.
12. Krajewski, S. M.; Crossman, A. S.; Akturk, E. S.; Suhrbier, T.; Scappaticci, S. J.; Staab, M. W.; Marshak, M. P. Sterically encumbered beta-diketonates and base metal catalysis. *Dalton Trans.* **2019**, *48*, (28), 10714-10722.
13. Crossman, A. S.; Marshak, M. P.,  $\beta$ -Diketones: Coordination and Application. In *Comprehensive Coordination Chemistry III*, Elsevier: 2021; Vol. 1-9, pp 331-365.
14. Mehrotra, R. C. Chemistry of metal  $\beta$ -diketonates. **1988**, *60*, (8), 1349-1356.
15. Kawaguchi, S. Variety in the coordination modes of  $\beta$ -dicarbonyl compounds in metal complexes. *Coord. Chem. Rev.* **1986**, *70*, 51-84.
16. Aromí, G.; Gamez, P.; Reedijk, J. Poly beta-diketones: Prime ligands to generate supramolecular metalloclusters. *Coord. Chem. Rev.* **2008**, *252*, (8-9), 964-989.
17. Bray, D. J.; Clegg, J. K.; Lindoy, L. F.; Schilter, D., Self-assembled Metallo-supramolecular Systems Incorporating  $\beta$ -Diketone Motifs as Structural Elements. In *Adv. Inorg. Chem.*, Eldik van R. Bowman-James, K., Ed. 2006; Vol. 59, pp 1-37.
18. Emsley, J.; Freeman, N. J.  $\beta$ -diketone interactions: Part 5. Solvent effects on the keto  $\rightleftharpoons$  enol equilibrium. *J. Mol. Struct.* **1987**, *161*, 193-204.
19. Gilli, P.; Bertolasi, V.; Pretto, L.; Ferretti, V.; Gilli, G. Covalent versus Electrostatic Nature of the Strong Hydrogen Bond: Discrimination among Single, Double, and Asymmetric Single-Well Hydrogen Bonds by Variable-Temperature X-ray Crystallographic Methods in  $\beta$ -Diketone Enol RAHB Systems. *J. Am. Chem. Soc.* **2004**, *126*, (12), 3845-3855.
20. Bock, B.; Flatau, K.; Junge, H.; Kuhr, M.; Musso, H. Bond Character of  $\beta$ -Diketone Metal Chelates. *Angew. Chem., Int. Ed.* **1971**, *10*, (4), 225-235.
21. Sanz, P.; M $\acute{o}$ , O.; Y $\acute{a}$ ñez, M.; Elguero, J. Resonance-assisted hydrogen bonds: A critical examination. Structure and stability of the enols of  $\beta$ -diketones and  $\beta$ -enaminones. *J. Phys. Chem. A* **2007**, *111*, (18), 3585-3591.
22. Hopmann, K. H.; Stuurman, N. F.; Muller, A.; Conradie, J. Substitution and isomerization of asymmetric  $\beta$ -diketonato rhodium(I) complexes: A crystallographic and computational study. *Organometallics* **2010**, *29*, (11), 2446-2458.
23. Fatta, A. M.; Lintved, R. L. Nephelauxetic and Spectrochemical Series for 1,3-Diketonates. Ligand Field Spectra of Some Tris(1,3-diketonato)chromium(III) Chelates. *Inorg. Chem.* **1971**, *10*, (3), 478-481.

24. Gericke, H. J.; Muller, A. J.; Swarts, J. C. Electrochemical illumination of intramolecular communication in ferrocene-containing tris  $\beta$ -diketonato aluminum(III) complexes; Cytotoxicity of Al(FcCOCHCOCF 3) 3. *Inorg. Chem.* **2012**, 51, (3), 1552-1561.
25. Ilmi, R.; Haque, A.; Khan, M. S. Synthesis and photo-physics of red emitting europium complexes: An estimation of the role of ancillary ligand by chemical partition of radiative decay rate. *J. Photochem. Photobiol., A* **2019**, 370, 135-144.
26. Siedle, A. R., Diketones and Related Ligands. In *Comprehensive Coordination Chemistry*, Wilkinson, G.; Gillard, R. D.; McCleverty, J. A., Eds. Pergamon: Oxford, UK, 1987; pp 365-412.
27. Pettinari, C.; Marchetti, F.; Drozdov, A.  $\beta$ -Diketones and Related Ligands. *ChemInform* **2004**, 35, (49).
28. Otway, D. J.; Rees, W. S. Group 2 element beta-diketonate complexes: synthetic and structural investigations. *Coord. Chem. Rev.* **2000**, 210, 279-328.
29. Drozdov, A.; Troyanov, S. The structural chemistry of iia group metal diketonates. *Main Group Met. Chem.* **1996**, 19, (9), 547-570.
30. Hampden-Smith, M. J.; Kostas, T. T. Chemical vapour deposition of copper from (hfac)CuL compounds. *Polyhedron* **1995**, 14, (6), 699-732.
31. Perrin, C. L.; Kim, Y.-J. Symmetry of Metal Chelates. *Inorg. Chem.* **2000**, 39, (17), 3902-3910.
32. Power, P. P. Stable two-coordinate, open-shell (d 1-d 9) transition metal complexes. *Chem. Rev.* **2012**, 112, (6), 3482-3507.
33. Cramer, C. J.; Tolman, W. B. Mononuclear Cu-O<sub>2</sub> Complexes: Geometries, Spectroscopic Properties, Electronic Structures, and Reactivity. *Acc. Chem. Res.* **2007**, 40, (7), 601.
34. Katritzky, A. R.; Wang, Z.; Wang, M.; Wilkerson, C. R.; Hall, C. D.; Akhmedov, N. G. Preparation of  $\beta$ -keto esters and  $\beta$ -diketones by C-acylation/deacetylation of acetoacetic esters and acetyl ketones with 1-acylbenzotriazoles. *J. Org. Chem.* **2004**, 69, (20), 6617-6622.
35. Farooqui, T.; Farooqui, A. A., Chapter 2 - Curcumin: Historical Background, Chemistry, Pharmacological Action, and Potential Therapeutic Value. In *Curcumin for Neurological and Psychiatric Disorders*, Farooqui, T.; Farooqui, A. A., Eds. Academic Press: 2019; pp 23-44.
36. Menon, V. P.; Sudheer, A. R., Antioxidant and anti-inflammatory properties of Curcumin. In *The Molecular Targets and Therapeutic Uses of Curcumin in Health and Disease*, Aggarwal, B. B.; Surh, Y.-J.; Shishodia, S., Eds. Springer US: Boston, MA, 2007; pp 105-125.
37. Sharifi-Rad, J.; Rayess, Y. E.; Rizk, A. A.; Sadaka, C.; Zgheib, R.; Zam, W.; Sestito, S.; Rapposelli, S.; Neffe-Skocińska, K.; Zielińska, D.; Salehi, B.; Setzer, W. N.; Dosoky, N. S.; Taheri, Y.; El Beyrouthy, M.; Martorell, M.; Ostrander, E. A.; Suleria, H. A. R.; Cho, W. C.; Maroyi, A.; Martins, N. Turmeric and Its Major Compound Curcumin on Health: Bioactive Effects and Safety Profiles for Food, Pharmaceutical, Biotechnological and Medicinal Applications. *Front. Pharmacol.* **2020**, 11, 01021.
38. Ault, A. The Nobel Prize in Chemistry for 2001. *J. Chem. Educ.* **2002**, 79, (5), 572.
39. Casey, C. P. 2005 Nobel Prize in Chemistry. Development of the Olefin Metathesis Method in Organic Synthesis. *J. Chem. Educ.* **2006**, 83, (2), 192.
40. Halford, B. NOBEL PRIZE IN CHEMISTRY. *Chem. Eng. News* **2010**, 88, (41), 7.
41. White, M. C. Base-Metal Catalysis: Embrace the Wild Side. *Adv. Synth. Catal.* **2016**, 358, (15), 2364-2365.
42. Beletskaya, I. P.; Cheprakov, A. V. Copper in cross-coupling reactions. The post-Ullmann chemistry. *Coord. Chem. Rev.* **2004**, 248, (21-24), 2337-2364.
43. Crossley, S. W. M.; Obradors, C.; Martinez, R. M.; Shenvi, R. A. Mn-, Fe-, and Co-Catalyzed Radical Hydrofunctionalizations of Olefins. *Chem. Rev.* **2016**, 116, (15), 8912-9000.
44. Surry, D. S.; Buchwald, S. L. Dialkylbiaryl phosphines in Pd-catalyzed amination: a user's guide. *Chem. Sci.* **2011**, 2, (1), 27-50.
45. Mendiola, D. J. Nacnac are you still there? The evolution of  $\beta$ -diketiminato complexes of nickel. *Angew. Chem., Int. Ed.* **2009**, 48, (34), 6198-6200.
46. Santini, C.; Marinelli, M.; Pellei, M. Boron-Centered Scorpionate-Type NHC-Based Ligands and Their Metal Complexes. *Eur. J. Inorg. Chem.* **2016**, (15-16), 2312-2331.
47. Pellei, M.; Lobbia, G. G.; Papini, G.; Santini, C. Synthesis and Properties of Poly(pyrazolyl)borate and Related Boron-Centered Scorpionate Ligands. Part B: Imidazole-, Triazole- and Other Heterocycle-Based Systems. *Mini-Rev. Org. Chem.* **2010**, 7, (3), 173-203.
48. Santini, C.; Pellei, M.; Lobbia, G. G.; Papini, G. Synthesis and Properties of Poly(pyrazolyl)borate and Related Boron-Centered Scorpionate Ligands. Part A: Pyrazole-Based Systems. *Mini-Rev. Org. Chem.* **2010**, 7, (2), 84-124.
49. Masui, H. Metalloaromaticity. *Coord. Chem. Rev.* **2001**, 219-221, 957-992.



50. Buck, E.; Song, Z. J.; Tschaen, D.; Dormer, P. G.; Volante, R. P.; Reider, P. J. Ullmann Diaryl Ether Synthesis: Rate Acceleration by 2,2,6,6-Tetramethylheptane-3,5-dione. *Org. Lett.* **2002**, 4, (9), 1623-1626.
51. Nandurkar, N. S.; Bhanushali, M. J.; Patil, D. S.; Bhanage, B. M. Synthesis of sterically hindered 1,3-diketones. *Synth. Commun.* **2007**, 37, (23), 4111-4115.
52. Monnier, F.; Taillefer, M. Catalytic C-C, C-N, and C-O Ullmann-type coupling reactions. *Angew. Chem., Int. Ed.* **2009**, 48, (38), 6954-6971.
53. Roy, D.; Uozumi, Y. Recent Advances in Palladium-Catalyzed Cross-Coupling Reactions at ppm to ppb Molar Catalyst Loadings. *Adv. Synth. Catal.* **2018**, 360, (4), 602-625.
54. Beletskaya, I. P.; Ananikov, V. P. Transition-metal-catalyzed C-S, C-Se, and C-te bond formation via cross-coupling and atom-economic addition reactions. *Chem. Rev.* **2011**, 111, (3), 1596-1636.
55. Cheng, B.; Yi, H.; He, C.; Liu, C.; Lei, A. Revealing the Ligand Effect on Copper(I) Disproportionation via Operando IR Spectra. *Organometallics* **2014**, 34, (1), 206-211.
56. Chi, K. M.; Shin, H. K.; Hampden-Smith, M. J.; Duesler, E. N.; Kostas, T. T. Synthesis and Characterization of ( $\beta$ -Diketonato)copper(I) Alkyne Complexes: Structural Characterization of (Hexafluoroacetylacetonato)(diphenylacetylene)copper(I). *Inorg. Chem.* **1991**, 30, (23), 4293-4294.
57. Doppelt, P.; Baum, T. H. Alkyne Complexes of Copper(I) (1,1,1,5,5,5-Hexafluoro-2,4-Pentanedionato): Syntheses and Characterization of H<sub>2</sub>-Bis(Trimethylsilyl)Acetylene) Copper(I) (Hfac), ( $\mu$ -H<sub>2</sub>-Bis(Trimethylsilyl)Acetylene) Bis(Copper(I) (Hfac) and a Series of (H<sub>2</sub>-Alkyne) Cu(Hfac) Complexes. *J. Organomet. Chem.* **1996**, 517, (1-2), 53.
58. Sherborne, G. J.; Adomeit, S.; Menzel, R.; Rabeah, J.; Brückner, A.; Fielding, M. R.; Willans, C. E.; Nguyen, B. N. Origins of High Catalyst Loading in Copper(i)-Catalysed Ullmann–Goldberg C–N Coupling Reactions. *Chem. Sci.* **2017**, 8, (10), 7203-7210.
59. Larson, A. T.; Crossman, A. S.; Krajewski, S. M.; Marshak, M. P. Copper(II) as a Platform for Probing the Steric Demand of Bulky beta-Diketonates. *Inorg. Chem.* **2020**, 59, (1), 423-432.
60. Sambigioglio, C.; Marsden, S. P.; Blacker, A. J.; McGowan, P. C. Copper catalysed Ullmann type chemistry: from mechanistic aspects to modern development. *Chem. Soc. Rev.* **2014**, 43, (10), 3525-3550.
61. Kundu, S.; Greene, C.; Williams, K. D.; Salvador, T. K.; Bertke, J. A.; Cundari, T. R.; Warren, T. H. Three-Coordinate Copper(II) Aryls: Key Intermediates in C–O Bond Formation. *J. Am. Chem. Soc.* **2017**, 139, (27), 9112-9115.
62. Akturk, E. S.; Scappaticci, S. J.; Seals, R. N.; Marshak, M. P. Bulky beta-Diketones Enabling New Lewis Acidic Ligand Platforms. *Inorg. Chem.* **2017**, 56, (19), 11466-11469.
63. Vigato, P. A.; Peruzzo, V.; Tamburini, S. The Evolution of  $\beta$ -Diketone or  $\beta$ -Diketophenol Ligands and Related Complexes. *Coord. Chem. Rev.* **2009**, 253, (7-8), 1099.
64. Darr, J. A.; Poliakoff, M. New Directions in Inorganic and Metal-Organic Coordination Chemistry in Supercritical Fluids. *Chem. Rev.* **1999**, 99, (2), 495-542.
65. Koepf-Maier, P.; Koepf, H. Non-platinum group metal antitumor agents. History, current status, and perspectives. *Chem. Rev.* **1987**, 87, (5), 1137-1152.
66. Dubler, E.; Buschmann, R.; Schmalke, H. W. Isomer abundance of bis( $\beta$ -diketonato) complexes of titanium(IV). Crystal structures of the antitumor compound budotitane [TiIV(bzac)<sub>2</sub>(OEt)<sub>2</sub>] and of its dichloro-derivative [TiIV(bzac)<sub>2</sub>Cl<sub>2</sub>] (bzac=1-phenylbutane-1,3-dionate). *J. Inorg. Biochem.* **2003**, 95, (2-3), 97-104.
67. Yam, V. W.-W.; Lo, K. K.-W. Recent advances in utilization of transition metal complexes and lanthanides as diagnostic tools. *Coord. Chem. Rev.* **1999**, 184, (1), 157-240.
68. Molander, G. A. Application of lanthanide reagents in organic synthesis. *Chem. Rev.* **1992**, 92, (1), 29-68.
69. Gross, T.; Chevalier, F.; Lindsey, J. S. Investigation of Rational Syntheses of Heteroleptic Porphyrinic Lanthanide (Europium, Cerium) Triple-Decker Sandwich Complexes. *Inorg. Chem.* **2001**, 40, (18), 4762-4774.
70. Sarada, G.; Sim, B.; Moon, C.-K.; Cho, W.; Kim, K.-H.; Sree, V. G.; Park, E.; Kim, J.-J.; Jin, S.-H. Synthesis and characterization of highly efficient blue Ir(III) complexes by tailoring  $\beta$ -diketonate ancillary ligand for highly efficient PhOLED applications. *Org. Electron.* **2016**, 39, 91-99.
71. Adachi, C.; Baldo, M. A.; Thompson, M. E.; Forrest, S. R. Nearly 100% internal phosphorescence efficiency in an organic light-emitting device. *J. Appl. Phys.* **2001**, 90, (10), 5048-5051.
72. de Bettencourt-Dias, A. Lanthanide-based emitting materials in light-emitting diodes. *Dalton Transactions* **2007**, (22), 2229-2241.

73. Abbati, G. L.; Cornia, A.; Fabretti, A. C.; Caneschi, A.; Gatteschi, D. A Ferromagnetic Ring of Six Manganese(III) Ions with a  $S = 12$  Ground State. *Inorg. Chem.* **1998**, *37*, (7), 1430-1431.
74. Angelova, O.; Matsichek, I.; Atanasov, M.; Petrov, G. Chelating modes of 3-substituted 2,4-pentanediones. Crystal and electronic structure of bis(3-cyano-2,4-pentanedionato)cobalt(II). *Inorg. Chem.* **1991**, *30*, (8), 1943-1949.
75. Silvernail, C. M.; Yap, G.; Sommer, R. D.; Rheingold, A. L.; Day, V. W.; Belot, J. A. An effective synthesis of alkyl  $\beta$ -cyano- $\alpha,\gamma$ -diketones using chlorosulfonylisocyanate and a representative Cu(II) complex. *Polyhedron* **2001**, *20*, (26), 3113-3117.
76. Tsiamis, C.; Tzavellas, L. C.; Stergiou, A.; Anesti, V. Variable Coordination and Conformation of the 3-Cyano-2,4-pentanedionato Anion in a Mixed-Ligand Binuclear Copper(II) Chelate. *Inorg. Chem.* **1996**, *35*, (17), 4984-4988.
77. Thambidurai, S.; Jeyasubramanian, K.; Ramalingam, S. K. Bis(benzotriazol-1-yl) methylimine as a novel cyanating agent for labile  $\beta$ -diketonates. *Polyhedron* **1996**, *15*, (22), 4011-4014.
78. Fackler, J. P.; Cotton, F. A. Electronic Spectra of  $\beta$ -Diketone Complexes. IV.  $\gamma$ -Substituted Acetylacetonates of Copper(II). *Inorg. Chem.* **1963**, *2*, (1), 102-106.
79. Hirsch, J.; Paulus, H.; Elias, H. Kinetics and Mechanism of the Formation and Acid Dissociation of Cobalt(II), Nickel(II), and Copper(II) Complexes with the Highly Enolized  $\beta$ -Diketone 3-(N-Acetylamido)pentane-2,4-dione (=Hamac) in Aqueous Solution. *Inorg. Chem.* **1996**, *35*, (8), 2343-2351.
80. Elias, H.; Wiegand, D.; Wannowius, K. X-ray structure analysis of the cobalt(III) complex formed with the ambidentate ligand 3-hydroxyiminopentane-2,4-dione: proof for N,O-fac-coordination and resonance charge delocalization. *Inorg. Chim. Acta* **1992**, *197*, (1), 21-24.
81. Nieuwenhuyzen, M.; Schobert, R.; Hampel, F.; Hoops, S. Reactions of dicarbonyltitanocenes with 2-diazo-1,3-diketones: O-,N- versus O-,O- chelation and self-assembly of a novel heteroleptic Ti5O6-cage compound. *Inorg. Chim. Acta* **2000**, *304*, (1), 118-121.
82. Krishnankutty, K.; Babu, D. K. Metal Complexes of 2-(2-Thiazolylazo)-1,3-dicarbonyls. *J. Indian Chem. Soc.* **1996**, 379-384.
83. S. Turner, S.; Collison, D.; E. Mabbs, F.; Halliwell, M. Preparation, magnetic properties and crystal structure of bis[3-(4-pyridyl)pentane-2,4-dionato]copper(II). *J. Chem. Soc., Dalton Trans.* **1997**, (7), 1117-1118.
84. Boldog, I.; Rusanov, E. B.; Chernega, A. N.; Sieler, J.; Domasevitch, K. V. Acentric Extended Solids by Self Assembly of 4,4'-Bipyrazolyis. *Angew. Chem., Int. Ed.* **2001**, *40*, (18), 3435-3438.
85. Sheldrick, G. M. A short history of SHELX. *Acta Crystallogr. Sect. A Found. Crystallogr.* **2008**, *64*, (1), 112-122.
86. Dolomanov, O. V.; Bourhis, L. J.; Gildea, R. J.; Howard, J. A. K.; Puschmann, H. OLEX2: A complete structure solution, refinement and analysis program. *J. Appl. Crystallogr.* **2009**, *42*, (2), 339-341.
87. CrysAlisPro 1.171.41.103a (Rigaku Oxford Diffraction). **2021**.
88. Sheldrick, G. M. SHELXT - Integrated space-group and crystal-structure determination. *Acta Crystallogr. Sect. A Found. Crystallogr.* **2015**, *71*, (1), 3-8.
89. Sheldrick, G. M. Crystal structure refinement with SHELXL. *Acta Crystallogr. Sect. C Struct. Chem.* **2015**, *71*, 3-8.
90. Kumpan, K.; Nathubhai, A.; Zhang, C.; Wood, P. J.; Lloyd, M. D.; Thompson, A. S.; Haikarainen, T.; Lehtiö, L.; Threadgill, M. D. Structure-based design, synthesis and evaluation in vitro of aryl naphthyridinones, arylpyridopyrimidinones and their tetrahydro derivatives as inhibitors of the tankyrases. *Bioorg. Med. Chem.* **2015**, *23*, (13), 3013-3032.
91. Emsley, J. In *The composition, structure and hydrogen bonding of the  $\beta$ -diketones*, Complex Chemistry, Berlin, Heidelberg, 1984//, 1984; Emsley, J.; Ernst, R. D.; Hathaway, B. J.; Warren, K. D., Eds. Springer Berlin Heidelberg: Berlin, Heidelberg, pp 147-191.
92. Dryden, R. P.; Winston, A. The Infrared Spectra of Some metal Chelates of  $\beta$ -Diketones. *J. Phys. Chem.* **1958**, *62*, (5), 635-637.
93. Slabzhennikov, S. N.; Ryabchenko, O. B.; Kuarton, L. A. Interpretation of the IR spectra of aluminum, gallium, and indium tris(acetylacetonates). *Russ. J. Coord. Chem.* **2006**, *32*, (8), 545-551.
94. Nakamoto, K., *Infrared and Raman Spectra of Inorganic and Coordination Compounds, Part B: Applications in Coordination, Organometallic, and Bioinorganic Chemistry*. Wiley: 2009.
95. Zhang, C.; Yang, P.; Yang, Y.; Huang, X.; Yang, X.-J.; Wu, B. High-Yield Synthesis of 1,3-Dimesityl-propane-1,3-dione: Isolation of Its Aluminum Complex as a Stable Intermediate. *Synth. Commun.* **2008**, *38*, (14), 2349-2356.

96. Fuson, R. C.; Ross, W. E.; McKeever, C. H. The Condensation of Paraformaldehyde with Aromatic Ketones. II.1 Mesityl Ketones. *J. Am. Chem. Soc.* **1939**, 61, (2), 414-417.
97. Johnson, C. K. *ORTEP, Report ORNL-5138, Oak Ridge National Laboratory, Oak Ridge, TN; 1976.*
98. Farrugia, L. WinGX and ORTEP for Windows: an update. *J. Appl. Cryst.* **2012**, 45, (4), 849-854.
99. He, C.; Zhang, G.; Ke, J.; Zhang, H.; Miller, J. T.; Kropf, A. J.; Lei, A. Labile Cu(I) Catalyst/Spectator Cu(II) Species in Copper-Catalyzed C–C Coupling Reaction: Operando IR, in Situ XANES/EXAFS Evidence and Kinetic Investigations. *J. Am. Chem. Soc.* **2013**, 135, (1), 488-493.
100. Gromilov, S. A.; Baidina, I. A. Regularities of crystal structures of Cu(II)  $\beta$ -diketonates. *J. Struct. Chem.* **2004**, 45, (6), 1031-1081.
101. Lebrun, P. C.; Lyon, W. D.; Kuska, H. A. Crystal Structure of Bis(2,4-Pentanedionato)Copper(II). *J. Crystallogr. Spectrosc. Res.* **1986**, 16, (6), 889.
102. Dey, S. K.; Bag, B.; Zhou, Z.; Chan, A. S. C.; Mitra, S. Synthesis, Characterization and Crystal Structure of a Monomeric and a Macrocyclic Copper (II) Complex with a Large Cavity Using Benzylacetylacetone Ligand. *Inorg. Chim. Acta* **2004**, 357, (7), 1991.
103. Starikova, Z. A.; Shugam, E. A. Crystal chemical data for inner complexes of  $\beta$ -diketonates. *J. Struct. Chem.* **1969**, 10, (2), 267-269.
104. Sans-Lenain, S.; Gleizes, A. Structural Features of Homo- and Heteroleptic Complexes of Copper(II) with 2,2,6,6-Tetramethyl-3,5-Heptanedione and 3-Chloro-2,4-Pentanedione. *Inorg. Chim. Acta* **1993**, 211, (1), 67.

## Ringraziamenti

“Mai dire mai, perché i limiti, come le paure, spesso sono solo un’illusione.” M.J.

Quando si giunge ad un traguardo, piccolo o grande che sia, il pensiero va sempre a coloro che ci hanno aiutati in questo percorso, perché nel nostro ricordo essi ci hanno spianato la strada rendendola meno difficile di quanto sarebbe stata.

Un sentito grazie ai miei relatori, Carlo Santini e Maura Pellei per la loro infinita disponibilità, l’immensa pazienza, per i loro indispensabili consigli e soprattutto per la loro grandissima organizzazione e dedizione al lavoro che sono state essenziali per crescere professionalmente e personalmente.

Vorrei ringraziare la Professoressa Luísa Margarida Martins che ha gentilmente accettato di seguirmi nella discussione della Tesi con l’Istituto Superior Técnico di Lisbona.

Ringrazio la mia correlatrice Miriam Caviglia, che in questi mesi di lavoro mi ha supportato con una grande dose di suggerimenti pratici nella ricerca in laboratorio e nella stesura della Tesi.

Un ringraziamento particolare va alla mia famiglia che è stata le fondamenta dei miei valori, un grande punto di riferimento e un costante sostegno.

Un grazie infinito va ai miei amici che sono una fonte inesauribile di spensieratezza, leggerezza, ascolto e sostegno.

Vorrei dedicare qualche riga per ricordare l’importanza che ha avuto il periodo di Double Degree a Lisbona, intrapreso inizialmente con assoluta incertezza e come una sfida, ma che si è dimostrato essere una delle esperienze che più mi hanno fatto crescere non solo a livello formativo, ma anche umano.